MOLECULAR DESIGN AND APPLICATION OF CHIRAL PORPHYRIN WITH MOLECULAR ASYMMETRY

（分子不斉ポルフィリンの設計とその応用）

KATSUAKI KONISHI

MOLECULAR DESIGN AND APPLICATION OF CHIRAL PORPHYRIN WITH MOLECULAR ASYMMETRY

A THESIS PRESENTED
TO
UNIVERSITY OF TOKYO

1993
BY

KATSUAKI KONISHI

PREFACE

The study presented in this thesis has been carried out under the direction of Professor Dr. Shohei Inoue during the period of April, 1987 - January, 1993, at the Department of Synthetic Chemistry at University of Tokyo. The studies are concerned with molecular design of chiral porphyrin with molecular asymmetry on the basis of an original concept, its use for stereochemical model systems of enzymatic reactions and properties, and its application for a novel chiral catalyst and receptor.

The author wishes to express his sincere gratitude to Professor Dr. Shohei Inoue for his valuable suggestions and encouragement throughout the work, and, to be much more important, leading him to the wonderful world of chemistry.

The author should express his supreme and special gratitude to Associate Professor Dr. Takuzo Aida for technical and practical instructions, constant discussions, and continuous encouragement during the course of this study.

The author is also grateful to Professor Dr. Reiko Kuroda, University of Tokyo, for her work of X-ray structural analysis.

Grateful acknowledgment is made to Messrs. Hideo Kubo, Minoru Igarashi, Kazuharu Miyazaki, Ken-ichiro Oda, Takashi Sugino, Kei Nishida, Yoshiki Mori, Lin-Chiu Chiang, Yuji Kozawa, Yoshio Furusho, Yoshinori Takahata, Kazuyuki Yahara, Hiroshi Toshishige, and Hideki Saito for their active collaborations

during the course of the study.

The author is also grateful to Associate Professor Dr. Mizuo Maeda, Kyushu University, and Drs. Atsunori Mori, Dae-won Chung, Masuyuki Yokoyama, Masato Aoyama, Toru Arai, Masakatsu Kuroki, and Hiroshi Sugimoto for their valuable discussions and kind advices.

The author deeply thanks Messrs. Yasuhiro Hirai, Kenzo Tanaka, Masashi Komatsu, Yoshihiko Watanabe, Kenji Shibata, Mrs. Hiroko Yasuda, Miss Kanako Kouda, and all members of Inoue Laboratory for their kind consideration.

Finally, the author expresses his deep and special gratitude to his parents, Mr. Takao Konishi and Mrs. Hiroko Konishi, for their affectionate encouragement throughout the work.

Katsuaki KONISHI

Department of Synthetic Chemistry
Faculty of Engineering
University of Tokyo

March, 1993

CONTENTS

GENERAL INTRODUCTION

The chemistry of tetrapyrrolic macrocycle and related compounds has received particular attention in relation to their prominent function in biological systems.[1] For example, metalloenzymes such as hemoglobin, myoglobin, catalase, cytochrome *c* peroxidase, and microsomal, hepatic, and bacterial cytochrome P-450s contain iron protoporphyrin IX in the active site, while pheophorbide and magnesium pheophorbide (chlorophyll) serve as a light-harvesting antenna and electron-transfer pigments in the photosynthetic process of plants and bacterias. Coenzyme vitamin B_{12} (5'-deoxyadenosylcobalamin), a cobalt corrin, serves as a cofactor for a variety of enzymatic reactions involving 1,2-interchange of hydrogen atom and another substituent on adjacent carbon atoms of the substrate.[2] In the biogenesis of methane in methanogenic bacteria, factor F-430, a nickel corphin, is believed to play a key role of hydrogenolysis of carbon-sulfur bonds.[3]

One of the current trends in this field is to mimic these naturally occurring process involving tetrapyrrolic macrocycle by simplified artificial systems. In this respect, synthetic porphyrin and metalloporphyrin have been served excellent model systems. Many chemists have participated in this research area, since the discovery of the improved, facile, and easy synthetic method of

5,10,15,20-tetraarylporphyrin by Adler *et al.*,[4] and the elaborate works on the synthesis of octaalkylporphyrin by Johnson or Smith.[1] Especially, iron-complexes of functinalized porphyrins, *e.g.*, "picket-fence porphyrin",[5] "strapped porphyrin",[6] "capped porphyrin",[7] or "tailed porphyrin",[8] have been extensively studied for the model system of hemoglobin with regard to the artificial occurrence of the reversible dioxygen binding property.

Iron porphyrins also act as oxidation catalysts of hydrocarbons, which is related to the function of cytochrome P-450 monooxygenase.[9] In 1979, Groves *et al.* reported for the first time that the oxidation of alkane or alkene with iodosobenzene (PhIO) is effectively catalyzed by the chloroiron complex of 5,10,15,20-tetraphenylporphyrin or protoporphyrin IX dimethylester.[10] Though iron is the metal present in biological systems, manganese has proven to be very effective. In fact, manganese porphyrins have been shown to be better catalysts for hydroxylation than iron porphyrins.[11] Chromium systems also perform this chemistry,[12] and nickel,[13] copper,[14] and ruthenium systems[15] have been reported, though the mechanisms of oxygen transfer may be somewhat different in these systems. Several different oxygen sources can be used in model systems. The most popular source, however, has been PhIO and its perfluoro derivative.[16] The perfluoro derivative reacts much faster than PhIO, mainly because of its greater

solubility. Sodium[17] and lithium[18] hypochlorite have also proven to be effective in a number of cases. Amine oxides, peroxides, and peracids, potassium persulfate, and sodium periodate work similarly.[19] Molecular oxygen itself is inactive in the manganese porphyrin systems without reducing agent such as ascorbate[20] or platinum and hydrogen.[21] Simple aerobic epoxidation of alkenes has been achieved by using a sterically hindered ruthenium porphyrin.[22]

With respect to the regio- and/or stereo-chemical course of the oxidation process by metalloporphyrin, remarkable steric effects of the porphyrin ligands have been recognized.[9] An iron or manganese complex of sterically hindered tetramesitylporphyrin has shown a higher reactivity toward *cis*-alkene than *trans*-alkene.[23] Recently, very high shape-selectivity (regioselectivity) has been achieved by using fuctinalized metalloporphyrin catalysts. Collman *et al.* has reported that a manganese "picnic-basket" porphyrin coupled with an anionic ligand effectively recognizes the shape of the substrates.[24]

◆◆◆◆◆ Natural and Artifical Chiral Porphyrins ◆◆◆◆◆

As described above, cytochrome P-450s catalyzes the metabolic oxidation reaction in biological systems. These reaction proceeds stereospecifically under the appropriate conditions. For example, selectivity in the metabolism of a

racemic mixture such as with warfarin[25] or amphetamine[26]; the predominant attack on one face of a plannar molecule, such as epoxidation of various polycyclic aromatic hydrocarbons [27] or simple alkenes[28], α-face hydroxylation of steroids;[29] the generation of chiral sulfoxides,[30] or selective removal of a prochiral hydrogen from a substrate[31] have been demonstrated. Furthermore, recently, cytochrome P-450$_{cam}$, which had been considered to be a specific enzyme for the hydroxylation of camphor and related compounds, also catalyzes the epoxidation of a simple alkene such as *cis*-β-methylstyrene with high enantioselectivity.[32]

In relation to the mechanism of this interesting asymmetric oxygen transfer, various synthetic chiral metalloporphyrin catalysts have been exploited. The representative catalysts bear chiral groups covalently linked to achiral porphyrin moieties, which model the essential role of the chiral protein molecule of cytochrome P-450 monooxygenases in the stereochemical course of the oxygen transfer process. In 1983, Groves *et al.* designed chiral iron catalysts bearing a binaphthyl moieties attached the atropisomers of tetrakis(*o*-aminophenyl)porphyrin for the first time, and obtained enantioselectivities ranging form 20 - 51 % *ee* in the epoxidation of styrene derivatives with iodosomesitylene.[33] One year later, Mansuy *et al.* reported asymmetric epoxidation of 4-chlorostyrene with comparable enantioselectivities

by using a chiral iron complex of basket-handle porphyrin incorporating L-phenylalanine.[34] Recently, Kodadek *et al.* have presented a chiral porphyrin in which the binaphthoic moieties are directly linked to the porphyrin meso carbons. This system gives slightly lower *ee*'s, but it was significantly more stable to the oxidation conditions, allowing much greater turnnumber.[35] Groves *et al.* have recently reported asymmetric hydroxylation of simple ethylbenzene, epoxidation of alkenes, and sulfoxidation of sulfides, using another basket-handle type chiral porphyrin catalysts.[36] Some other examples of asymmetric oxidation catalyzed by chiral porphyrin complexes have been reported on the basis of a similar methodology.[37]

There have been a few reports concerning the use of chiral porphyrin for the function other than monooxygenase-like asymmetric oxidation. Kodadek *et al.* have reported asymmetric cyclopropanation by using rhodium complexes of chiral wall porphyrin and fortress porphyrin as catalysts.[38] Ohkubo *et al.* have employed a chiral manganese porphyrin for the enantioselective oxidation of tryptophan as a model of tryptophan 2,3-dioxygenase.[39] Chiral recognition of racemic phosphines has been achieved by using a chiral ruthenium porphyrins.[40]

◆◆◆◆◆ Scope of the Present Thesis ◆◆◆◆◆

In the present thesis, the author will describe design of a conceptually new chiral porphyrin with "molecular asymmetry" derived from "enantiotopic (prochiral)" porphyrin, and its application for the stereochemical model of the biological functions and also for the novel catalyst or receptor.

What is Chiral Porphyrin with *"Molecular Asymmetry"?*

Despite the extensive development of studies to understand the role of the metal (iron) ion in hemoproteins, little attention has been paid with respect to the structure of the ligand itself. As described above, the porphyrin ligand of P-450 is protoporphyrin IX, which has "enantiotopic faces", and, therefore, upon coordination with the chiral protein moleculethe, protoheme itself should become chiral ("molecular asymmetry") and the active site takes a diastereoisomeric structure. In connection with this, the coordinated protoheme has been proposed to exist as either of two possible optically active diastereoisomers as a result of a stereospecific discrimination between the faces of the heme ("chiral orientation") by the chiral cysteine residue for cytochromes,[41] histidine for hemoglobin[42]and myoglobin, and tyrosine for catalase.[43] The X-ray crystallographic works of some hemoproteins demonstrated the stereochemically unique face available to O_2 and other ligands is exactly the same in P-450_{cam}, microsomal P450s, globins, and

catalase, whereas cytochrome *c* peroxidase exhibits the opposite orientation.[44]

By mimicking the chiral structure and the orientation of the protoheme itself in the active site of hemoproteins, the author has developed a series of chiral porphyrin with "molecular asymmetry" based on a novel concept regarding the prochirality of porphyrin carrying specifically arranged peripheral substituents. Likewise protoporphyrin IX in hemoproteins, porphyrins carrying specifically arranged peripheral substituents has enantiotopic faces and thus prochiral. Appropriate modification (*e.g.*, N-substitution, Co(III) insertion, strapping, meso-substitution) to one of the enantiotopic faces should give a chiral porphyrin.

Chapter 1 is concerned with synthesis, separation, circular dichroism and X-ray crystallographic determination of the absolute stereochemistry of a chiral N-substituted etioporphyrin I.

Chapter 2 is concerned with optical resolution of chiral alkyl- and aryl-cobalt(III)etioporphyrins I, their racemization profiles, and also its use for a tool to deduce the mechanism of the transfer reaction of alkyl or aryl group between metal and nitrogen.

Chapter 3 is concerned with separation of an enantiomeric pair, thermal- and/or photo-induced racemization of chiral meso-substituted ("armed") porphyrin complexes.

Chapter 4 is concerned with asymmetric oxidation of olefin and sulfide catalyzed by metal complexes of chiral strapped porphyrin as a novel stereochemical model of the enzyme P-450.

Chapter 5 is concerned with enantioselective binding of carboxylate anions of N-protected amino acids with the zinc complex of a chiral N-alkylated strapped porphyrin, where unprecedentedly high enantioselectivity is achieved.

Chapter 6 is concerned with diastereoselective and asymmetric reduction of carbonyl compounds with alcohol catalyzed by achiral aluminum porphyrin.

Reference and Notes

1. (a) *Porphyrin and Metalloporphyrin;* Smith, K. M., Ed.; Elsevier: New York, 1975. (b) *The Porphyrins;* Dolphin, D., Ed.; Academic Press: New York, 1978.

2. (a) Woodward, R. B. *Pure Appl. Chem.* **1988**, *33*, 145. (b) Abeles, R. H.; Dolphin, D. *Acc. Chem. Res.* **1976**, *9*, 114.

3. *The Bioinorgnic Chemistry of Nickel;* Lanchester, J. R., Ed.; VCH Publishers: New York, 1988.

4. Adler, A. D.; Longo, F. R.; Finnel, J. Goldmacher, J.; Assour, J.; Korsakoff, L. *J. Org. Chem.* **1967**, *32*, 476.

5. (a) Collman, J. P.; Gange, R. R.; Halbert, T. R.; Marchon, J.-C.; Reed, C. A. *J. Am. Chem. Soc.* **1973**, *95*, 7860. (b) Collman, J. P.; Brauman, J. I.; Iverson, B. L.; Sessler, J. L.; Morris, R, M,; Gibson, Q. H. *J. Am. Chem. Soc.* **1983**, *105*, 3052. (c) Eshima, K.; Yuasa, M.; Nishide, H.; Tschida, E. *J. Chem. Soc., Chem. Commun.*, **1985**, 130.

6. Ogoshi, H,; Sugimoto, H,; Yoshida, Z. *Tetrahedron Lett.* **1976**, 4476.

7. Alwong, J.; Baldwin, J. E.; Huff, J. *J. Am. Chem. Soc.*, **1975**, *97*, 227.

8. (a) Chang, C. K.; Traylor, T. G. *Proc. Natl. Acad. Sci. USA* **1973**, *70*, 2647. (b) Traylor, T. G.; Chang, C. K.; Geibel, J.; Berzinis, A.; Mincey, T.; Canonn, J. *J. Am. Chem. Soc.* **1979**, *101*, 6716.

9. *Cytochrome P-450;* Ortiz de Montellano, P. R., Ed.; Plenum Press: New York, 1986.

10. Groves, J. T.; Nemo, T. E.; Myers, R. S. *J. Am. Chem. Soc.* **1979**, *101*, 1032.

11. Collman, J. P.; Kodadek, T.; Raybuck, S. A.; Meuiner, B. *Proc. Natl. Acad. Sci. USA* **1983**, *80*, 7039.

12. Groves, J. T.; Kruper, W. J. Jr. *J. Am. Chem. Soc.* **1979**, *101*, 7613.

13. Koolu, J. D.; Kochi, J. K. *Inorg. Chem.* **1987**, *26*, 908.

14. Tai, A. F.; Margerum, L. D.; Valentine, J. S.; *J. Am. Chem. Soc.* **1986**, *108*,

5006.

15. Leung, T.; James, B. R.; Dolphin, D. *Inorg. Chim. Acta* **1983**, *79*, 180.

16. Traylor, T. G.; Marsteres, J. C. Jr.; Nakano, T.; Dunlap, B. E. *J. Am. Chem. Soc.* **1985**, *107*, 5537.

17. Guilmet, E.; Meuiner, B. *Nouv. J. Chim.* **1982**, *6*, 511.

18. Collman, J. P.; Brauman, J. I.; Meuiner, B.; Raybuck, S. A.; Kodadek, T. *Proc. Natl. Acad. Sci. USA* **1984**, *81*, 3245.

19. Meunier, B. *Bull. Soc. Chim. Fr.* **1986**, 578.

20. Mansuy, D.; Fontecave, M.; Bartoli, J. F. *J. Chem. Soc., Chem. Commun.*, **1983**, 253.

21. Tabushi. I.; Koga, N. *J. Am. Chem. Soc.* **1979**, *101*, 6456.

22. J. T. Groves.; Quinn, R. *J. Am. Chem. Soc.* **1985**, *107*, 5790.

23. (a) Groves, J. T.; Nemo, T. E. *J. Am. Chem Soc.* **1983**, *105*, 5786. (b) Coll-

man, J. P.; Brauman, J. I.; Meunier, B.; Hayashi, T.; Kodadek. T.; Raybuck, S. A. *J. Am. Chem Soc.* **1985**, *107*, 2000.

24. Collman, J. P.; Zhang, X.; Hembre, R. T.; Brauman, J. I. *J. Am. Chem. Soc.* **1990**, *112*, 5356.

25. Kaminsky, L. S.; Fasco, M. J.; Guengerich, F. P. *J. Biol. Chem.* **1980**, *255*, 85.

26. Cho, A. K.; Wright, J. *Life Sci.* **1978**, *22*, 363.

27. Miwa, G. T.; Lu, A. Y. H. The Topology of the Mammalian Cytochrome P-450 Active Site. In *Cytochrome P-450;* Ortiz de Montellano, P. R., Ed.; Plenum Press: New York, 1986.

28. (a) Harris, C.; Philpot, R. M.; Hernandez, O.; Bend, J. R. *J. Pharmacol. Exp. Ther.* **1989**, *248*, 492. (b) Foureman, G. L.; Harris, C.; Guengerich, F. P.; Bend, J. R. *J. Pharmacol. Exp. Ther.* **1986**, *236*, 144.

29. Waxman, D. J.; Ko, A.; Walsh, C. *J. Biol. Chem.* **1983**, *258*, 11937.

30. (a) Waxman, D. J.; Light, D. R.; Walsh, C. *Biochemistry* **1982**, *21*, 2499.

(b) Takata, T.; Yamazaki, M.; Fujimori, K.; Kim, Y. H.; Iyanagi, T.; Oae, S. *Bull. Chem. Soc. Jpn.* **1983**, *56*, 2300.

31. Tullman, R. H.; WAlsh, J. S.; Miwa, G. T. *Fed. Proc.* **1984**, *43*, 346.

32. Ortiz de Montellano, P. R.; Fruetel, J. A.; Collins, J. R.; Camper, D. L.; Loew, G. H. *J. Am. Chem. Soc.* **1991**, *113*, 3195.

33. Groves, J. T.; Myers, R. S. *J. Am. Chem. Soc.* **1983**, *105*, 5791.

34. Mansuy, D.; Battioni, P.; Renaud, J. P.; Guerin, P. *J. Chem. Soc., Chem. Commun.*, ***1985***, 155.

35. O'Malley, S; Kodadek, T. J. *J. Am. Chem. Soc.* **1989**, *111*, 9116.

36. (a) Groves, J. T.; Viski, P. *J. Am. Chem. Soc.* **1989**, *111*, 8537. (b) Groves, J. T.; Viski, P. *J. Org. Chem.* **1990**, *55*, 3628.

37. (a) Naruta, Y.; Tani, F.; Maruyama, K. *Chem. Lett.* ***1989***, 1269. (b) Naruta, Y.; Tani, F.; Maruyama, K. *J. Chem. Soc., Chem. Commun.*,

1990, 1378. (c) Naruta, Y.; Tani, F.; Ishihara, N.; Maruyama, K. *J. Am. Chem. Soc.* **1991**, *113*, 1378. (d) Naruta, Y.; Tani, F.; Maruyama, K. *Tetrahedron Asymmetry:* **1991**, *2*, 533. (e) Naruta, Y.; Ishihara, N.; Tani, F.; Maruyama, K. *Chem. Lett.* **1991**, 1933. (f) Naruta, Y.; Tani, F.; Maruyama, K. *Tetrahedron. Lett.* **1992**, *33*, 1269. (g) Collman, J. P.; Zhang, X.; Hembre, R. T.; Brauman, J. I. *J. Am. Chem. Soc.* **1990**, *112*, 5356. (h) Collamn, J. P.; Zhang, X.; Lee, V. J.; Brauman, J. I. *J. Chem. Soc., Chem. Commun.*, ***1992***, 1647. (i) Halterman, R. L.; Jan, S.-T. *J. Org. Chem.* **1991**, *56*, 5253.

38. (a) O'Malley, S; Kodadek, T. *Tetrahedorn Lett.* **1989**, *111*, 9116. (b) Maxwell, J. L.; O'Malley, S; Brown, K.; Kodadek, T. *Organometallics* **1992**, *11*, 645. (c) O'Malley, S; Kodadek, T. *Organometallics* **1992**, *11*, 2299.

39. (a) Ohkubo, K.; Sagawa, T.; Kuwata, M.; Hata, T.; Ishida, H. *J. Chem. Soc., Chem. Commun.*, **1989**, 352. (b) Ohkubo, K.; Sagawa, T.; Ishida, H. *Inorg. Chem.* **1992**, 2682.

40. (a) Le Maux, P.; Bahri, H,: Simonneaux, G. *J. Chem. Soc., Chem. Commun.*, **1992**, 1350.

41. (a) Ortiz de Montellano, P. R.; Kunze, K. L.; Belian, H. S. *J. Biol. Chem.*

1983, *258*, 45. (b) Kunze, K. L.; Mangold, B. L. K.; Wheeler, C.; Belian. H. S.; Ortiz de Montellano, P. R. *J. Biol. Chem.* **1983**, *258*, 4202.

42. Perutz, M. F.; Muirhead, H.; Cox, J. M.; Guaman, L. G. *Nature* **1983**, *219*, 131.

43. Murphy, M. R. N.; Reid, T. J.; Sicignano, A.; Tanaka, N.; Rossmann, M. G. *J. Mol. Biol.* **1981**, *152*, 465.

44. Poulous, T. L.; Freer, S. T.; Alden, R. A.; Xuong, N. H.; Edwards, S. L.; Hamilin, R. C.; Kraut, J. *J. Biol. Chem.* **1978**, *257*, 10427.

CHAPTER 1

Chiral N-Substituted Porphyrin. Synthesis, Circular Dichroism, and Crystallographic Determination of Absolute Stereochemistry.

Abstract

Chiral N-(2-hydroxyalkyl)etioporphyrins I were prepared in excellent yields by nucleophilic ring-opening of epoxides such as ethylene oxide, propylene oxide, and styrene oxide with the lithium salt of etioporphyrin I having enantiotopic faces, and the optical isomers were resolved by HPLC. In the case of the reactions with mono-substituted epoxides bearing asymmetric carbon atoms, either of the two possible diastereoisomers was preferentially formed. Based on the X-ray crystallography of the bromozinc complex of an isomer of *N*-((*R*)-2-(4'-bromobenzoyloxy)-2-phenylethyl)etioporphyrin I, derived with (*R*)-styrene oxide, the configurations of the four possible diastereoisomers of *N*-(2-hydroxy-2-phenylethyl)etioporphyrin I were elucidated, and the signs of their circular dichroism peaks were correlated with the absolute configurations at the alkylated nitrogen atoms.

Introduction

There are various naturally occurring and artificial porphyrins with enantiotopic faces (prochiral) due to specific arrangements of the peripheral substituents, and they are possibly converted into chiral porphyrins. From a biological viewpoint, chiral *N*-substituted porphyrins with asymmetric nitrogen atoms are the most attractive series.[1] Ortiz de Montellano et al. has demonstrated that the prosthetic heme group, iron protoporphyrin IX, is denatured into *N*-substituted protoporphyrins IX during the interaction of drugs (alkene, alkyne, and so on) with cytochrome P-450 in animal livers and reactions of aryl and alkyl-hydrazines with hemoglobin (**Scheme 1**).[2] Since

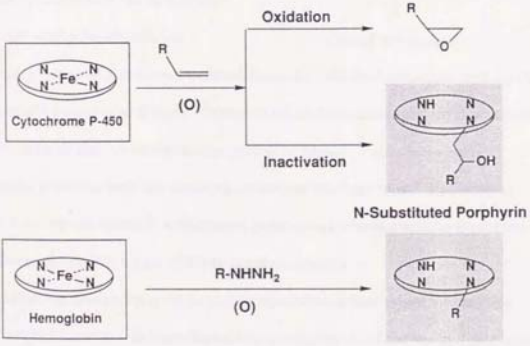

Scheme 1

protoporphyrin IX has enantiotopic faces, the *N*-substituted derivatives derived from hemoproteins are chiral due to the presence of the *N*-substituents on either of the two faces, and their circular dichroism profiles are expected to provide a versatile tool for deducing the absolute orientation of the prosthetic heme groups in hemoproteins, which are generally not easily accessible. In fact, some optically active *N*-substituted protoporphyrins IX have been isolated from the metabolic systems, and on the basis of the patterns and signs of their circular dichroism spectra, the absolute orientations of the prosthetic heme groups in hemoproteins have been discussed together with the stereochemistry of the reactions.[3] However to date, there are no chiral *N*-substituted porphyrins whose absolute structures have been defined in terms of X-ray crystallography.

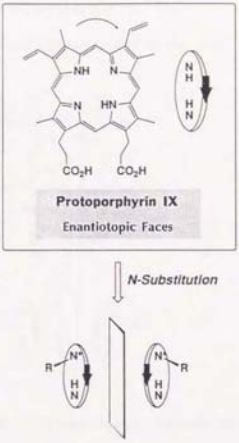

Likewise protoporphyrin IX in hemoproteins, etioporphyrin I (**1a**) has enantiotopic faces due to the alternating arrangement of the methyl and ethyl groups along the periphery of the porphyrin ring (*C4h* symmetry), and has enantiotopic faces (prochiral). Recently, Kubo *et al.* have succeeded in the

resolution of the optical antipodes of *N*-methyletioporphyrin I (**2a**) *N*-ethyletioporphyrin I (**3a**) and by HPLC and characterized as the zinc

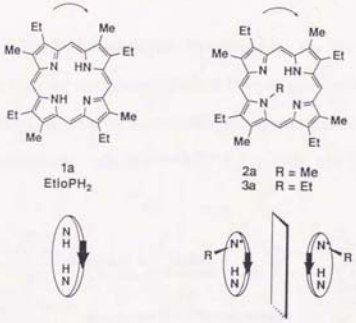

complex possessing a chiral axial ligand such as L-methoxypropionate by NMR spectroscopy. This provided an evidence of prochirality of type I porphyrin originating from its enantiotopic faces.[4]

In the present chapter, the author wishes to describe the first crystallographic determination of the absolute configuration of a chiral *N*-substituted etioporphyrin I, taking advantage of the novel, efficient synthetic route to chiral *N*-(2-hydroxyalkyl)porphyrins related to the products of the inactivation of cytochrome P-450 with olefins,[5] and a successful resolution of their stereoisomers by HPLC. The author also provides the definitive correlation of the X-ray crystallography - based structure with the circular dichroism.

Results and Discussion

Synthesis of *N*-(2-Hydroxyalkyl)porphyrins. For the synthesis of a series of *N*-(2-hydroxyalkyl)etioporphyrins I (**4** - **6**), the novel, efficient route was exploited, which involves nucleophilic ring-opening of epoxides with lithiated etioporphyrin I (**1b**) (**Scheme 2**).[6,7] Typically, to a THF solution (20

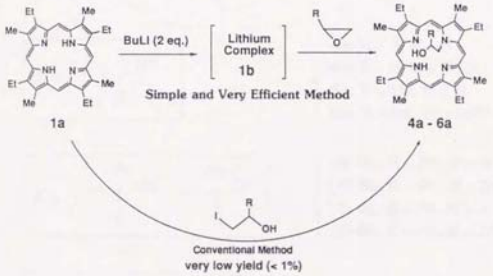

Scheme 2

mL) of etioporphyrin I (**1a**, 1 mmol) was added a hexane solution of *n*-BuLi (2 mmol) at -78 °C in a nitrogen atmosphere, and the mixture was stirred for 1 h. Then, ethylene oxide (10 mmol) was added, and the mixture was allowed to warm to room temperature. After stirring for 20 h, the reaction mixture was treated with methanolic zinc acetate followed by aq. NaCl, affording the chlorozinc complex of *N*-(2-hydroxyethyl)etioporphyrin I (**4b**) in 96 % yield.

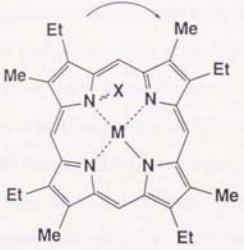

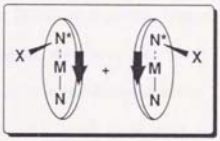

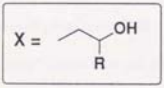

4a: R = H, M = H
4b: R = H, M = ZnCl
5a: R = Me, M = H
5b: R = Me, M = ZnCl

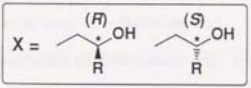

(*R*)-**6a:** R = Ph, M = H
(*R*)-**6b:** R = Ph, M = ZnCl
(*S*)-**6a:** R = Ph, M = H
(*S*)-**6b:** R = Ph, M = ZnCl

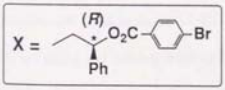

(*R*)-**7b:** M = ZnBr

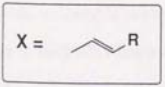

(*R*)-**8b:** M = ZnCl

When mono-substituted epoxides such as propylene oxide and styrene oxide bearing asymmetric carbon atom were employed for the above reaction, they were cleaved exclusively at the O-CH_2 bonds with retention of configuration, to give **5b** and **6b**, respectively, in 78 and 76 % yields. Use of the lithiated porphyrin generated from the equimolar reaction of **1a** with *n*-BuLi for the ring-opening of styrene oxide resulted in the decrease of the yield of **6b** (44 %) along with the recovery of **1a** (38 %). In all these cases, no polyalkylated products such as *N*, *N'*-disubstituted porphyrins were formed, even though an excess amount of *n*-BuLi was employed for the preparation of the lithiated porphyrin (**1b**). In contrast to this efficient method, employment of the conventional one-pot method involving electrophilic *N*-substitution with alkyl iodides resulted in the formation of *N*-(2-hydroxyalkylporphyrins) in very low yields (< 1 %) (**Scheme 2**).[8]

Resolution of Stereoisomers. Due to the enantiotopic structure of etioporphyrin I (**1a**), **4** should be racemic, while **5** and **6** should be mixtures of diastereoisomers. The isomers of **4a** - **6a** in the free-base forms were resolved by HPLC on silica gel coated with cellulose tris(3,5-dimethylphenylcarbamate) as a chiral stationary phase. For example, racemic **4a** provided two elution peaks with comparable peak areas at 17.1 (fraction I: **4a**-[FI]) and 38.9 min (fraction II: **4a**-[FII]); **Figure 2 (A)**). On the other hand, for diastereoisomeric *N*-((*R*)-2-hydroxy-2-phenylethyl)etioporphyrin I ((*R*)-**6a**) derived with (*R*)-styrene oxide, two elution peaks at 14.8 ((*R*)-**6a**-[FI]) and 37. 8 min

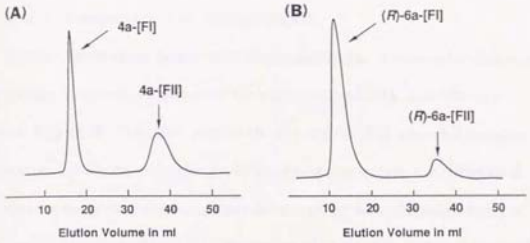

Figure 2. HPLC profiles of (**A**) **4a** and (**B**) (*R*)-**6a** using the analytical column (see **Experimental Section**) with hexane/2-propanol/diethylamine (95/5/0.1 v/v) as eluent at room temperature monitored at 390 nm.

((*R*)-**6a**-[FII]) with different peak areas (ratio of 2 : 1 for (*R*)-**6a**-[FI]/(*R*)-**6a**-[FII]) were observed (**Figure 2 (B)**). The same was true for (*S*)-**6a** derived with (*S*)-styrene oxide (peak area ratio of 1 : 2 for (*S*)-**6a**-[FI] (retention time: 15.5 min)/(*S*)-**6a**-[FII]) (retention time: 41.2 min), indicating the possible discrimination of the two enantiotopic faces of **1b** in the *N*-alkylation with chiral epoxides. The diastereoisomeric ratio could be estimated also from the ^{1}H NMR in $CDCl_3$ of a diastereoisomeric mixture of (*R*)-**6b** ((*S*)-**6b**). It showed two doublet signals at δ 5.49 and 5.43, assignable to the ortho protons of *N*-$CH_2CH(Ph)OH$, respectively, in (*R*)-**6b**-[FI] ((*S*)-**6b**-[FII]) and (*R*)-**6b**-[FII] ((*S*)-**6b**-[FI]) with the peak intensity ratio of 2 :

1. Similarly, the mole ratio of the two diastereoisomers of **5b** was 3 : 2 as determined from the ^{1}H NMR based on the intensity ratio of the signals at δ -1.11 and -1.15 assignable to *N*-$CH_2CH(CH_3)OH$.

Circular Dichroism Spectra of Stereoisomers. The circular dichroism (CD) profiles of the stereoisomers of the zinc complexes (**4b**) and (**6b**) are shown in **Figure 3**. The enantiomers **4b**-[FI] and **4b**-[FII] provided negative and positive CD bands, respectively, in the Soret region (426 nm) (**Figure 3 (A)**), which were perfect mirror images of each other with the magnitudes of molar molecular ellipticity ($|[\Theta]|$, deg·cm^2·dmol^{-1}) being ca. 5,000. These CD profiles were very similar to those of the enantiomers of the zinc complex of *N*-methyl- or *N*-ethyl-etioporphyrin I. In contrast, the diastereoisomers of **6b** showed split Cotton effects with enhanced intensities (**Figure 3 (B)**), where the mirror-image spectral patterns for (*R*)-**6b**-[FI] and (*S*)-**6b**-[FII] ((*R*)-**6b**-[FII] and (*S*)-**6b**-[FI]) indicate that these are the enantiomeric pair. The splitting and enhancement of the CD spectra thus observed are obviously due to the induced CD associated with the presence of the chiral, chromophoric *N*-substituent in proximity to the porphyrin chromophore. In fact, the analogous chlorozinc complex derived with achiral octaethylporphyrin and (*R*)-styrene oxide provided a very similar CD pattern to those of (*R*)-**6b**. When (*R*)-**6b**-[FI] ((*R*)-**6b**-[FII]) was mixed with an equimolar amount of (*S*)-**6b**-[FI] ((*S*)-**6b**-[FII]) to cancel the contribution of the induced CD, the resulting spectrum was virtually identical to that of **4b**-[FI] (**4b**-[FII]) (**Figure 3 (A)**). On the other hand, the *N*-styryl derivatives **8b**-[FI] (**8b**-[FII]), derived from

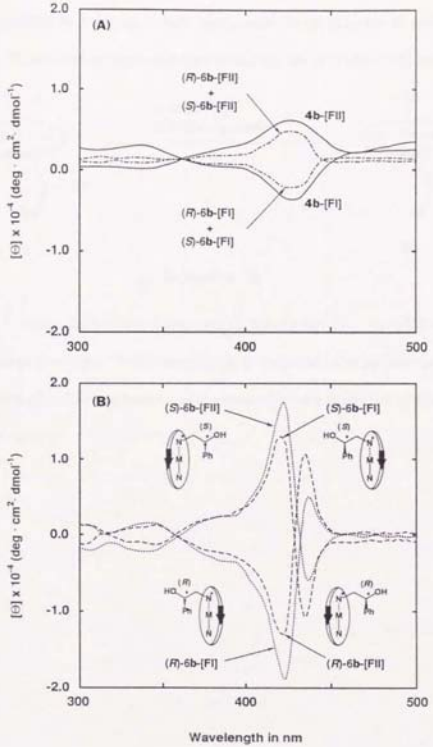

Figure 3. Circular dichroism spectra of the chlorozinc complexes of the isomers of chiral *N*-(2-hydroxyethyl)etioporphyrin I (**4b**) and *N*-(2-hydroxy-2-phenylethyl)etioporphyrin I (**6b**). The arrows in the schematic illustrations of the isomers indicate the Me → Et turn in each pyrrole unit.

6b-[FI] (**6b**-[FII]) by treatment with methanesulfonyl chloride in pyridine (**Scheme 3**), showed an opposite sign to that of **4b**-[FI] (**4b**-[FII]) with a

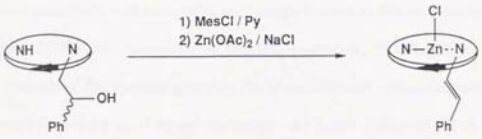

6a 8b

Scheme 3

comparable magnitude in the Soret region, where **8b**-[FI] (**8b**-[FII]) showed a positive (negative) sign. This observation is considered to be associated with the presence of a chromophore (styryl group) directly attached to the porphyrin unit.

Determination of the Absolute Stereochemistry by X-ray crystallography and Correlation with the Circular Dichroism. The X-ray diffraction analysis was successful on a single crystal of the bromozinc complex ((*R*)-**7b**-[FI]), derived from the diastereoisomer (*R*)-**6b**-[FI] by esterification of the hydroxy group in the *N*-substituent with 4-bromobenzoyl chloride followed by axial ligand exchange with NaBr (**Scheme 4**). A dark

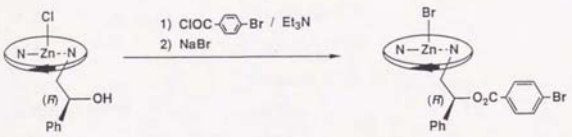

(*R*)-6b-[FI] (*R*)-7b-[FI]

Scheme 4

red cubic single crystal suitable for X-ray work was obtained by slow diffusion of cyclohexane vapor into a toluene solution of (*R*)-**7b**-[FI], which was originally precipitated as needles from a benzene / cyclohexane / ethanol solution. The crystallographic data and experimental conditions of this crystal are given in **Table 1**. The crystal contained 0.3 cyclohexane and 0.3 ethanol molecules of solvation being disordered. **Figure 4** shows the molecular structure of the porphyrin moiety, where one of the ethyl substituents (C(40) carbon) is disordered. The crystal packing is given in a stereoview in **Figure 5**. **Table 2** lists the positional parameters of the atoms of the porphyrin moiety. The bond distances, and bond angles are given in **Table 3** and **4**, respectively.

Table I. Crystal Data and Experimental Conditions.

Formula	$ZnBr_2C_{47}H_{48}N_4O_2 \cdot 0.3C_2H_5OH \cdot 0.3C_6H_{12}$
Formula Weight	965.19
Crystal System	orthorhombic
Space Group	$P2_12_12$
a / Å	28.933 (6)
b / Å	13.171 (3)
c / Å	13.942 (3)
V / Å^3	5313 (2)
temperature / °C	23 °C
F(000)	1896
Radiation	Mo Kα (λ = 0.71069 Å)
Dc / g · cm^{-3}	1.158
Z	4
Crystal Size / mm	0.35 x 0.50 x 0.20
m (Mo Kα) / cm^{-1}	20.0
Diffractometer	Rigaku AFC-5R
Maximum 2θ / °	60.1
Scanning Rate / ° min^{-1}	4.0
Scan Width / °	0.76 + 0.30 tan θ
Number of Unique Reflections	2468
R	0.086
Rw	0.116
GOF	3.89

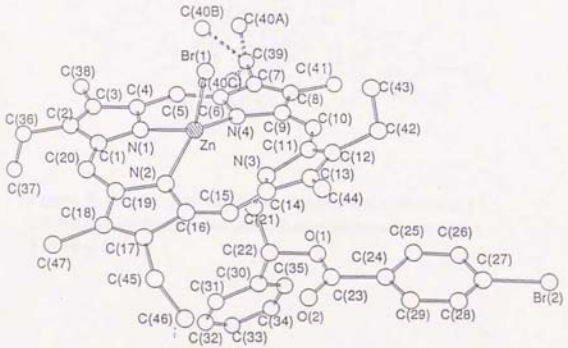

Figure 4. X-ray crystal structure of the bromozinc complex of (*S*)-*N*-((*R*)-2-(4'-bromobenzoyloxy)-2-phenylethyl)etioporphyrin I ((*R*)-**7b**-[FI]). Hydrogen atoms are omiitted for clarity.

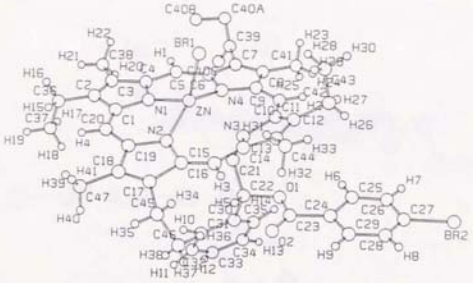

Figure 5. X-ray crystal structure of the bromozinc complex of (*S*)-*N*-((*R*)-2-(4'-bromobenzoyloxy)-2-phenylethyl)etioporphyrin I ((*R*)-**7b**-[FI]).

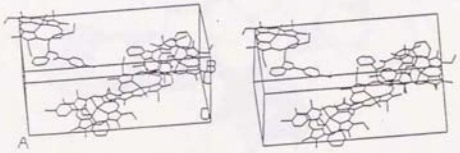

Figure 6. Crystal packing in an unit cell of the bromozinc complex of (*S*)-*N*-((*R*)-2-(4'-bromobenzoyloxy)-2-phenylethyl) etioporphyrin I ((*R*)-**7b**-[FI]) in a stereodiagram.

(**A**)

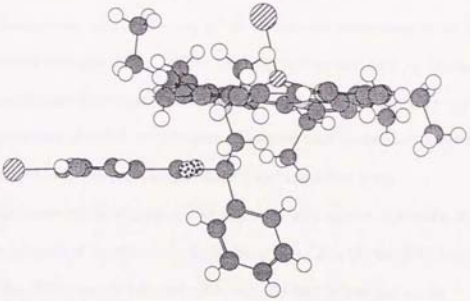

(**B**)

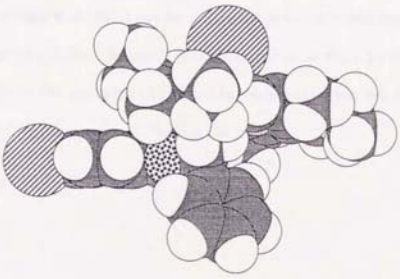

Figure 7. Ball and stick (**A**) and space-filling (**B**) models of (*S*)-*N*-((*R*)-2-(4'-bromobenzoyloxy)-2-phenylethyl)etioporphyrin I ((*R*)-**7b**-[FI]) based on the crystal structure.

The molecular structure of (*R*)-**7b**-[FI] (**Figure 5**) showed that the *N*-alkylated pyrrole ring is tilted by 29° from the reference plane of the three non-alkylated nitrogen atoms. When the molecule is viewed from the same side of the alkylated nitrogen atom, a clockwise methyl → ethyl turn appears at the β-positions of every pyrrole unit. Based on this molecular structure, the configurations of the precursor (*R*)-**6b**-[FI] and the other three diastereoisomers can be elucidated as schematically shown in **Figure 3 (B)**. Thus, the isomers of the free-base **6a** eluting first ((*R*)-, (*S*)-**6a**-[FI]) and second ((*R*)-, (*S*)-**6a**-[FII]) respectively take (*S*)- and (*R*)-configurations at the alkylated nitrogen atoms. When these stereochemical profiles are correlated with the CD spectra of the mixtures (*R*)-**6b**-[FI] + (*S*)-**6b**-[FI] and (*R*)-**6b**-[FII] + (*S*)-**6b**-[FII] in **Figure 3 (A)**, it can be concluded that the chiral free-base *N*-alkyletioporphyrin I (**2a - 6a**) with (*S*)-configuration at the alkylated nitrogen atom provides a negative CD band in the Soret region, while the antipode with (*R*)-configuration a positive CD band.

Table 2. Positinal Parameters (Å) and Thermal Parameters ($Å^2$).[a]

atom	x	y	z	B (eq.)
Br(1)	0.8471 (1)	0.0362 (2)	-0.0084 (3)	6.6 (2)
Br(2)	0.601 (1)	-0.4824 (3)	-0.4333 (3)	9.2 (2)
Zn	0.8808 (9)	-0.1292 (2)	0.0061 (2)	4.2 (1)
O(1)	0.8069 (5)	-0.406 (1)	-0.207 (1)	5 (1)
O(2)	0.8303 (7)	-0.365 (2)	-0.364 (1)	10 (2)
N(1)	0.9354 (7)	-0.154 (2)	0.095 (1)	4 (1)
N(2)	0.9255 (7)	-0.15 (2)	-0.109 (1)	4 (1)
N(3)	0.8277 (8)	-0.222 (2)	-0.109 (1)	5 (1)
N(4)	0.8359 (7)	-0.212 (2)	0.099 (1)	4 (1)
C(1)	0.9809 (8)	-0.135 (2)	0.076 (2)	3.4 (5)
C(2)	1.005 (1)	-0.132 (2)	0.164 (2)	4.2 (6)
C(3)	0.9786 (8)	-0.159 (2)	0.236 (2)	3.3 (5)
C(4)	0.9333 (8)	-0.167 (2)	0.192 (2)	4 (6)
C(5)	0.89 (1)	-0.203 (2)	0.235 (2)	5.1 (6)
C(6)	0.8463 (9)	-0.22 (2)	0.195 (2)	4.4 (6)
C(7)	0.807 (1)	-0.255 (2)	0.242 (2)	5.2 (6)
C(8)	0.7743 (9)	-0.263 (2)	0.181 (2)	4.6 (6)
C(9)	0.79 (1)	-0.235 (2)	0.089 (2)	4.6 (7)
C(10)	0.7653 (7)	-0.236 (2)	0.006 (2)	4.8 (5)
C(11)	0.778 (1)	-0.213 (2)	-0.082 (2)	5.1 (7)
C(12)	0.7565 (8)	-0.175 (2)	-0.158 (2)	4.2 (6)
C(13)	0.787 (1)	-0.157 (2)	-0.231 (2)	5.3 (7)
C(14)	0.8321 (8)	-0.177 (2)	-0.204 (2)	4 (6)
C(15)	0.8727 (8)	-0.16 (2)	-0.248 (2)	4.4 (6)
C(16)	0.9141 (9)	-0.155 (2)	-0.209 (2)	4.5 (6)
C(17)	0.96 (1)	-0.143 (2)	-0.256 (2)	5.3 (7)
C(18)	0.995 (1)	-0.129 (2)	-0.194 (2)	5.1 (6)
C(19)	0.975 (1)	-0.134 (2)	-0.097 (2)	4.8 (6)

C(20)	0.9986	(8)	-0.123	(2)	-0.012	(2)	4.7 (5)
C(21)	0.8515	(8)	-0.319	(2)	-0.089	(2)	4.3 (6)
C(22)	0.853	(1)	-0.385	(2)	-0.176	(2)	5.4 (6)
C(23)	0.802	(1)	-0.393	(3)	-0.302	(3)	6.9 (8)
C(24)	0.7508	(9)	-0.417	(2)	-0.329	(2)	5.2 (7)
C(25)	0.715	(1)	-0.441	(2)	-0.262	(2)	6.5 (8)
C(26)	0.672	(1)	-0.46	(2)	-0.295	(2)	6.3 (7)
C(27)	0.662	(1)	-0.454	(2)	-0.392	(2)	5.7 (7)
C(28)	0.693	(1)	-0.425	(2)	-0.455	(2)	7.4 (8)
C(29)	0.737	(1)	-0.409	(2)	-0.424	(2)	5.6 (7)
C(30)	0.876	(1)	-0.491	(2)	-0.156	(2)	5.6 (6)
C(31)	0.925	(1)	-0.493	(3)	-0.164	(2)	8.1 (9)
C(32)	0.946	(1)	-0.589	(3)	-0.125	(3)	10 (1)
C(33)	0.922	(1)	-0.664	(3)	-0.09	(3)	7.4 (9)
C(34)	0.876	(1)	-0.658	(3)	-0.082	(3)	9 (1)
C(35)	0.853	(1)	-0.057	(3)	-0.11	(2)	7.1 (8)
C(36)	1.055	(1)	-0.116	(2)	0.171	(2)	5.8 (7)
C(37)	1.0821	(1)	-0.21	(3	0.174	(2)	7.6 (9)
C(38)	0.987	(1)	-0.17	(2)	0.337	(2)	6.3 (8)
C(39)	0.807	(1)	-0.275	(3)	0.359	(3)	9 (1)
C(40A)	0.801	(2)	-0.208	(5)	0.415	(5)	5 (1)
C(40B)	0.841	(6)	-0.21	(1)	0.45	(1)	9 (5)
C(40C)	0.829	(3)	-0.341	(8)	0.385	(7)	7 (3)
C(41)	0.726	(1)	-0.297	(2)	0.199	(2)	6.2 (7)
C(42)	0.706	(1)	-0.157	(2)	-0.157	(2)	6.6 (8)
C(43)	0.699	(1)	-0.052	(3)	-0.134	(3)	11 (1)
C(44)	0.78	(1)	-0.106	(3)	-0.325	(2)	8.2 (9)
C(45)	0.961	(1)	-0.156	(2)	-0.373	(2)	6.3 (8)
C(46)	0.949	(1)	-0.262	(3)	-0.408	(3)	11 (1)
C(47)	1.048	(1)	-0.12	(3)	-0.212	(2)	6 (7)
H(1)	0.8933		-0.2126		0.3032		5.1
H(2)	0.7332		-0.2514		0.0068		5.7
H(3)	0.8694		-0.1494		-0.3155		5.8
H(4)	1.0308		-0.1062		-0.0117		5.5

H(5)	0.8666	-0.3523	-0.2262	6.3
H(6)	0.7212	-0.4459	-0.1972	7.4
H(7)	0.6479	-0.4763	-0.2543	7.5
H(8)	0.6829	-0.4122	-0.5228	10
H(9)	0.7588	-0.3876	-0.4717	6.3
H(10)	0.9448	-0.4352	-0.1853	7.4
H(11)	0.9777	-0.6049	-0.1462	7.5
H(12)	0.9374	-0.7156	-0.0568	10
H(13)	0.8562	-0.7109	-0.0611	6.3
H(14)	0.8196	-0.5595	-0.0958	11.5
H(15)	1.0671	-0.0781	0.1127	12.8
H(16)	1.0634	-0.074	0.2237	8.6
H(17)	1.0731	-0.2424	0.2324	10.5
H(18)	1.074	-0.2499	0.1214	8.1
H(19)	1.1139	-0.1958	0.1752	6.3
H(20)	0.9767	-0.2376	0.3553	6.3
H(21)	1.0162	-0.158	0.3533	9.3
H(22)	0.9657	-0.1236	0.3715	9.3
H(23)	0.7101	-0.2536	0.2441	6.8
H(24)	0.7076	-0.2958	0.1404	6.8
H(25)	0.725	-0.3645	0.2232	6.8
H(26)	0.6931	-0.1686	-0.2142	7.8
H(27)	0.6932	-0.1989	-0.1067	7.8
H(28)	0.7121	-0.0395	-0.663	12
H(29)	0.7126	-0.009	-0.1738	12
H(30)	0.6665	-0.0399	-0.1249	12
H(31)	0.7978	-0.0465	-0.323	9.5
H(32)	0.7946	-0.1521	-0.372	9.5
H(33)	0.07501	-0.0984	-0.3362	9.5
H(34)	0.9382	-0.1115	-0.3979	6.3
H(35)	0.9901	-0.1403	-0.3992	6.3
H(36)	0.919	-0.2794	-0.3817	12.8
H(37)	0.9478	-0.2631	-0.4744	12.8
H(38)	0.971	-0.3081	-0.3836	12.8

H(39)	1.0639	-0.1153	-0.1531	6.3
H(40)	1.0577	-0.1726	-0.2496	6.3
H(41)	1.0519	-0.0555	-0.2457	6.3
H(42)	0.8822	-0.3045	-0.6955	5.2
H(43)	0.8356	-0.3533	-0.0396	5.2

[a] Estimated standard deviations in paretheses. The atom-labeling figure is shown in **Figure 4**.

Table 3. Intramolecular distances (Å) involving the nonhydrogen atoms.

Atoms		Distance	Atoms		Distance
Br(1)	Zn	2.394 (4)	C(11)	C(12)	1.34 (3)
Br(2)	C(27)	1.88 (3)	C(12)	C(13)	1.36 (3)
Zn	N(1)	2.04 (2)	C(12)	C(42)	1.48 (3)
Zn	N(2)	2.08 (2)	C(13)	C(14)	1.39 (3)
Zn	N(4)	2.13 (2)	C(13)	C(44)	1.5 (4)
O(1)	C(22)	1.43 (3)	C(14)	C(15)	1.34 (3)
O(1)	C(23)	1.34 (4)	C(15)	C(16)	1.32 (3)
O(2)	C(23)	1.26 (3)	C(16)	C(17)	1.49 (3)
N(1)	C(1)	1.37 (3)	C(17)	C(18)	1.34 (3)
N(1)	C(4)	1.36 (3)	C(17)	C(45)	1.64 (4)
N(2)	C(16)	1.44 (3)	C(18)	C(19)	1.47 (3)
N(2)	C(19)	1.47 (3)	C(18)	C(47)	1.56 (4)
N(3)	C(11)	1.48 (3)	C(19)	C(20)	1.38 (3)
N(3)	C(14)	1.46 (3)	C(21)	C(22)	1.5 (3)
N(3)	C(21)	1.47 (3)	C(22)	C(30)	1.57 (4)
N(4)	C(6)	1.37 (3)	C(23)	C(24)	1.55 (4)
N(4)	C(9)	1.36 (3)	C(24)	C(25)	1.43 (3)
C(1)	C(2)	1.4 (3)	C(24)	C(29)	1.39 (4)

C(1)	C(20)	1.34	(3)	C(25)	C(26)	1.35	(3)
C(2)	C(3)	1.31	(3)	C(26)	C(27)	1.4	(3)
C(2)	C(36)	1.47	(3)	C(27)	C(28)	1.31	(4)
C(3)	C(4)	1.45	(3)	C(28)	C(29)	1.36	(3)
C(3)	C(38)	1.44	(3)	C(30)	C(31)	1.41	(4)
C(4)	C(5)	1.47	(3)	C(30)	C(35)	1.39	(4)
C(5)	C(6)	1.39	(3)	C(31)	C(32)	1.5	(5)
C(6)	C(7)	1.38	(3)	C(32)	C(33)	1.31	(4)
C(7)	C(8)	1.29	(3)	C(33)	C(34)	1.33	(4)
C(8)	C(39)	1.64	(4)	C(34)	C(35)	1.39	(4)
C(8)	C(9)	1.41	(3)	C(35)	C(37)	1.46	(4)
C(8)	C(41)	1.49	(3)	C(39)	C(40A)	1.2	(6)
C(9)	C(10)	1.37	(3)	C(39)	C(40B)	1.59	(6)
C(10)	C(11)	1.31	(4)	C(39)	C(40C)	1.13	(9)
C(45)	C(46)	1.51	(4)	C(42)	C(43)	1.43	(5)

[a] Estimated standard deviaitions in paretheses.

Table 4. Intramolecular bond angles (°) involving the nonhydrogen atoms.[a]

Atoms			Angle
Br(1)	Zn	N(1)	120.8 (6)
Br(1)	Zn	N(2)	107.8 (6)
Br(1)	Zn	N(4)	105.5 (6)
N(1)	Zn	N(2)	88.2 (7)
N(1)	Zn	N(4)	91 (8)
N(2)	Zn	N(4)	141.5 (9)
C(22)	O(1)	C(23)	112 (2)
Zn	N(1)	C(1)	127 (2)
Zn	N(1)	C(4)	126 (2)
C(1)	N(1)	C(4)	105 (2)

Zn	N(2)	C(16)	128	(2)
Zn	N(2)	C(19)	120	(2)
C(16)	N(2)	C(19)	110	(2)
C(11)	N(3)	C(14)	107	(2)
C911)	N(3)	C(21)	118	(2)
C(14)	N(3)	C(21)	119	(2)
Zn	N(4)	C(6)	120	(2)
Zn	N(4)	C(9)	130	(2)
C(6)	N(4)	C(9)	107	(2)
N(1)	C(1)	C(2)	108	(2)
N(1)	C(1)	C(20)	125	(2)
C(2)	C(1)	C(20)	127	(2)
C(1)	C(2)	C(3)	112	(2)
C(1)	C(2)	C(36)	124	(2)
C(3)	C(2)	C(36)	124	(2)
C(2)	C(3)	C(38)	133	(2)
C(4)	C(3)	C(38)	123	(2)
N(1)	C(4)	C(3)	111	(2)
N(1)	C(4)	C(5)	119	(2)
C(4)	C(5)	C(6)	132	(3)
N(4)	C(6)	C(7)	108	(2)
C(5)	C(6)	C(7)	127	(3)
C(6)	C(7)	C(8)	108	(3)
C(6)	C(7)	C(39)	122	(3)
C(8)	C(7)	C(39)	129	(3)
C(7)	C(8)	C(9)	110	(3)
C(7)	C(8)	C(41)	128	(3)
C(9)	C(8)	C(41)	123	(3)
N(4)	C(9)	C(8)	106	(2)
N(4)	C(9)	C(10)	127	(3)
C(8)	C(9)	C(11)	126	(3)
N(3)	C(11)	C(10)	120	(3)
N(3)	C(11)	C(12)	106	(2)
C(10)	C(11)	C(12)	134	(3)

C(11)	C(12)	C(13)	111	(2)
C(11)	C(12)	C(42)	121	(3)
C(13)	C(12)	C(42)	128	(3)
C(12)	C(13)	C(14)	112	(3)
C(12)	C(13)	C(44)	130	(3)
C(14)	C(13)	C(44)	117	(3)
N(3)	C(14)	C(13)	104	(2)
N(3)	C(14)	C(15)	124	(2)
C(13)	C(14)	C(15)	133	(3)
C(14)	C(15)	C(16)	128	(3)
N(2)	C(16)	C(15)	128	(2)
N(2)	C(16)	C(17)	102	(2)
C(15)	C(16)	C(17)	130	(3)
C(16)	C(17)	C(18)	114	(3)
C(16)	C(17)	C(45)	116	(2)
C(18)	C(17)	C(19)	130	(3)
C(17)	C(18)	C(47)	107	(2)
C(17)	C(18)	C(47)	131	(3)
N(2)	C(19)	C(18)	106	(2)
N(2)	C(19)	C(20)	127	(2)
C(18)	C(19)	C(20)	127	(3)
C(1)	C(20)	C(19)	126	(2)
N(3)	C(21)	C(22)	112	(2)
O(1)	C(22)	C(21)	109	(2)
O(1)	C(22)	C(30)	107	(2)
C(21)	C(22)	C(30)	112	(2)
O(1)	C(23)	O(2)	130	(3)
O(1)	C(23)	C(24)	109	(3)
O(2)	C(23)	C(24)	121	(3)
C(23)	C(24)	C(25)	125	(3)
C(23)	C(24)	C(29)	119	(3)
C(25)	C(24)	C(29)	116	(3)
C(24)	C(25)	C(26)	119	(3)
C(25)	C(26)	C(27)	121	(3)

Br(2)	C(27)	C(26)	119	(3)
Br(2)	C(27)	C(28)	120	(3)
C(26)	C(27)	C(28)	121	(3)
C(27)	C(28)	C(29)	119	(3)
C(24)	C(29)	C(28)	124	(3)
C(22)	C(30)	C(31)	116	(3)
C(22)	C(30)	C(35)	123	(3)
C(31)	C(30)	C(35)	120	(3)
C(30)	C(31)	C(32)	113	(3)
C(31)	C(32)	C(33)	124	(3)
C(32)	C(33)	C(34)	120	(4)
C(33)	C(34)	C(35)	121	(3)
C(30)	C(35)	C(34)	121	(3)
C(2)	C(36)	C(37)	113	(3)
C(7)	C(39)	C(40A)	122	(5)
C(7)	C(39)	C(40B)	128	(6)
C(7)	C(39)	C(40C)	116	(6)
C(12)	C(42)	C(43)	108	(3)
C(17)	C(45)	C(46)	114	(3)

[a] Estimated standard deviaitions in paretheses.

Conclusion

The interest in the chirality of *N*-substituted porphyrin family with asymmetric core nitrogen atom has emerged since the discovery of the optical activities of some *N*-substituted protoporphyrins IX isolated as the inactivation products of cytochrome P-450 in metabolic processes. The patterns and signs of the unique circular dichroism profiles of the inactivation products provided a tool for deducing the orientation of the prosthetic heme groups in hemoproteins. However, there were no chiral *N*-substituted porphyrins with crystallographically defined structures. The present chapter describes the novel, efficient synthetic route to chiral *N*-(2-hydroxyalkyl)porphyrins, resolution of the optical isomers by HPLC, and the first example of a crystallographically defined chiral *N*-substituted porphyrin bearing asymmetric nitrogen atom. The definitive correlation enabled here between the absolute structure and the circular dichroism of this particular type of chiral compound would not only offer the basic contribution to the hemoprotein chemistry but also provide a potentially useful knowledge in the general field of chemistry.

Experimental Section

Materials.

Tetrahydrofuran (THF) was distilled over sodium benzophenone ketyl just before use. Ethylene oxide was purified by trap-to- trap distillation over KOH and CaH_2. Propylene oxide was distilled under atmospheric pressure over KOH and CaH_2. (*R*)- and (*S*)-Styrene oxide were purchased from Aldrich and Merck, respectively and used as received. Butyllithium (1.6 M in hexane, Aldrich) was used as received. Etioporphyrin I (**1a**, EtioPH$_2$) was synthesized from *tert*-butyl 4-ethyl-3,5-dimethylpyrrole-2-carboxylate and recrystallized from chloroform ($CHCl_3$)/methanol (MeOH).[9]

Chloro(*N*-(2-hydroxyethyl)etioporphyrinato)zinc (4b). To a THF solution (20 mL) of etioporphyrin I (**1a**, 1 mmol) was added a hexane solution of n-BuLi (2 mmol) at -78 °C in a nitrogen atmosphere, and the mixture was stirred for 1 h to generate the dilithium complex (**1b**). Then, ethylene oxide (10 mmol) was added, and the mixture was allowed to warm to room temperature. After stirring for 20 h, the reaction mixture was treated with methanolic zinc acetate, washed with aqueous NaCl, dried over anhydrous Na_2SO_4, and filtered out. The filtrate was evaporated to dryness under reduced pressure, and the residue dissolved in a minimum volume of $CHCl_3$ was loaded on an alumina column (Merck, Art. 1097) prepared from a $CHCl_3$ slurry. A purple fraction eluted with $CHCl_3$ containing 10 % MeOH was

collected and washed with saturated aqueous NaCl. The separated organic layer was dried over anhydrous Na_2SO_4 and filtered. The filtrate was evaporated to dryness, and the residue was recrystallized from CH_2Cl_2 / hexane to give **4b** as a purple powder (96 % yield). UV-vis λmax, nm (log ε): 623 (3.50), 583 (4.04), 540 (3.90), 434 (5.04), 424 (5.09), 308 (4.08). ^{1}H NMR: δ 10.33, 10.31, 10.19, 10.18 (s x 4, 4H, meso), 4.09 - 3.95 (m, 8H, pyr-CH_2CH$_3$), 3.64, 3.63, 3.59, 3.49 (s x 4, 12H, pyr-CH$_3$), 1.96 - 1.75 (m, 12H, pyr-CH$_2$CH_3), 0.64 (q, 2H, *N*-CH$_2$CH_2OH), -0.76 (br, 1H, *N*-CH$_2$CH$_2$O*H*), -4.97 (t, 2H, *N*-CH_2CH$_2$OH).

***N*-(2-hydroxyethyl)etioporphyrin (4a)**. To a CH_2Cl_2 solution (5 mL) of the zinc complex (**4b**) (50 mg) was added trifluoroacetic acid (1mL). After stirring for 30 min, the reaction mixture was neutralized with aq. ammonia, and the organic layer separated was washed with saturated aq. NaCl, dried over anhydrous Na2SO4, and evaporated to dryness under reduced pressure at room temperature to give free-base porphyrin (**4a**) quantitatively as a purple powder. FAB-HRMS for $C_{34}H_{43}N_4O$ (MH^+): calcd m/z 523.3423; obsd 523.3433. UV-vis λmax, nm (log ε): 641 (3.43), 585 (3.69), 535 (3.80), 505 (4.03), 409 (5.00)

Chloro(*N*-((*RS*)-2-hydroxypropyl)etioporphyrinato)zinc (5b). 5b was prepared in 78 % yield from **1b** and racemic propylene oxide in a manner similar to that described for the preparation of **4b**. UV-vis λmax , nm (log ε): 623 (3.49), 581 (4.00), 540 (3.88), 433 (5.01), 423 (5.06), 353 (4.32). ^{1}H NMR (diastereoisomeric mixture): δ 10.35 - 10.18 (m, 4H, meso), 4.12 - 4.00 (m, 8H,

pyr-CH_2CH_3), 3.64 - 3.45 (m, 12H, pyr-CH_3), 1.96 - 1.66 (m, 12H, pyr-CH_2CH_3), 0.64 (m, 2H, *N*-$CH_2CH(CH_3)OH$), -0.41, -0.47 (d x 2, 1H, diastereoisomeric *N*-$CH_2CH(CH_3)OH$), -0.11, -1.15 (d x 2, 3H, diastereoisomeric *N*-$CH_2CH(CH_3)OH$), -5.20 - -4.92 (m, 2H, *N*-$CH_2CH(CH_3)OH$).

***N*-((*RS*)-2-Hydroxypropyl)etioporphyrin I (5a).** **5a** was obtained from the corresponding zinc complex **5b** in a manner similar to that described for the preparation of **4a**. FAB-HRMS for $C_{34}H_{43}N_4O$ (MH^+): calcd m/z 537.3593; obsd 537.3621. UV-vis λmax, nm (log ε): 642 (3.37), 584 (3.68), 536 (3.78), 505 (3.96), 409 (4.96).

Chloro(*N*-((*R*)-2-hydroxy-2-phenylethyl)etioporphyrinato)zinc ((*R*)-6b) and Chloro(*N*-((*S*)-2-hydroxy-2-phenylethyl)etioporphyrinato)zinc ((*S*)-6b.) (*R*)-**4b** and (S)-**4b** was prepared in 76 % yield from **1b** and (*R*)-styrene oxide and (*S*)-styrene oxide, respectively, in a manner similar to that described for the preparation of **2b**. UV-vis λmax, nm (log ε): 622 (3.45), 583 (3.89), 542 (3.81), 434 (4.86), 424 (4.94), 346 (4.25). ^{1}H NMR: for (*R*)-**6b**-[FI] and (*S*)-**6b**-[FII]: δ 10.38, 10.09 (s x 2, 2H, meso), 10.15 (s, 2H, meso), 6.79 (t, 1H, *p*-C_6H_5), 6.65 (dd, 2H, *m*-C_6H_5), 5.49 (d, 2H, *o*-C_6H_5), 4.12 - 3.75 (m, 8H, pyr-CH_2CH_3), 3.66, 3.64, 3.57, 3.33 (s x 4, 12H, pyr-CH_3), 1.96 - 1.75 (m, 12H, pyr-CH_2CH_3), 0.96 (m, 2H, *N*-$CH_2CH(C_6H_5)OH$), 0.09 (br, 1H, *N*-$CH_2CH(C_6H_5)OH$), -4.95 - -4.70 (m, 2H, *N*-$CH_2CH(C_6H_5)OH$); for (*R*)-**6b**-[FII] and (*S*)-**6b**-[FI]: δ 10.32, 10.15, 10.13, 10.12 (s x 4, 4H, meso), 6.76 (t, 1H, *p*-C_6H_5), 6.61 (dd, 2H, *m*-C_6H_5), 5.43 (d, 2H, *o*-C_6H_5), 4.10 - 3.76 (m, 8H,

pyr-CH_2CH_3), 3.62, 3.59, 3.56, 3.44 (s x 4, 12H, pyr-CH_3), 1.96 - 1.75 (m, 12H, pyr-CH_2CH_3), 0.92 (m, 2H, *N*-$CH_2CH(C_6H_5)OH$), 0.10 (br, 1H, *N*-$CH_2CH(C_6H_5)OH$), -4.93 - -4.67 (m, 2H, *N*-$CH_2CH(C_6H_5)OH$).

***N*-((*R*)-2-hydroxy-2-phenylethyl)etioporphyrin I ((*R*)-6a) and *N*-((*S*)-2-hydroxy-2-phenylethyl)etioporphyrin I ((*S*)-6a)** (*R*)-6a ((*S*)-6a) was obtained from the corresponding zinc complex (*R*)-**6b** ((*S*)-**6b**) in a manner similar to that described for the preparation of **4a**. FAB-HRMS for $C_{34}H_{43}N_4O$ (MH^+): calcd m/z 599.3750; obsd 599.3752. UV-vis λmax, nm (log ε): 643 (3.24), 585 (3.69), 538 (3.77), 506 (3.83), 408 (4.90).

Chloro(*N*-styryletioporphyrinato)zinc (8b). To a pyridine solution of (5 mL) of the free-base porphyrin (*R*)-**6a** or (*S*)-**6a** (20 mg) was added methanesulfonyl chloride (3 drops). After stirring for 40 h at room temperature, the reaction mixture was poured into 2N HCl (20 mL) and extracted with $CHCl_3$. The organic layer separated was successively washed saturated aq. $NaHCO_3$ and aq. NaCl, dried over anhydrous Na_2SO_4, and filtered out. The filtrate was evaporated to dryness under reduced pressure, and the residue dissolved in a minimum volume of $CHCl_3$ was loaded on an alumina column (Merck, Art. 1097) prepared from a $CHCl_3$ slurry. The red fraction eluted with $CHCl_3$ was evaporated to give *N*-styryletioporphyrin I (FAB-HRMS for $C_{34}H_{43}N_4O$ (MH^+): calcd m/z 581.3644; obsd 581.3650), which was converted into the chlorozinc complex and purified as described in the preparation of **4b** to give **8b** (95 % from **6a**). UV-vis λmax, nm (log ε): 628 (3.71), 588 (4.13), 541 (3.97), 429 (5.02), 371 (4.51) ^1H NMR δ 10.40, 10.38,

10.17, 10.16 (s x 4, 4H, meso), 10.15 (s, 2H, meso), 6.25 (t, 1H, *p*-C_6H_5), 6.03 (dd, 2H, *m*-C_6H_5), 4.28 (d, 2H, *o*-C_6H_5), 4.15 - 3.78 (m, 8H, pyr-CH_2CH_3), 3.64, 3.61, 3.59, 3.58 (s x 4, 12H, pyr-CH_3), 1.96 - 1.75 (m, 12H, pyr-CH_2CH_3), 0.96 (d, J = 14 Hz, 1H, *N*-CH=C*H*(C_6H_5)), 0.09 (d, J = 14 Hz, 1H, *N*-C*H*=CH(C_6H_5))

Optical Resolution by HPLC.

Resolutions of the stereoisomers of **4a** - **6a** were carried out by using 0.46 x 250 mm (the analytical column) or 20 x 500 mm (the preparative column) HPLC column packed with silica gel coated with cellulose tris(3,5-dimethylphenylcarbamate) as a chiral stationary phase. HPLC experiments with the analytical column were performed on a JASCO Type TWINCLE equipped with a JASCO Type 875-UV variable wavelength detector at a flow rate of 1.0 mL·min^{-1} at room temperature and monitored at 390 nm. HPLC experiments with the preparative column were performed on a JASCO Type 887-PU pump equipped with a JASCO Type 875-UV variable wavelength detector, a JASCO Type 802-SC system controller, and a JASCO Type 892-01 column selector at a flow rate of 10.0 mL·min^{-1} at room temperature and monitored at 350 nm. The HPLC column pack was prepared by the method reported by Okamoto *et. al.*[10]

Resolution of the Antipodes of 4a. 4a (4 mg) was dissolved in CCl_4 (20 mL), and an aliquot (20 μL) of the solution was subjected to HPLC with the analytical column using hexane/2-propanol/diethylamine (95/5/0.1 v/v/v) as eluent. Two peaks were observed with the retention times of 17.1 (**4a**-[FI])

and 38.9 min (**4a**-[FII]), respectively. For miligram-scale resolution, 3-mL portions of a solution (100 mg of **4a** in 50 mL of eluent) was loaded on the preparative column with hexane/2-propanol/diethylamine (85/15/0.1 v/v) as eluent. The resolved antipodes were converted into chlorozinc complexes, and purified by chromatography on an alumina and recrystallization from CH_2Cl_2 / hexane as described in the preparation of **4b**.

Resolution of the Stereoisomers of 5a. Under similar conditions as for **4a**, two peaks were observed with the retention times of 15.5 ((*R*)-**5a**-[FI] and (*S*)-**5a**-[FI]) and 34.5 min ((*R*)-**5a**-[FII] and (*S*)-**5a**-[FII]).

Resolution of the Stereoisomers of (*R*)-6a. Under similar conditions as for **4a**, two peaks were observed with the retention times of 14.8 ((*R*)-**6a**-[FI]) and 37.8 min ((*R*)-**6a**-[FII]). The miligram-scale resolution was performed as described in the resolution of the antipodes of **4a**.

Resolution of the Stereoisomers of (*S*)-6a. Under similar conditions as for **4a**, two peaks were observed with the retention times of 15.5 ((*S*)-**6a**-[FI]) and 41.2 min ((*S*)-**6a**-[FII]).

Bromozinc complex of (*S*)-*N*-((*R*)-2-(4'-bromobenzoyloxy)-2-phenylethyl)etioporphyrin I ((*R*)-7b-[FI]). To a THF solution (10 mL) of (*R*)-**6b**-[FI] (80 mg) was added 4-bromobenzoyl chloride (350 mg) dissolved in THF (5 mL) and triethylamine (0.5 mL) at room temperature. After stirring for 40 h at 45 °C under dry nitrogen, the reaction mixture was successively washed with 2N aq. NaOH and saturated aq. NaCl, dried over anhydrous Na_2SO_4, and filtered out. The filtrate was evaporated to dryness under

reduced pressure, and the residue dissolved in a minimum volume of $CHCl_3$ was loaded on a silica gel column (Merck, Art. 7734) prepared from a $CHCl_3$ slurry. A violet fraction eluted with $CHCl_3$ containing 10 % MeOH was collected and washed with saturated aqueous NaBr. The separated organic layer was dried over anhydrous Na_2SO_4 and filtered. The filtrate was evaporated to dryness, and the residue was recrystallized from benzene / ethanol / cyclohexane to give (*R*)-**7b**-[FI] as purple needles (65 % yield). UV-vis λmax, nm (log ε): 627 (3.58), 585 (3.97), 542 (3.84), 434 (4.92), 424 (4.98) 346 (4.35). ^{1}H NMR δ 10.29, 10.25, 10.18, 10.16 (s x 4, 4H, meso), 7.81 - 7.67 (m, AA'BB' system, 4H, BrC_6H_4), 6.60 (t, 1H, *p*-C_6H_5), 6.46 (dd, 2H, *m*-C_6H_5), 5.38 (d, 2H, *o*-C_6H_5), 4.20 - 3.90 (m, 8H, pyr-CH_2CH_3), 3.66, 3.64, 3.58, 3.40 (s x 4, 12H, pyr-CH_3), 1.99 - 1.86 (m, 12H, pyr-CH_2CH_3), 0.92 (m, 2H, *N*-$CH_2CH(C_6H_5)O_2C$), -4.87 - -4.39 (m, 2H, *N*-$CH_2CH(C_6H_5)O_2C$)

X-Ray Crystallography.

Intensity data were collected on a Rigaku AFC-5R (rotating anode) diffractometer at 23 °C with Mo Kα (λ = 0.71069 Å) radiation and refined by full-matrix least squares techniques. No crystal decay was observed. Absorption correction was applied based on azimuthal scans of three reflections. The maximum and minimum transmission factors were 1.00 and 0.89, respectively. Out of 8560 reflections observed, as few as 2488 satisfied $I > 3\sigma(I)$, thus only the heavier atoms (*i.e.* Br, Zn, O and N) were refined anisotropically. One of the ethyl substituents (C(40) carbon) was disordered.

The final *R*, *Rw* and GOF were 0.086, 0.116 and 3.89, respectively. All the calculations were carried out on a Vax station 3200 by using the TEXSAN program system (Molecular Structure Corporation, Texas, 1987).

Measurements.

^{1}H NMR spectra were measured in $CDCl_3$ on a JEOL Type GSX-270 spectrometer operating at 270 MHz, where the chemical shifts were determined with respect to internal $CHCl_3$ (δ 7.28). Absorption and spectra were measured in $CHCl_3$ on a JASCO Type U-best 50 spectrometer by using a quartz cell of 1-cm path length. Circular dichroism spectra were recorded on a Jasco Type J-720 spectropolarimeter with the following parameters: sensitivity, 10 mdeg; step resolution, 2 nm / data; response, 4 sec; scan speed, 50 nm·min^{-1}; accumulation, 16 times, using a quartz cell of 1-cm path length; optical density of sample ($CHCl_3$), 2.0 at 424 nm (2.3×10^{-5} M). All the CD spectra were corrected by subtracting those of the corresponding racemates.

References and Notes.

1. Lavallee, D. K. *The Chemistry and Biochemistry of N-Substituted Porphyrins*; VCH: New York, 1987.

2. (a) Ortiz de Montellano, P. R. *Annu. Rep. Med. Chem.* **1984**, *19*, 201. (b) Ortiz de Montellano, P. R.; Correia, M. A. *Annu. Rev. Pharmacol. Toxicol.* **1983**, *23*, 481.

3. (a) Ortiz de Montellano, P. R.; Kunze, K. L.; Beilan, H. S. *J. Biol. Chem.* **1983**, *258*, 45. (b) Kunze, K. L.; Mangold, B. L. K.; Wheeler, C.; Beilan, H. S.; Ortiz de Montellano, P. R. *J. Biol. Chem.* **1983**, *258*, 4202. (c) Ortiz de Montellano, P. R.; Mangold, B. L. K.; Wheeler, C.; Kunze, K. L.; Reich, N. O. *J. Biol. Chem.* **1983**, *258*, 4208. (d) Augusto, O,; Kunze, K. L.; Ortiz de Montellano, P. R. *J. Biol. Chem.* **1982**, *257*, 6231. (e) Ortiz de Montellano, P. R.; Kunze, K. L. *Biochemistry* **1981**, *20*, 7266. (f) Swanson, B. A.; Ortiz de Montellano, P. R. *J. Am. Chem. Soc.* **1991**, *113*, 8146.

4. Kubo, H.; Aida, T.; Inoue, S.; Okamoto, Y. *J. Chem. Soc., Chem. Commun.*, **1988**, 1015.

5. Ortiz de Montellano, P. R.; Beilan, H. S.; Kunze, K. L.; Mico, B. A. *J. Biol. Chem*. **1981**, *256*, 4395.

6. For preparation and characterization of dilithium salts of porphyrins: (a) Arnold, J. *J. Chem Soc., Chem. Commun. 1990*, 976. (b) Buchler, J. W.; De Cian, A.; Fischer, J.; Hammerschmitt, P.; Weiss, R. *Chem. Ber.* **1991**, *124*, 1051.

7. This method is applicable for *N*-2-hydroxyalkylation of porphyrins carrying other peripheral substituents such as octaethylporphyrin ($OEPH_2$), tetraphenylporphyrin ($TPPH_2$), and 2,7,12,17-tetramesityl-3,8,13,18-tetramethylporphyrin.

8. Cavaleiro, J. A. S.; Condesso, M. F. P. N.; Jackson, A. H.; Neves, M. G. P. M. S.; Rao, K. R. N.; Sadashiva, B. K. *Tetrahedron Lett.*, **1984**, *25*, 6047. Another conventional method utilizing cobalt porphyrins (Setsune, J.; Dolphin, D. *J. Org. Chem*. **1985**, *50*, 2958) involves multi-step redox process, and not convenient for large-scale synthesis.

9. Evans, B.; Smith, K. M. *Tetrahedron* **1977**, 32, 629.

10. (a) Okamoto, Y.; Hatada, K. *Chem. Lett.* **1986**, 1237. (b) Okamoto, Y.; Kawashima, M; Hatada, K. *J. Chromatogr.* **1986**, 363, 173.

CHAPTER 2

Stereochemical Studies on Reversible Metal - Nitrogen Transfer of Alkyl and Aryl Groups in Chiral Cobalt(III) Porphyrins.

Abstract

Resolution of the antipodes of chiral σ-alkyl- and σ-aryl-cobalt(III) complexes of etioporphyrin I was first achieved, where the latter was shown to be much more stable than the former toward thermal racemization. Use of these antipodes for stereochemical studies on the mechanism of reversible cobalt - nitrogen transfer of alkyl and aryl groups in cobalt porphyrins revealed that the transfers from cobalt to nitrogen and from nitrogen to cobalt both take place in intramolecular fashions.

Introduction

During the xenobiotic metabolism of phenylhydrazine, the prosthetic group of hemoproteins is denaturated into an abnormal green pigment, which has been identified as *N*-phenylprotoporphyrin IX.[1] Ortiz de Montellano *et. al.* have demonstrated that this reaction occurs *via* the transient formation of a protein-stabilized intermediate bearing a σ-phenyl - iron bond (**Scheme 1 (A)**). Model studies have demonstrated that σ-aryl groups bonded to iron(III) porphyrins undergo oxidative transfer reaction to the pyrrole nitrogen upon aerobic acid workup, giving the corresponding N-substituted porphyrins (**Scheme 1 (B)**).[2] Furthermore, iron(II) *N*-substituted porphyrins, possible

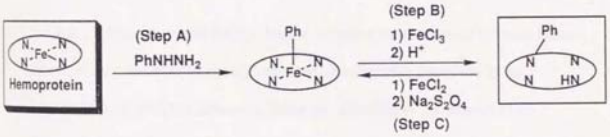

Scheme 1

intermediate species for the formation of the iron-free *N*-substituted porphyrins, can revert to the parent organoiron(III) porphyrins by reductive transfer in the presence of sodium dithionite (**Scheme 1 (C)**).[3] A similar reversible transfer occurs in the case of cobalt porphyrins[4-6] (**Scheme 2**), which

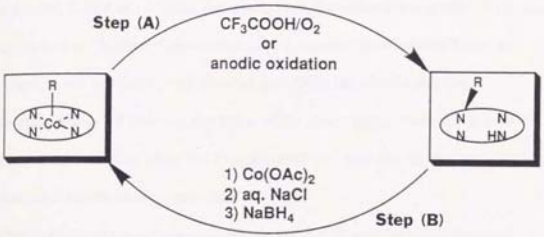

Scheme 2

has been extensively studied by double labeling method coupled with mass spectrometry in order to clarify whether the transfer proceeds in an intramolecular or intermolecular fashion. Dolphin *et. al.* observed no deuterium scrambling when the mixture of ethyl(tetraphenylporphinato) cobalt(III) and ethyl-d_5-(*2,3,7,8,12,13,17,18*-d_8-tetraphenylporphinato)cobalt(III) was subjected to electrochemical oxidative transfer, but a considerable scrambling when the mixture of (*N*-ethyltetraphenylporphinato)cobalt(II) and (*N*-ethyl-d_5-2,3,7,8,12,13,17,18-d_8- tetraphenylporphinato)cobalt(II) was subjected to reductive transfer with $NaBH_4$, and concluded that the oxidative

cobalt to nitrogen transfer (**Step (A)**) occurs *intramolecularly*, while the reductive nitrogen to cobalt transfer (**Step (B)**) occurs *intermolecularly*.[4] On the other hand, Callot *et. al.* later reinvestigated the reductive transfer using the combination of (*N*-phenyl-d_5-tetraphenyl-d_{20}-porphinato)cobalt(II) and its nondeuterated analogue, and claimed that **Step (B)** should also occur *intramolecularly*. This is on the basis of the observations that the degree of deuterium scrambling after the transfer reaction depends on the heating time of the mass spectrometry, and that o-phenyl-d_5-(tetraphenyl-d_{20}-porphinato)cobalt(III) and its nondeuterated analogue scrambles only by subjecting the mixture to mass spectroscopy.[5] Therefore, to date, the consensus has been given only for the *intramolecular* mechanism of the oxidative cobalt to nitrogen transfer (**Step (A)**), while the mechanism of the reductive nitrogen to cobalt transfer (**Step (B)**) has remained ambiguous due to the thermal lability of the cobalt - carbon bonds in organocobalt(III) porphyrins.

In the present paper, the author wish to provide a conclusive answer to the transfer mechanism by a novel approach using cobalt(II) complexes of chiral *N*-substituted etioporphyrins I (**2**) and chiral organocobalt(III) etioporphyrins I (**3**). Etioporphyrin I is of C_{4h} symmetry due to the alternating arrangement of the methyl and ethyl groups along the periphery of the porphyrin ring, and has enantiotopic faces (prochiral). Therefore, *N*-substituted etioporphyrins I and

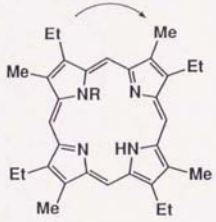

1a **R = Me**
1b **R = Et**
1c **R = Ph**

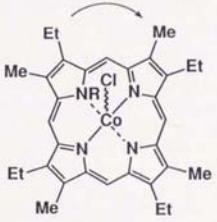

2a **R = Me**
2b **R = Et**
2c **R = Ph**

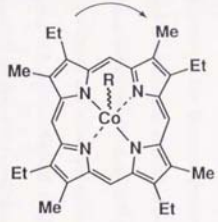

3a **R = Me**
3b **R = Et**
3c **R = Ph**

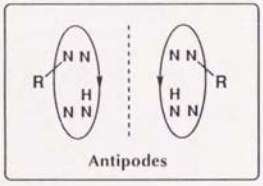

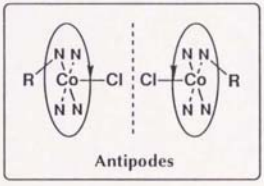

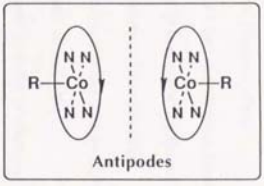

cobalt(III) etioporphyrins I should be chiral due to the presence of the *N*-substituents and/or the axial groups on either of the two enantiotopic faces. the author have recently succeeded in the resolution of the optical antipodes of *N*-methyletioporphyrin I (**1a**) by HPLC.[7] This achievement prompted the author to attempt the resolution of the optical antipodes of other *N*-substituted homologous and organocobalt(III) etioporphyrins I, and to study the stereochemical course of the reversible cobalt - nitrogen transfer of alkyl and aryl groups in these chiral cobalt porphyrins.

Results and Discussion

Resolution and Thermal Stability of the Optical Antipodes of Chiral Organocobalt(III) Etioporphyrins I (3a - 3c). The antipodes of a series of chiral organocobalt(III) etioporphyrins I (**3a - 3c**) were successfully resolved by HPLC on silica gel coated with cellulose tris(3,5-dimethylphenylcarbamate) with hexane/2-propanol (97/ 3 v/v) as eluent.[7] For example, phenyl(etioporphyrinato)cobalt(III) (**3c**) showed two elution peaks (**[F1]** and **[F2]**, the first and second fractions, respectively) with comparable peak areas (**Figure 1**), whose circular dichroism spectra were perfect mirror image of each other (**Figure 2**).

The antipodes of **3c** are very reluctant to undergo thermal racemization. When a hexane/2-propanol (99/1 v/v) solution of the antipode **[F1]** was kept at 60 °C for 4 h and analyzed by HPLC, no peak corresponding to the antipode **[F2]** appeared (**Figure 3 (A)**). Quite surprisingly, no racemization was observed even upon refluxing in toluene for 24 h. In contrast, for obtaining the antipodes of the ethyl homologue (**3b**) in optically pure forms, it is necessary to collect the eluates in test tubes kept in the dark at a low temperature such as -78 °C. The antipode **3b-[F1]** hardly underwent racemization below 30 °C in hexane/2-propanol (99/1 v/v), but gradually racemized at a higher temperature such as 47 °C, where the enantiomeric excess (*ee*) decreased to 69 and 9 % in 25 and 100 min, respectively (**Figure 3 (B)**). Compared with the ethyl and phenyl

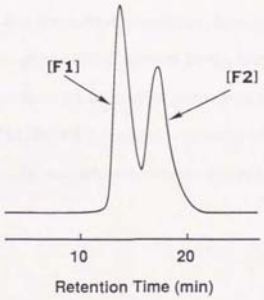

Figure 1. HPLC profile of phenyl(etioporphyrinato)cobalt(III) (**3c**) with analytical column (see **Experimental Section**) at a flow rate of 0.5 mL·min^{-1} using hexane/2-propanol (97/3 v/v) as eluent at room temperature monitored at 390 nm. **[F1]** and **[F2]** denote the first and second eluted fractions, respectively.

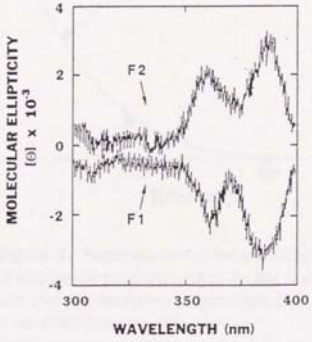

Figure 2. CD spectra of the antipodes of phenyl(etioporphyrinato)cobalt(III) (**3c**) in CH_2Cl_2 (5.9 x 10^{-6} M) in a quartz cell of 1-cm path length.

homologues (**3b, 3c**), the methyl homologue (**3a**) appears to racemize much more easily. Although the HPLC pattern for the methyl homologue (**3a**) was almost the same as those for **3b** and **3c**, reanalysis of the eluate corresponding to the antipode [**F1**] (**3a**-[**F1**]) provided a virtually identical HPLC pattern to that of the racemic **3a** even when the eluate was collected and stored at -78 °C before analysis.

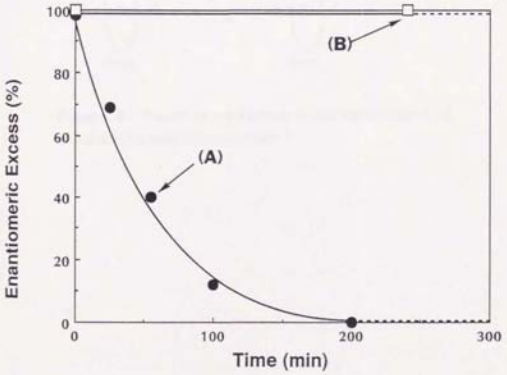

Figure 3. Racemizations of the antipodes ([**F1**]) of ethyl(etioporphyrinato)cobalt(III) (**3b**) at 47 °C (**A**) and phenyl(etioporphyrinato)cobalt(III) (**3c**) at 60 °C (**B**) in hexane/2-propanol (99/1 v/v).
Enantiomeric excess (*ee*) was determined by HPLC.

Racemization of the alkyl complexes of cobalt(III) etioporphyrin I (**3a, 3b**) possibly occurs *via* thermal homolysis of the σ-alkyl - cobalt bond followed by recombination of the resulting alkyl radical and cobalt(II) porphyrin (**Figure 4**).[8] Therefore, the σ-aryl - cobalt bond in cobalt(III) porphyrin is much more stable than the corresponding σ-alkyl - cobalt bond toward thermal homolysis.

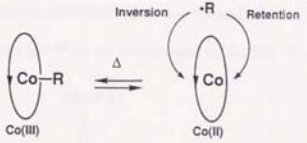

Figure 4. Plausible mechanism of the racemization of chiral alkylcobalt(III)etioporhyrin I.

Stereochemical Profiles of the Transfer Reactions Between Nitrogen and Cobalt. To investigate the stereochemical course of the transfer reactions (**Scheme 3**), the antipode of chiral chloro(*N*-ethyletioporphyrinato)cobalt(II) (**2b-[F1]** (**X = Cl**)), derived from optically pure *N*-ethyletioporphyrin I (**1b-[F1]**; (**I**) in **Figure 5**),[7] was treated with $NaBH_4$ in THF/EtOH at -10 °C for 5 min (**Step (B)**), where ethyl(etioporphyrinato)cobalt(III) (**3b**) was formed with only a slight decrease in enantiomeric excess (80 % *ee*, as determined by HPLC; (**II**) in **Figure 5**; peak

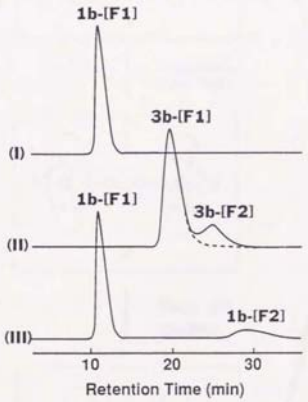

Figure 5. HPLC profiles of the starting *N*-ethyletioporphyrin I (**1b-[F1]**) (**I**), ethyl(etioporphyrinato)cobalt(III) (**3b**) formed by the reductive transfer (**Step (B)**) (**II**), and **1b** reproduced by the subsequent oxidative transfer (**Step (A)**) (**III**). Eluents: Hexane/2-propanol/diethylamine (95/5/0.1 v/v) (flow rate: 1.0 mL·min^{-1}) for (**I**) and (**III**), hexane/2-propanol (97/3) (flow rate: 0.5 mL·min^{-1}) for (**II**).

area ratio of **[F1]** and **[F2]** being 9 : 1). It is likely that the racemization observed here is not associated with the transfer reaction but due to the lability of the cobalt - carbon bond of the product **3b**, since optically pure **3b** was

Scheme 3

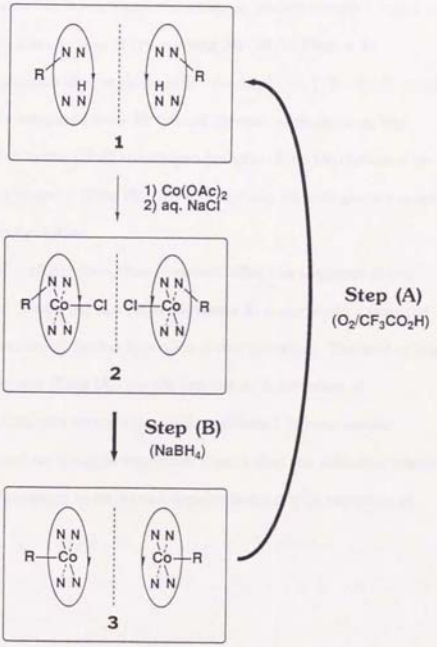

observed to racemize to the same degree after stirring for 5 min in THF/EtOH at -10 °C in the presence of $NaBH_4$. When the 9 : 1 mixture of the antipodes of **3b** thus obtained after the transfer reaction was treated with CF_3CO_2H in CH_2Cl_2 at room temperature (~20 °C) under aerobic condition (**Step (A)**), *N*-ethyletioporphyrin I (**1b**) was produced without any decrease in enantiomeric excess (80 % *ee*), where the antipode predominantly formed had the same configuration as that of the starting **2b** ((**III**) in **Figure 5**).

When the antipode of phenylcobalt(III) etioporphyrin I (**3c-{F1}**), which is much more stable compared with **3b** toward thermal racemization, was similarly subjected to the cobalt to nitrogen transfer (**Step (A)**) followed by nitrogen to cobalt transfer (**Step (B)**), **3c** was reproduced with perfect retention of the original configuration.

Retention of configuration, thus observed, after the sequence of two transfer reactions (**Steps (A)** and **(B)** in **Scheme 3**) is obviously a result of either double retention or double inversion of configuration. The acid-catalyzed oxidative transfer step (**Step (A)**) should proceed with retention of configuration, taking into account the well-established *intramolecular* mechanism. Therefore, it can be concluded clearly that the reductive transfer step (**Step (B)**) also occurs in an *intramolecular* fashion with retention of configuration.

Experimental Section

Materials. Tetrahydrofuran (THF) and benzene (C_6H_6) were distilled over sodium benzophenone ketyl just before use. Ethanol (EtOH) was distilled over Mg treated with iodine and stored over molecular sieves 4A. Phenyllithium (2.0 M in cyclohexane/ether (70/30 v/v, Aldrich) was used as received. Etioporphyrin I (EtioPH$_2$) was synthesized from *tert*-butyl 4-ethyl-3,5-dimethylpyrrole-2-carboxylate and recrystallized from chloroform ($CHCl_3$)/methanol (MeOH).[9] Pyridinobromocobalt(III) etioporphyrin I was prepared according to the procedure reported by Dolphin and Johnson.[10]

***N*-Methyletioporphyrin (1a).** In a 500-mL round bottom flask equipped with a reflux condenser were placed etioporphyrin I (1.20 g , 2.5 mmol), $CHCl_3$ (200 mL), methyl iodide (10 mL), and acetic acid (25 mL), and the mixture was stirred at 55 °C. After 40 h, the reaction mixture was poured into saturated aq. $NaHCO_3$. The organic layer separated was washed successively with aq. ammonia (28 %) and saturated aq. NaCl, dried over anhydrous Na_2SO_4, and evaporated to dryness. The residue dissolved in a minimum volume of dichloromethane (CH_2Cl_2)/hexane (50/50 v/v) was loaded on an alumina column (Merck, Art. 1097, activity II ~ III) prepared from hexane slurry. Unreacted etioporphyrin I was first eluted with CH_2Cl_2/hexane (50/50 v/v) as a red band. The second violet band eluted with CH_2Cl_2 was concentrated to a small volume

(ca. 50 mL) and then heptane (100 mL) was added. The mixture was slowly evaporated to leave a dark purple powder, which was identified as **1a** (0.75 g, 61 % yield) by absorption and ^{1}H NMR spectra.[11]

***N*-Ethyletioporphyrin I (1b).** EtioPH$_2$ (200 mg, 0.42 mmol), $CHCl_3$ (20 mL), ethyl iodide (20 mL), and acetic acid (1 mL) were added at room temperature to a 100-mL glass tube, which was then sealed and placed in an oil bath thermostated at 90 °C. After 7 days, the tube was opened and the reaction mixture was poured into saturated aq. $NaHCO_3$. The organic layer separated was treated similarly to the case for **1a**, affording **1b** (98 mg, 47 % yield) as a dark purple powder. HRMS Calcd for $C_{34}H_{43}N_4$ (MH^+), m/z 507.3488, obsd m/z 507.3475. UV-vis: λmax (log ε) 406 (4.95), 505 (3.90), 538 (3.71), 584 (3.63), 641 (3.27). ^{1}H NMR: δ10.11 (s, 2H, meso), 9.96 (s, 2H, meso), 3.83 - 3.98 (m, 8H, pyr-C*H*$_2$CH$_3$), 3.66 - 3.27 (s x 4, 12H, pyr-CH$_3$), 1.88 - 1.42 (m, 8H, pyr-CH$_2$C*H*$_3$), -2.32 (t, 3H, *N*-CH$_2$C*H*$_3$), -3.22 (br, 1H, NH), -5.22 (q, 2H, *N*-C*H*$_2$CH$_3$).

Chloro(*N*-methyletioporphyrinato)cobalt(II) (2a). To a 50-mL round bottom flask containing a CH_2Cl_2 solution (5 mL) of **1a** (200 mg, 0.41 mmol) were added an acetonitrile (CH_3CN) suspension (30 mL) of $CoCl_2$·6H_2O (380 mg, 1.6 mmol) and 2 drops of 2,6-di-*tert*-butylpyridine. After the mixture was stirred at room temperature for 2 h, the solvent was removed under reduced pressure. The residue dissolved in CH_2Cl_2 (12 mL) was washed successively

with water and saturated aq. NaCl, dried over anhydrous Na_2SO_4, and filtered. The filtrate was evaporated to dryness under reduced pressure and the residue dissolved in a minimum volume of $CHCl_3$ was loaded on an alumina column (Merck, Art. 1097, activity II ~ III) prepared from $CHCl_3$ slurry. A green fraction eluted with $CHCl_3$/MeOH (90/10 v/v) was collected and washed with saturated aq. NaCl. The organic layer separated was dried over anhydrous Na_2SO_4 and filtered. The filtrate was evaporated to dryness and the residue was recrystallized from $CHCl_3$/ether to give **2a** (178 mg, 78% yield) as purple crystals. Anal. Calcd for $C_{33}H_{39}N_4CoCl \cdot H_2O$: C, 67.63; H, 6.71; N, 9.56. Found: C, 67.35; H, 6.92; N, 9.28. UV-vis: λmax (log ε) 309 (4.14), 389 (4.64), 424 (4.78), 540 (3.80), 585 (3.91). ^{1}H NMR:[12] δ43.59, 31.91, 21.81, 18.61 (s x 4, 12H, pyr-CH_3), 38.23, 29.05, 28.35, 22.93, 21.32, 20.93, 18.61, 17.03 (s x 8, 8H, pyr-CH_2CH_3), 12.87, 10.86, -4.41, -4.98 (s x 4, 4H, meso), 11.64, 9.23, 8.17, 4.81 (s x 4, 12H, pyr-CH_2CH_3), -56.87 (s, 3H, *N*-CH_3).

Chloro(*N*-ethyletioporphyrinato)cobalt(II) (2b). **2b** was prepared in 85 % yield from **1b** in a similar manner to that described for the preparation of **2a**. Anal. Calcd for $C_{34}H_{41}N_4CoCl \cdot H_2O$: C, 66.07; H, 7.01; N, 9.06. Found: C, 66.30; H, 6.86; N, 8.80. UV-vis: λmax (log ε) 310 (4.18), 383 (4.67), 427 (4.85), 542 (3.84), 585 (3.96). ^{1}H NMR:[12] δ40.88, 29.67, 20.24, 16.66 (s x 4, 12H, pyr-CH_3), 35.66, 26.41, 26.08, 19.84, 18.99, 18.42, 16.22, 15.49 (s x 8, 8H, pyr-CH_2CH_3), 10.02, 7.66, -5.68, -6.37 (s x 4, 4H, meso), 9.65, 6.39, 5.70, 2.62 (s

x 4, 12H, pyr-CH_2CH_3), -44.80 (s, 3H, *N*-CH_2CH_3), -121.33 (br, 2H, *N*-CH_2CH_3).

Chloro(*N*-phenyletioporphyrinato)cobalt(II) (2c). To a 50-mL round bottom flask containing an aerated CH_2Cl_2 solution (14 mL) of phenyl(etioporphyrinato)cobalt(III) (**3c**, preparation: see below) (70 mg, 110 μmol) was added CF_3CO_2H (7 mL) at room temperature. The color of the solution turned rapidly from red to green. The reaction mixture, after stirring for 30 min at room temperature, was neutralized with aq. ammonia (28 %). The organic layer separated was washed with saturated aq. NaCl, dried over anhydrous Na_2SO_4, and evaporated to dryness under reduced pressure. To the residue dissolved in CH_2Cl_2 (2 mL) was added an CH_3CN suspension (10 mL) of $Co(O_2CCH_3)_2{\cdot}4H_2O$ (150 mg, 602 μmol), and the mixture was stirred for 30 min at room temperature. After the solvent was removed, the residue was dissolved in CH_2Cl_2, and the solution was washed successively with water and saturated aq. NaCl, dried over anhydrous Na_2SO_4 followed by filtration. The filtrate was evaporated to dryness, and the residue was chromatographed on alumina (Merck, Art. 1097, activity II ~ III). Unreacted **3c** was eluted as a red band with $CHCl_3$. When the eluent was changed to $CHCl_3$/MeOH (90/10 v/v), a green band was eluted, which after evaporation to dryness gave **2c** (35 mg, 49 % yield) as purple crystals. UV-vis: λmax (log ε) 308 (4.21), 384 (4.74), 425 (4.89), 538 (3.90), 586 (4.03). ^{1}H NMR:[12] δ41.23, 29.58, 20.85, 16.40 (s x 4, 12H, pyr-CH_3), 35.90, 26.82, 26.08, 19.60, 19.31, 18.91, 16.40, 15.22 (s x 8, 8H,

pyr-CH_2CH_3), 10.92, 8.83, -6.42, -7.08 (s x 4, 4H, meso), 9.56, 6.16, 5.61, 2.81 (s x 4, 12H, pyr-CH_2CH_3), 1.50 (s, 3H, C_6H_5, m-H and p-H), -57.60 (s, 2H, C_6H_5, o-H).

Methyl(etioporphyrinato)cobalt(III) (3a). To a 300-mL round bottom flask equipped with a three-way stopcock containing chloro(*N*-methyletioporphyrinato)cobalt(II) (**2a**) (35 mg, 60 μmol) and $NaBH_4$ (60 mg), THF (100 mL) was added under dry nitrogen at room temperature, and the mixture was stirred in the dark for 1 h. Then, the solvent was removed under reduced pressure at room temperature and the residue dissolved in a minimum volume of CH_2Cl_2 was loaded on a dry silica gel column (silica gel 60; Merck, Art. 7734). A red fraction eluted with CH_2Cl_2 was collected in a flask kept in the dark and evaporated to dryness under reduced pressure at room temperature. Recrystallization of the residue from CH_2Cl_2/hexane gave a reddish brown powder, which was identified to be **1a** (28 mg, 94 % yield) by ^1H NMR and absorption spectra.[10]

Ethyl(etioporphyrinato)cobalt(III) (3b). **3b** was similarly prepared from chloro(*N*-ethyletioporphyrinato)cobalt(II) (**2b**) in 95 % yield, and identified by ^1H NMR and absorption spectra.[10]

Phenyl(etioporphyrinato)cobalt(III) (3c). To a 50-mL round bottom flask fitted with a three-way stopcock containing a C_6H_6 suspension (5 mL) of pyridinobromocobalt(III) etioporphyrin I (50 mg, 65 μmol), an ether/cyclohexane

(70/30 v/v) solution (0.2 mL) of phenyllithium (400 μmol) was dropwise added under dry nitrogen, and the mixture was stirred at room temperature. After 6 min, MeOH (10 mL) was added, and the resulting solution was slowly concentrated to a small volume to give a reddish brown powder, which was identified to be **1c** (23 mg, 56 % yield) by ^{1}H NMR and absorption spectra.[10]

Procedures.

Optical Resolution by HPLC.

Resolutions of the optical antipodes of **1a - 1b** and **3a - c** were carried out by using 0.46 x 250 mm (the analytical column) or 20 x 500 mm (the preparative column) HPLC column packed with silica gel coated with cellulose tris(3,5-dimethylphenylcarbamate) as a chiral stationary phase. HPLC experiments with the analytical column were performed on a JASCO Type TWINCLE equipped with a JASCO Type 875-UV variable wavelength detector at a flow rate of 0.5 or 1.0 mL·mi*N*·$^{-1}$ at room temperature and monitored at 390 nm. HPLC experiments with the preparative column were performed on a JASCO Type 887-PU pump equipped with a JASCO Type 875-UV variable wavelength detector, a JASCO Type 802-SC system controller, and a JASCO Type 892-01 column selector at a flow rate of 10.0 mL·min^{-1} at room temperature and monitored at 350 nm. The HPLC column pack was prepared by the method reported by Okamoto *et. al.*[13]

Resolution of the Antipodes of 1b. **1b** (4 mg) was dissolved in CCl_4 (20

mL), and an aliquot (20 μL) of the solution was subjected to HPLC with the analytical column using hexane/2-propanol/diethylamine (95/5/0.1 v/v/v) as eluent at a flow rate of 1.0 mL·min^{-1}. Two peaks were observed with the retention times of 10.9 (**1b-[F1]**) and 28.6 min (**1b-[F2]**), respectively. For miligram-scale resolution, 3-mL portions of a solution (100 mg of **1b** in 50 mL of CCl_4) was loaded on the preparative column with hexane/2-propanol/diethylamine (85/15/0.1 v/v) as eluent.

Resolution of the Antipodes of 3a. A 10-μL portion of a CCl_4 solution of **3b** (2 mg/20 mL) was subjected to HPLC resolution with the analytical column using hexane/2-propanol (97/3 v/v) as eluent at a flow rate of 1.0 mL·min^{-1}. Two peaks were observed with the retention times of 6.3 (**3a-[F1]**) and 7.4 min (**3a-[F2]**), respectively. However, the isolation of the antipodes in optically pure forms was unsuccessful due to rapid racemization (see text).

Resolution of the Antipodes of 3b. Under similar conditions as for **3a** at a flow rate of 0.5 mL·min^{-1}, two peaks were observed with the retention times of 19.7 (**3b-[F1]**) and 24.8 min (**3b-[F2]**), respectively. An eluate containing **3b-[F1]** was collected in a test tube kept in the dark at -78 °C, and the volatile fraction was stripped off by bubbling nitrogen gas at 0 °C. Reanalysis of the residue dissolved in toluene or hexane/2-propanol (97/3 v/v) gave a single peak with the retention time of 19.7 min, demonstrating the 100 % enantiomeric excess (*ee*) of the antipode.

Resolution of the Antipodes of 3c. Under the same conditions as for **3b**, two peaks with the retention times of 13.3 and 16.9 min were observed (**Figure 1**). A milligram-scale resolution of the antipodes of **3c** was carried out similarly to that for **1b** using the preparative column with hexane/2-propanol (95/5 v/v) as eluent, where 2-mL portions of a CCl_4 solution of **3c** (30 mg /50 mL) were injected repeatedly.

Transfer of Ethyl Group Between Nitrogen and Cobalt.

$NaBH_4$ (5 mg, 132 μmol) was added at -10 °C under dry nitrogen to a 20-mL Schlenk tube containing a deoxygenated THF/EtOH (40/60 v/v) solution (2 mL) of the antipode (**[F1]**) of chloro(*N*-ethyletioporphyrinato)cobalt(II) (**2b**) (10 mg, 17 μmol) derived from optically pure *N*-ethyletioporphyrin I (**1b-[F1]**). After the complete consumption of **2b**, as determined by thin layer chromatography, the mixture was taken down to dryness at -10 °C under reduced pressure. A small aliquot of the resulting **3b** was dissolved in cold CCl_4 (ca. 0 °C), and the solution was subjected to HPLC analysis to determine the enantiomeric excess. To the remaining **3b** dissolved in CH_2Cl_2 at -78 °C was added CF_3CO_2H (0.3 mL), and the mixture was then allowed to expose to air and warm to 20 °C. After stirring for 5 min, the reaction mixture was treated with aq. ammonia (28 %), and the organic layer separated was washed with saturated aq. NaCl, dried over anhydrous Na_2SO_4, and evaporated to dryness under reduced pressure at room temperature. The residue dissolved in

a minimum volume of CH_2Cl_2 was chromatographed on alumina (Merck, Art. 1097, activity II ~ III) with CH_2Cl_2 as eluent. A violet band was collected, and evaporated to dryness to give **1b** (3.4 mg, 41 % based on starting **1b**), which was subjected to HPLC analysis to determine the enantiomeric excess.

Transfer of Phenyl Group Between Nitrogen and Cobalt.

To a 50-mL round bottom flask containing a CH_2Cl_2 solution (7 mL) of the antipode (**[F2]**) of phenyl(etioporphyrinato)cobalt(III) (**3c**) (26 mg, 42 μmol) was added CF_3CO_2H (1 mL) at room temperature, and the the mixture was stirred for 30 min at room temperature under aerobic condition. The reaction mixture was neutralized with aq. ammonia, and the organic layer separated was washed with saturated aq. NaCl, dried over anhydrous $Na2SO_4$, and evaporated to dryness under reduced pressure at room temperature. To the residue dissolved in CH_2Cl_2 (3 mL) was added an CH_3CN suspension (15 mL) of $Co(O_2CCH_3)_2{\cdot}4H_2O$ (78 mg, 313 μmol), and the mixture was stirred at room temperature for 30 min. After the volatile fraction was removed from the reaction mixture, the residue was treated by a similar procedure as described for the preparation of racemic **2c** to give **2c** (10 mg, 35 % yield), which was identified by thin layer chromatography and absorption spectrum. To a 100-mL round bottom flask containing a THF solution (30 mL) of **2c** thus obtained (15 μmol) was added $NaBH_4$ (18 mg, 476 μmol) at room temperature under dry nitrogen, and the mixture was stirred for 1h. The reaction mixture

was treated similarly to the case for **3a** to give **3c** (9 mg, 98 % yield), which was analyzed by HPLC to determine the enantiomeric excess.

Measurements.

^{1}H NMR spectra were measured in $CDCl_3$ on a JEOL Type GSX-270 spectrometer operating at 270 MHz, where the chemical shifts were determined with respect to internal $CHCl_3$ (δ 7.28). Absorption and circular dichroism spectra were measured in CH_2Cl_2 on a JASCO Type U-best 50 spectrometer and a JASCO Type J-500 spectropolarimeter, respectively, by using a quartz cell of 1-cm path length.

Conclusion

The chemistry of chiral compounds is of general interest and significance particularly from a biological standpoint. The present paper describes the first successful resolution of the optical antipodes of chiral organocobalt(III) complexes of etioporphyrin I, where the chirality is arising from the axial bonding of alkyl or aryl group from either side of the two enantiotopic faces of the metalloporphyrin plane. To our knowledge, these are the first C_{4h}-symmetric chiral organometallic compounds to be resolved, whose chirality is provided by labile metal - carbon bonding. From racemization profiles of the antipodes, the cobalt - carbon bond in σ-arylcobalt(III) porphyrin is much more stable than that in the σ-alkylcobalt homologue toward thermal homolysis. The above achievements enabled the author to make a novel stereochemical approach to the mechanism of a biologically important model reaction, the reversible transfer of alkyl (aryl) group between metal and nitrogen in cobalt porphyrins, and to conclude clearly that the transfers from metal to nitrogen and from nitrogen to metal both occur intramolecularly.

References and Notes

1. Lavallee, D. K., *The Chemistry and Biochemistry of N-Substituted Porphyrins*; VCH New York, 1987; pp 261-298. and references cited therein.

2. (a) Ortiz de Montellano, P. R.; Kunze, K. L. *J. Am. Chem. Soc.* **1981**, 103, 6534. (b) Kunze, K. L.; Ortiz de Montellano, P. R. *J. Am. Chem Soc.* **1981**, 103, 4225. (c) Augusto, O.; Kunze, K. L.; Ortiz de Montellano, P. R. *J. Biol. Chem.* **1982**, 257, 6231. (d) Kunze, K. L.; Ortiz de Montellano, P. R. *J. Am. Chem. Soc.* **1983**, 105, 1380. (e) Ortiz de Montellano, P. R.; Kunze, K. L.; Beilan, H. S. *J. Biol. Chem.* **1983**, 258, 45.

3. (a) Mansuy, D.; Battioni, P.; Dupre, D.; Sartori, E. *J. Am. Chem. Soc.* **1982**, *104*, 6159. (b) Battioni, P.; Mahy, J. P.; Gillet, G.; Mansuy, D. *J. Am. Chem. Soc.* **1983**, *105*, 1388. (c) Battioni, P.; Mahy, J. P.; Delaforge, M.; Mansuy, D. *Eur. J. Biochem.* **1983**, *134*, 241. (d) Mansuy, D.; Battioni, P.; Mahy, J. P.; Gillet, G. *Biochem. Biophys. Res. Commun.*, **1982**, *106*, 30.

4. Dolphin, D.; Halko, D. J.; Johnson, E. *Inorg. Chem.* **1981**, *20*, 4348.

5. (a) Callot, H. J.; Schaeffer, E. *Tetrahedron Lett.* **1980**, 21, 1335. (b) Callot, H. J.; Metz, F. *J. Chem. Soc., Chem. Commun.*, **1982**. 947. (c) Callot, H. J.; Metz, F.; Cromer, R. *Nouv. J. Chim.* **1984**, 8, 759.

6. Ogoshi, H.; Watanabe, E.; Koketsu, N.; Yoshida, Z. *J. Chem. Soc., Chem. Commun.*, **1974**, 943.

7. (a) Kubo, H.; Aida, T.; Inoue, S.; Okamoto, Y. *J. Chem. Soc., Chem. Commun.*, **1988**, 1015. (b) Konishi, K.; Miyazaki, K.; Aida, T.; Inoue, S. *J. Am. Chem. Soc.* **1990**, 112, 5639.

8. (a) Abeles, R. H.; Dolphin, D. *Acc. Chem. Res.* **1976**, *9*, 114. (b) Halpern, J. *Acc. Chem. Res.* **1982**, *15*, 238. (c) Halpern, J. *Science*, **1985**, 869. (c) Guilard, R.; Kadish, K .M. *Chem. Rev.* **1988**, *88*, 1121. (d) Tsou, T-T.; Loots, M.; Halpern, J. *J. Am. Chem. Soc.* **1982**, *104*, 623. (e) Geno, M. K.; Halpern, J. *J. Am. Chem. Soc.* **1987**, *109*, 1238.

9. Evans, B.; Smith, K. M. *Tetrahedron* **1977**, 32, 629.

10. (a) Clarke, D. A.; Dolphin, D.; Grigg, R.; Johnson, A. W.; Pinnock, H. A. *J. Chem. Soc. (C)*, **1968**, 881. (b) ref. 5c.

11. McEwen, W. K. *J. Am. Chem. Soc.* **1946**, 68, 711.

12. Assignments were made by reference to those for acetato(N-methyl- or ethyl-octaethylporphinato)cobalt(II) (Aoyagi, K.; Toi, H.; Aoyama, Y.; Ogoshi, H. *Chem. Lett.* **1987**, 467).

13. (a) Okamoto, Y.; Hatada, K. *Chem. Lett.* **1986**, 1237. (b) Okamoto, Y.; Kawashima, M; Hatada, K. *J. Chromatogr.* **1986**, 363, 173.

CHAPTER 3

Photo- and Thermal-induced Conformational Ruffling of Distorted Porphyrin. Optical Resolution and photochemical Behaivor of Chiral 'Armed' Porphyrin Complexes .

Abstract

The optical antipodes of a chiral *meso*-substituted porphyrin, α-pivaloylaminoetioporphyrin I, and its metal complexes of zinc and copper were resolved by HPLC. Racemization (flipping of the amide "arm") took place easily in the free-base form, but the metal complexes were much more reluctant to racemize, the $\Delta G^{\ddagger}$ values at 28.5 °C being 24.2 and 21.7 kcal·mol^{-1} for the zinc and copper complexes, respectively. As for the zinc complex, the racemization was remarkably accelerated under irradiation at Soret- and Q-bands with the quantum yields (Φ) at 28.5 °C, respectively, of 3.3×10^{-3} and 2.5×10^{-3}. In contrast, photoinduced racemization was not observed for the copper complex.

Introduction

Photo- and thermal-induced molecular motions ("ruffling") of tetrapyrrole macrocycles continue to be of general significance and increasing interest. There have been many works concerning the ruffled conformation of porphyrin skeleton in a solid state, which has been extensively studied by X-ray crystallography. However, to date, only limited examples of the "ruffling" phenomena in solution have been reported. Whitten and co-workers have reported the thermal- and photo-induced atropisomerization of the metal complexes of picket-fence porphyrins.[1] In the present chapter, the author wishes to describe the flipping phenomena of the *meso* substituent of porphyrin, as studied by the thermal- and photo-induced racemization profiles of the optical antipodes of a chiral "armed" porphyrin and its metal complexes (1), and provides a novel type of thermal and photoinduced conformational "ruffling" of tetrapyrrole macrocycles.

Results and Discussion

Optical Resolution of Chiral "Armed" Porphyrin Complexes. The "armed" porphyrin (**1**),[2] derived from etioporphyrin I (**2**), is considered to be distorted from the planarity due to the steric repulsion between the *meso* substituent and neighboring β substituents at the periphery .[3] Since **2** has enantiotopic faces (C_{4h} symmetry), the "armed" porphyrin (**1**) should be chiral due to the presence of the "amide arm" on either of the two enantiotopic faces of the porphyrin plane (**Scheme 1**). In fact, the zinc complex **1b** (zinc α-pivaloylaminoetioporphyrin I, (α-PivNHEtioP)Zn) showed two completely

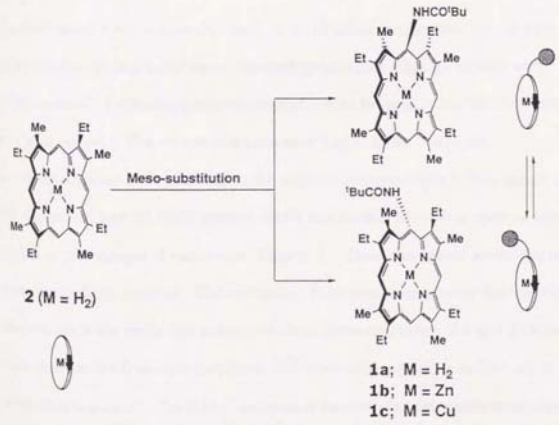

Scheme 1

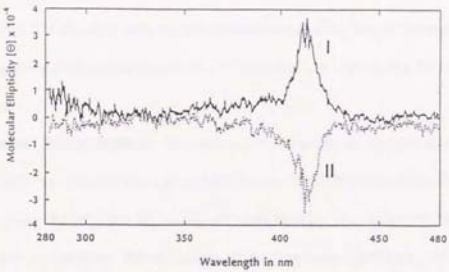

Figure 1. CD spectra of the antipodes of (α-PivNHEtioP)Zn (**1b**) in hexane/EtOH/$CHCl_3$ (70/20/10 v/v). I and II correspond to antipodes I and II in the text, respectively. Spectra were measured by using a quartz cell of 1-cm path length.

resolved peaks with comparable peak areas (fraction I; retention time of 10.9 min., fraction II; 36.5 min.) when chromatographed on silica gel coated with cellulose tris(3, 5-dimethylphenylcarbamate) with hexane/EtOH/$CHCl_3$ (70/20/10 in v/v) as eluent.[4] The compounds corresponding to these two peaks, fractionated, were both identical to the original zinc porphyrin (**1b**) in terms of the absorbtion and ^1H NMR spectra, while the circular dichroism spectra were perfect mirror images of each other (**Figure 1**). Thus, the optical antipodes of **1b** were successfully resolved. The antipodes of the copper porphyrin (**1c**) were also resolved perfectly under the same conditions (retention times, 8.9 and 24.3 min), while those of the free-base porphyrin (**1a**) were only partially resolved (60 % enantiomeric purity). The HPLC analysis of **1a** exhibited two peaks (retention

times, 8.4 and 16.9 min.) with significant tailing and leading in between, indicating the possibility of concomitant racemization during the HPLC separation.

Thermal Racemization. The antipodes of the metal complexes (**1b**) and (**1c**) gradually racemized when stored in hexane/EtOH/$CHCl_3$ (70/20/10 in v/v) at a temperature higher than 20 °C, but no racemization was observed below 0 °C (**Figure 2**).[5] In contrast, the antipodes of the free-base porphyrin (**1a**) are much easier to racemize, since the antipode I with 60 % enantiomeric purity, even when stored at 0 °C, gave in only 1 h an almost identical HPLC pattern as observed for the racemic **1a**. The rate constants for racemization in

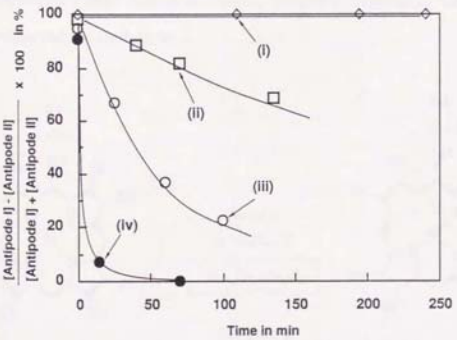

Figure 2. Racemizations of the **antipodes I** of (α-PivNHEtioP)Zn (**1b**) at 0 °C (i), 28.5 °C (ii), 40 °C (iii), and (α-PivNHEtioP)Cu (**1c**) at 28.5 °C (iv) in hexane/EtOH/$CHCl_3$ (70/20/10 in v/v, 7.1 x 10^{-5} M) [**Antipode I**] and [**Antipode II**], as determined by HPLC.

hexane/EtOH/$CHCl_3$ (70/20/10 in v/v) were measured as a function of temperature in range of 0 °C ~ 40 °C, which gave the activation free energies ($\Delta G^{\ddagger}$) of 24.2 and 21.7 kcal·mol^{-1} for the thermal racemization of **1b** and **1c** at 28.5 °C.[6] The racemization takes place *via* the flipping of the "amide arm" from one side of the porphyrin plane to the other through a coplanar transition state possibly as a consequence of a thermally induced conformational ruffling of the porphyrin skeleton (**Scheme 2**). Thus, the above results indicate that the insertion of metal atom into the porphyrin core provides the porphyrin skeleton with an enhanced rigidity, so that the thermally induced ruffling is much restrained compared with the free-base form. Zinc porphyrins appear to be conformationally more rigid than copper porphyrins, considering the higher $\Delta G^{\ddagger}$ value observed for **1b** than **1c**.

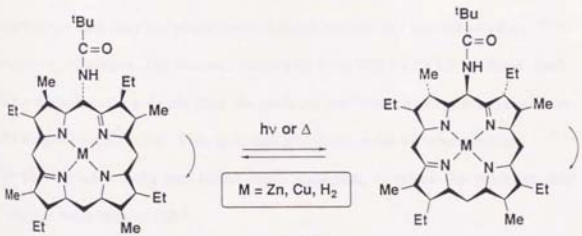

Scheme 2

Photoinduced Racemization. Of greater interest is the photoinduced racemization phenomenon observed for the antipodes of (α-PivNHEtioP)Zn (**1b**). As exemplified in **Figure 3**, the enantiomeric purity (enantiomeric excess, *e.e.*) of the antipode (fraction I) of **1b** was decreased rapidly with time when the degassed solution of the antipode (solvent: hexane/EtOH/$CHCl_3$ (70/20/10 in v/v), 7.1×10^{-5} M) at 28.5 °C was exposed to monochromatized light with a wavelength of 410 nm corresponding to the Soret band,[7] and complete racemization was attained in only 30 min. In contrast, it took more than two days in the dark to achieve the complete racemization under the same conditions. A quite similar photoinduced racemization was also observed when the antipode of **1b** was irradiated at the Q-band (580 nm).[7] The quantum yields (Φ) at the initial stage upon irradiation at Soret- and Q-bands were 3.3×10^{-3} and 2.5×10^{-3}, respectively, during the initial 3 min. at 28.5 °C.[8] Taking into account the fact that the photoinduced racemization was not quenched at all by admission of oxygen, the almost comparable quantum yields for the Soret- and Q-band excitations indicate that the photoinduced racemization originates from the singlet excited state. This is in sharp contrast with the photoinduced atropisomerization of a zinc picket-fence porphyrin, for which the triplet excited state has been implicated.[1]

Racemization of the antipodes of the copper porphyrin (**1c**) upon irradiation was also examined under similar conditions, in which however no photo-

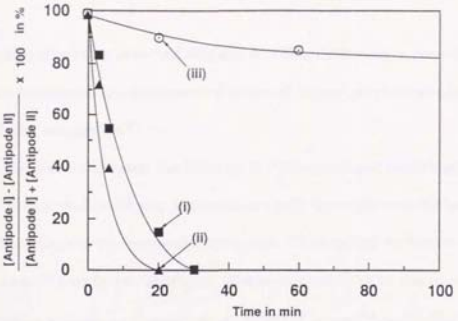

Figure 3. Racemizations of the **antipode I** of (α-PivNHEtioP)Zn (**1b**) in hexane/EtOH/$CHCl_3$ (70/20/10 in v/v, 7.1 x 10^{-5} M) at 28.5 °C under the irradiation at 410 nm (i), 580 nm (ii), and in the dark (iii). [**Antipode I**] and [**Antipode II**], as determined by HPLC.

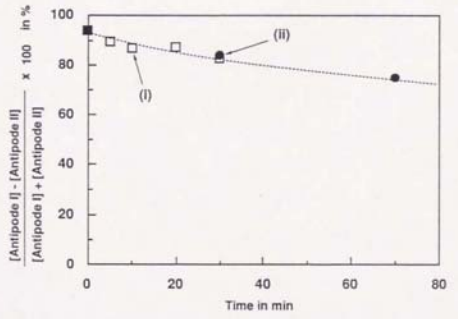

Figure 4. Racemizations of the **antipode I** of (α-PivNHEtioP)Cu (**1c**) in hexane/EtOH/$CHCl_3$ (70/20/10 in v/v, 7.5 x 10^{-5} M) at 0 °C under the irradiation at 400 nm (i) and in the dark (ii). [**Antipode I**] and [**Antipode II**], as determined by HPLC.

acceleration effect was observed (**Figure 4**). This difference is possibly due to the short lifetimes of the photoexcited states of copper porphyrins compared with those of zinc porphyrins.[9]

In the present chapter, the thermal and photoinduced conformational ruffling of distorted porphyrin skeletons are well demonstrated (**Scheme 2**), taking advantage of the successful resolution of the optical antipodes of chiral "single-armed" porphyrin complexes. Mechanistic studies on the photoinduced racemization process are in progress using other "armed" porphyrins with a variety of central metals.

References and Notes

1. (a) Freitag, R. A.; Mercer-Smith, J. A.; Whitten, D. G. *J. Am. Chem. Soc.* **1981**, 103, 1226. (b) Freitag, R. A.; Whitten, D. G. *J. Phys. Chem.* **1983**, 87, 3918.

2. **1a**; α-NH_2EtioPH_2, prepared by nitration of **2** with fuming HNO_3 followed by reduction with $SnCl_2$/HCl (Bonnett, R.; Stephenson, G. F. *J. Org. Chem.* **1971**, 36, 2791), was condensed with pivaloyl chloride in dry CH_2Cl_2/NEt_3. The reaction mixture was treated with aqueous ammonia, and then purified by column chromatography on silica gel with CH_2Cl_2 as eluent followed by recrystallization from CH_2Cl_2/MeOH. Yield; 81%. ^{1}H NMR ($CDCl_3$); δ10.13 and 10.12 ((s, 1H) x 2, meso β and δ), 9.96 (s, 1H, meso γ), 9.33 (s, 1H, amide-NH), 4.20 - 4.02 (m, 8H, CH_2CH_3), 3.64 - 3.46 (m, 12H, CH_3), 1.64 - 1.91 (m, 12H, CH_2CH_3), 1.81 (s, 9H, $^tC_4H_9$), –3.33 (br, 2H, core-NH). UV-vis (CH_2Cl_2); λ_{max} (log ε) 402 (5.03), 502 (4.18), 535 (3.65), 572 (3.58), and 627 nm (3.32). HRMS; 578.8264 calcd for $C_{37}H_{48}N_5O$ 578.8280. Treatements of **1a** with metal acetates gave the corresponding metal complexes in quantitative yields. **1b**; ^{1}H NMR

($CDCl_3$); δ9.89 (s, 1H, meso γ), 9.80 ((s, 1H) x 2, meso β and δ), 9.44 (s, 1H, NH), 3.98 - 3.93 (m, 8H, CH_2CH_3), 3.44 - 3.54 (m, 12H, CH_2CH_3), 1.74 - 1.82 (m, 12H, CH_3), 1.78 (s, 9H, $^tC_4H_9$). UV-vis (CH_2Cl_2); λ_{max} (log ε) 411 (5.47), 542 (4.26), and 580 nm (4.20). **1c**; UV-vis (CH_2Cl_2); λ_{max} (log ε) 402 (4.95), 530 (3.69), and 566 nm (3.84).

3. Comparison of the spectral data for **1a** and **1b** with those for etioporphyrin I and its zinc complex shows bathochromic shifts for the electronic absorptions (5 - 11 nm) and upfield-shifts for the ^1H NMR signals of the *meso* protons (0.1 - 0.2 ppm). Such spectral profiles have been claimed to be due to the lack of coplanarity of porphyrin disk: (a) Abraham, R. J.; Jackson, A. H.; Kenner, G. W.; Warburton, D. *J. Chem Soc.* **1960**, 853. (b) Burbidge, P. A.; Collier, G. L.; Jackson, A. H.; Kenner, G. W. *J. Chem. Soc.* B **1967**, 930. (c) Gong, L-C.; Dolphin, D. *Can. J. Chem.* **1985**, 63, 401.

4. Column: Chiralcell OD (Daicel), fow rate: 1.0 mL-min.$^{-1}$, room temperature, monitored at 410 nm, the eluates collected in flasks cooled at -78 °C.

5. The antipodes of the homologue of **1b** with a smaller amide group such as zinc α-acetylaminoetioporphyrin I were also resolved, whose racemization profiles were similar to those for **1b**.

6. Rate constants and activation parameters at 28.5 °C. For **1b**, $k = 2.1 \times 10^{-4}$ s^{-1}, $\Delta H^{\ddagger} = 29.4$ kcal·mol^{-1}, $\Delta S^{\ddagger} = 7.3$ eu. For **1c**, $k = 1.4 \times 10^{-3}$ s^{-1}, $\Delta H^{\ddagger} = 22.4$ kcal·mol^{-1}, $\Delta S^{\ddagger} = 2.8$ eu.

7. A quartz cell containig **1b** or **1c** in hexane/EtOH/$CHCl_3$ (70/20/10 in v/v), thermostated at 28.5 °C, was illuminated by a 500-W Xenon arc lamp from a distance of 4.3 cm through a band-path (bandwidth 10 nm) filter and another filter to cut heat.

8. Quauntum yields were obtained from the change in the enantiomeric purity of **1b** during the initial 3 min., at which the contribution of the thermal racemization was negligibly small (see: (**ii**) in **Figure 3**).

9. (a) Asano, M.; Kaizu, Y.; Kobayashi, H. *J. Chem. Phys.* **1988,** 89, 6567. (b)

Kim, D.; Holten, D.; Gouterman, M. *J. Am. Chem. Soc.* **1984**, 106, 2793. (c) Kobayashi, T.; Huppert, D.; Straub, K. D.; Rentzepis, P. M. *J. Chem. Phys.* **1979**, 70, 1720. (d) Brookfield, R. L.; Ellul, H.; Harriman, A .; Porter, G. *J Chem. Soc., Faraday Trans. 2* **1986**, 82, 219. (e) Harriman, A.; Richoux, M. C. *J. Chem. Soc., Faraday Trans. 2* **1980**, 76, 1618.

CHAPTER 4

Asymmetric Oxidation of Olefins and Sulfides Catalyzed by Metal Complexes of Chiral "Strapped" Porphyrin with Diastereotopic Faces.

Abstract

The optical antipodes of chiral *p*-xylylene-, *m*-xylylene-, and dodecamethylene-strapped porphyrins were resolved by HPLC. Asymmetric epoxidation of prochiral olefins such as styrene derivatives and vinylnaphthalene by iodosobenzene was achieved by using the manganese complexes of the antipodes of *p*-xylylene-strapped porphyrin as catalysts in the presence of imidazole, and the optically active epoxides were obtained in 42 - 58 % *ee*. When imidazole was absent, the epoxides with the opposite configuration were formed in lower *ee*. In the presence of imidazole, the enantioselectivity of the reaction depended on the structure of the strap in the catalyst, while no such dependence was observed in the absence of imidazole. When imidazole was present in the competitive oxidation of styrene with more-substituted olefins, the *p*-xylylene-strapped catalyst showed higher selectivity for styrene than (Etiop)MnCl, while the selectivity decreased in the absence of imidazole. The iron complex of chiral *p*-xylylene-strapped porphyrin effectively catalyzed the asymmetric oxidation of sulfides by iodosobenzene in the presence of imidazole.

Introduction

Cytochrome P-450 is one of the most attractive metalloenzymes, which catalyze metabolic oxygen transfer processes. The active site of cytochrome P-450 is an iron porphyrin bound to a cysteine thiolate group of the chiral protein molecule (**Figure 1**).[1] It has been also noted that the oxidation of prochiral olefins or sulfides mediated by cytochrome P-450 takes place enantioselectively under appropriate conditions.[2,3] In relation to the mechanism of this interesting asymmetric oxygen transfer, various chiral metalloporphyrin catalysts have been exploited.[4-7] The representative catalysts bear chiral groups such as binaphthyl and peptide groups covalently linked to achiral porphyrin moieties (**Figure 2**), which model the essential

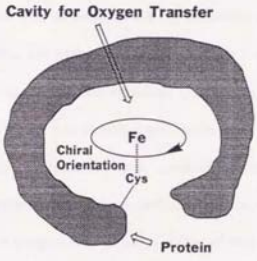

Figure 1. Schematic representation of the active site of cytochrome P-450.

role of the chiral protein molecule of cytochrome P-450 in the stereochemical course of the oxygen transfer process.

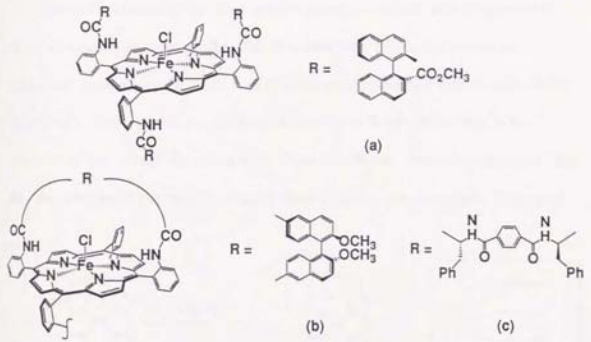

Figure 2. Examples of chiral metalloporphyrins for asymmetric oxidation. (a) ref 4a; (b) refs 4b and 4c; (c) ref 5a.

In the present paper will be described a fundamentally new strategy for structurally modeling the active site of cytochrome P-450 in asymmetric oxidation of prochiral olefins and sulfides. The porphyrin ligand of P-450 is protoporphyrin IX, which has enantiotopic faces, and, therefore, the active site has a diastereoisomeric structure upon coordination with the chiral cysteine thiolate group (**Figure 3**, (**I**)). In connection with this, the coordinated protoheme has been proposed to exist as either of two possible optically active diastereoisomers as a result of a stereospecific discrimination between the faces of the heme by the chiral thiolate group. Thus, the oxygen transfer in

the metabolic process has been considered to occur predominantly on either of the two chemically inequivalent, diastereotopic faces of the active site.[1]

The catalysts exploited here are the manganese and iron complexes of chiral strapped porphyrins (**2c, 2d, 3c, and 4c**). Since the precursor dihexyldeuteroporphyrin II (**1**) is of C_{2h} symmetry and has enantiotopic faces (prochiral), the strapped porphyrins derived from **1** are chiral due to the presence of the "strap" on either side of the two faces. Thus, the catalysts (**2c, 2d, 3c, and 4c**) have two chemically inequivalent, diastereotopic faces, and

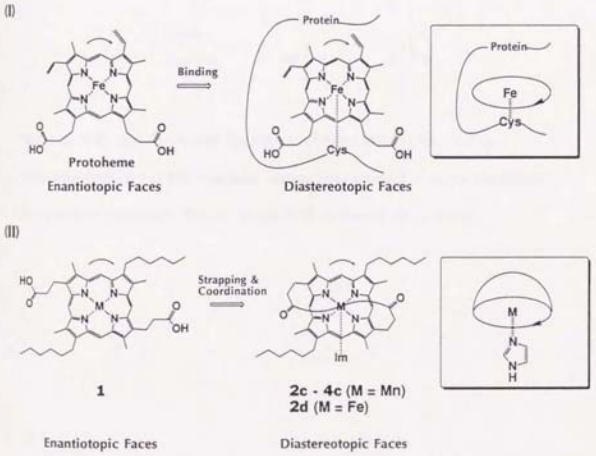

Figure 3. Active Site of cytochrome P-450 (**I**) and the metal complex of chiral strapped porphyrin coordinated by imidazole as a structual model system (**II**).

model the stereochemical structure of the P-450 active site. When an axially coordinating ligand is present on the non-strapped face, the oxygen transfer reaction is expected to occur exclusively on the strapped face of the catalyst (**Figure 3, (II)**).

By using these novel P-450 model catalysts (**2c, 2d, 3c, and 4c**), the author has attempted asymmetric oxidation of prochiral olefins and/or sulfides

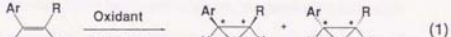

(1)

(2)

(**eq. 1** and **2**), and discussed the effects of coordinating base on the enantioselectivity of the reaction, taking into account also the results of competitive oxidation of olefin pairs with different steric bulks.

Results and Discussion

Optical Resolution of Chiral Strapped Porphyrin. The antipodes of a series of chiral strapped porphyrins (**2a** - **4a**) were obtained in optically pure forms by means of HPLC on silica gel coated with cellulose tris(3,5-dimethylphenylcarbamate). For example, zinc complex of *p*-xylylene-strapped porphyrin ((*p*-XYSP)Zn, **2b**) showed two peaks (fractions I and II) with comparable peak areas when chromatographed with hexane/ethanol/diethylamine (96/3/1 v/v) as eluent (**Figure 4**). The compounds corresponding to these two peaks were fractionated, both of which were found to be identical to the original **2b** in terms of the absorption

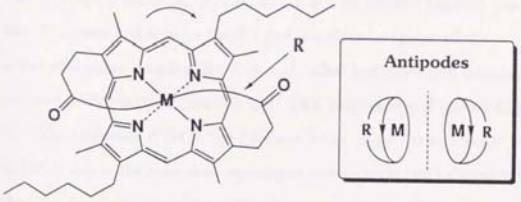

2a M = H_2
2b M = Zn
2c M = MnCl
2d M = FeCl

R = —NHCH$_2$—C$_6$H$_4$—CH$_2$NH—

3a M = H_2
3c M = MnCl

R = —NHCH$_2$—C$_6$H$_3$(CH$_2$NH—)—

4a M = H_2
4c M = MnCl

R = —NH-(CH$_2$)$_{12}$-NH—

spectra, while the circular dichroism (CD) spectra were perfect mirror-images of each other (**Figure 5(A)**). Fraction I provided a positive CD band in the Soret region (410 nm) and fraction II a negative band. Thus, these two antipodes are denoted here as [+]- and [-]-**2b**, respectively. The free-base porphyrin **2a** derived from [+]-**2b** also exhibited a positive CD band at the Soret region (401 nm) ([+]-**2a**), and that from [-]-**2b** a negative band ([-]-**2a**). The same was true for the CD profiles of the antipodes of the chloromanganese complex (**2c**) ([+]- and [-]-**2c**) and chloroiron complex (**2d**) ([+]- and [-]-**2d**) derived from [+]- and [-]-**2a**, respectively (**Figures 5(B)** and **(C)**). The antipodes of **2a** in the free-base forms could not be directly resolved by HPLC due to the poor peak separation under similar HPLC conditions. On the other hand, the antipodes of the chloroiron complex (**2d**) were successfully separated.[8] An attempted HPLC resolution of the manganese complex (**2c**) also failed due to its too strong affinity toward the column pack. In sharp contrast to **2a**, the antipodes of the free-base *m*-xylylene-strapped porphyrin (*m*-XYSPH$_2$, **3a**) and dodecamethylene-strapped porphyrin (DMSPH$_2$, **4a**) could be directly resolved by HPLC with the same column pack and showed strong CD bands at the Soret regions (401 nm) (**Figures 5(D)** and **(F)**).

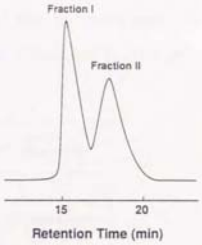

Figure 4. HPLC profile of **2b** using the analytical column (see **Experimental Section**) with hexane/ethanol/diethylamine (91/8/1 v/v) as eluent at room temperature monitored at 390 nm.

However, as for **3a**, the antipode obtained as the first fraction showed a negative CD band at the Soret region (401 nm) ((-)-**3a**), and the second fraction a positive band. ((+)-**3a**). Thus, the order of elution of the (+)- and (-)-antipodes of **3a** was opposite to that of **4a**.

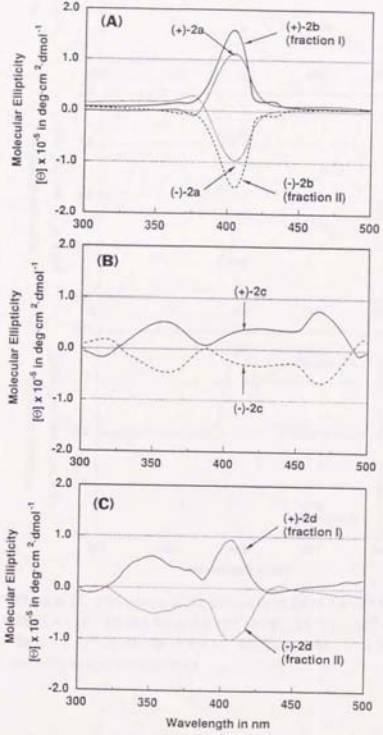

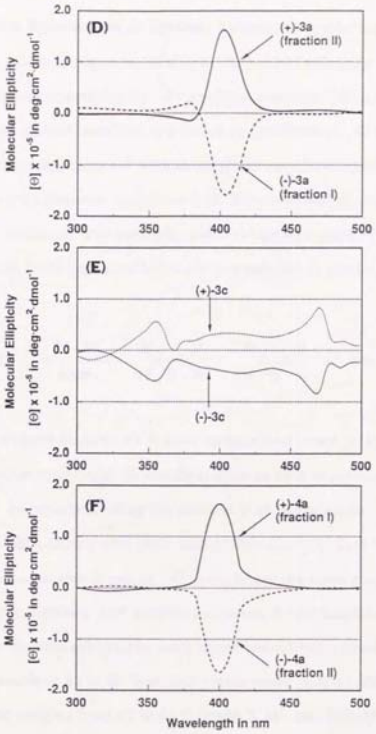

Figure 5. CD spectra of the antipodes of **2a** (1.1 x 10^{-5} M), **2b** (3.4 x 10^{-6} M) (**A**), **2c** (1.0 x 10^{-5} M) (**B**), **2d** (1.0 x 10^{-5} M) (**C**), **3a** (8.1 x 10^{-6} M) (**D**), **3c** (3.8 x 10^{-6} M) (**E**), and **4a** (1.1 x 10^{-5} M) (**F**) in $CHCl_3$ at room temperature.

Asymmetric Epoxidation of Olefins. Typically, epoxidation of olefins was carried out under nitrogen in CH_2Cl_2 at -20 - -10 °C using the antipodes of the chloromanganese complexes **2c** - **4c** as chiral catalysts, 100 equiv of iodosobenzene as oxidant, and 500 equiv of olefin (**Scheme 3**). As shown in **Table I**, the epoxidation occurred with satisfactory enantioselectivities when the antipodes of *p*-xylylene-strapped catalyst (**2c**) were used as catalysts in the presence of imidazole. For example, use of (+)-**2c** as a catalyst with 10 equiv of imidazole for the epoxidation of styrene resulted in the formation of

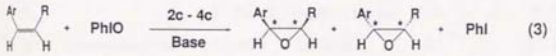

(3)

optically active styrene oxide in 43 % yield (determined based on the initial amount of iodosobenzene)[9] with (*R*)-configuration in 49 % enantiomeric excess (*ee*) (**run 1**).[10,11] As expected, using the catalyst with the opposite configuration ((-)-**2c**), (*S*)-styrene oxide was preferentially formed (45 % yield) in a comparable enantiomeric excess (48 % *ee*) under the same conditions (**run 2**). Similarly, 4-chloro- and 4-methyl-styrenes, 2-vinylnaphthalene, indene, and 1,2-dihydronaphthalene were enantioselectively epoxidized in the presence of imidazole in 42 to 58 % *ee* with yields based on the initial amount of iodosobenzene ranging from 32 to 65 % (**runs 7, 11 - 14**). Substituted imidazoles such as 1-ethyl- and 2-methyl-imidazoles worked similarly to non-substituted imidazole for the asymmetric epoxidation (**runs 5** and **9**), while use of 2-phenylimidazole resulted in a remarkable decrease in

Table I. Asymmetric Epoxidation of Olefins by Chiral Manganese Porphyrins.[a]

Run	Olefin	Catalyst	Base	Yield, %[b, c]	*ee*, %	Confign.
1	styrene	[+]-**2c**	imidazole	43	49	(*R*)-(+)
2		[-]-**2c**	imidazole	45	48	(*S*)-(-)
3		[+]-**2c**	none	72	18	(*S*)-(-)
4		[+]-**2c**	1-ethylimidazole	68	50	(*R*)-(+)
5	4-chlorostyrene	[-]-**2c**	imidazole	41	42	(*S*)-(-)
6		[-]-**2c**	2-methylimidazole	40	42	(*S*)-(-)
7		[-]-**2c**	2-phenylimidazole	36	8	(*S*)-(-)
8	4-methylstyrene	[+]-**2c**	imidazole	56	47	(*R*)-(+)[d]
9	2-vinylnaphthalene	[+]-**2c**	imidazole	65	42	(*R*)-(+)[d]
10	indene	[+]-**2c**	imidazole	58	58	(1*R*,2*S*)-(-)
11	1,2-dihydronaphthalene	[+]-**2c**	imidazole	32	52	(1*R*,2*S*)-(+)
12	styrene	[+]-**3c**	1-ethylimidazole	27 (5)	30	(*R*)-(+)
13		[+]-**3c**	none	18 (4)	16	(*S*)-(-)
14	styrene	[+]-**4c**	1-ethylimidazole	33 (14)	17	(*R*)-(+)
15		[+]-**4c**	none	30 (10)	16	(*S*)-(-)

[a] $[Olefin]_0/[PhIO]_0/[base]_0/[catalyst]_0$ = 900 μmol/180 μmol/18 μmol/1.8 μmol in CH_2Cl_2 (1.0 mL) at -20 - -10 °C under N_2 for 3 h. [b] By GC based on the amount of iodosobenzene charged. [c] No carbonyl compounds were detected unless otherwise noted. The numbers in parentheses are the yields of phenylacetaldehyde. [d] From analogy of the ^1H NMR profile with that of (*R*)-styrene oxide in the presence of Eu(hfc)3.

enantioselectivity (**run 10**). In a more polar solvent such as acetonitrile under similar conditions, asymmetric epoxidation of styrene also occurred with a comparable enantioselectivity to that in CH_2Cl_2 (**run 6**). On the other hand, use of a less polar solvent such as toluene/CH_2Cl_2 (50/50) resulted in lowering the chemical yield and enantiomeric excess of the product (**run 8**). When the chiral *m*-xylylene-strapped catalyst ([-]-**3c**) was used coupled with 1-ethylimidazole, (*R*)-styrene oxide was formed in 30 % *ee* (27 % yield) under similar conditions (**run 15**). Use of the chiral catalyst bearing dodecamethylene strap ([+]-**4c**) resulted in a significant decrease in enantiomeric excess of the epoxide (17 % *ee*; (*R*), 33 % yield) along with the formation of a considerable amount of phenylacetaldehyde (**run 17**). Thus, in the presence of imidazole, the enantioselectivity of the reaction varies with the structure of the strap in the catalyst. However, it should be also noted that (*R*)-epoxides were always formed predominantly using as catalysts the [+]-antipodes of **2c** - **4c** providing positive CD bands in the Soret regions, while the formation of (*S*)-epoxides was favored when the catalysts with the opposite configuration ([-]-antipodes) were employed.

In sharp contrast, when styrene was epoxidized in the absence of imidazole using **2c** as catalyst (**run 3**), the epoxide with the opposite

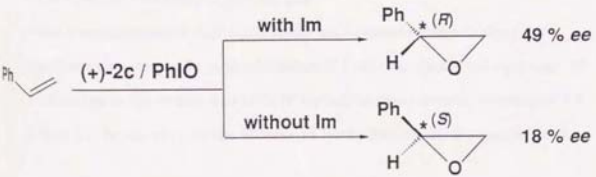

configuration to that in the presence of imidazole (**run 1**) was formed. The same was true for the reactions using **3c** and **4c** as catalysts (**runs 16** and **18**, **runs 15** and **17**). Furthermore, the observed % *ee* of the products were all low in the range of 16 - 18 %, indicating that the strap part of the catalyst does not affect the enantioselectivity of the reaction.

Competitive Epoxidation. In connection with the mechanism of the above asymmetric oxygen transfer, styrene and more-substituted olefins were competitively oxidized using **2c** as catalyst in the presence or absence of imi-

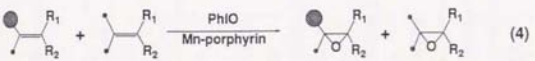

(4)

dazole (**Scheme 4**), and the substrate selectivities were compared with those of (EtioP)MnCl as a non-strapped catalyst. As shown in **Table II**, **2c** coupled with 1-ethylimidazole showed substrate selectivities for styrene competing with other olefins. For example, the oxidation of an equimolar mixture of styrene and *trans*-β-methylstyrene (250 equiv each) with iodosobenzene (100 equiv) catalyzed by racemic **2c** in the presence of 1-ethylimidazole (10 equiv) at -10 °C resulted in the conversion ratio of styrene to *trans*-β-methylstyrene of 3.2 : 1 (**run 1**). In contrast, in the absence of 1-ethylimidazole, the preference for

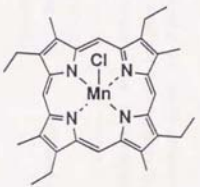

(EtioP)MnCl

Table II. Competitive Epoxidation of Olefins by Manganese Porphyrins. [a]

run	olefin **A**	olefin **B**	catalyst system [b]	yield in % [c, d]		conv. of olefin **A**
				epoxide **A**	epoxide **B**	conv. of olefin **B**
1	styrene	*trans*-β-methylstyrene	**2c** / NEIm	58	18	3.2 : 1
2			**2c**	21	42	0.5 : 1
3			(EtioP)MnCl / NEIm	13 (13)	62	0.4 : 1
4	styrene	β,β-dimethylstyrene	**2c** / NEIm	50	21	2.3 : 1
5			(EtioP)MnCl / NEIm	12 (17)	55	0.5 : 1
6	styrene	*cis*-2-octene	**2c** / NEIm	55	6	9.1 : 1
7			**2c**	37	16	2.4 : 1
8			(EtioP)MnCl / NEIm	16 (26)	40	1.0 : 1
9	styrene	2-methyl-2-pentene	**2c** / NEIm	64	10	6.6 : 1
10			(EtioP)MnCl / NEIm	20 (26)	40	1.2 : 1

[a] [Olefin A]$_0$/[olefin B]$_0$/[PhIO]$_0$/[base]$_0$/[catalyst]$_0$ = 250 μmol/250 μmol/100 μmol/10 μmol/1 μmol in CH_2Cl_2 (0.5 mL) at -10 °C under N_2 for 1 h. [b] NEIm: 1-ethylimidazole. [c] By GC based on the amount of iodosobenzene charged. [d] No carbonylcompounds were detected otherwise noted. The numbers in parentheses are the yields of phenylacetaldehyde.

styrene was reduced to give the ratio of 0.5 : 1 (**run 2**), which is very close to that observed with the (EtioP)MnCl/1-ethylimidazole system (0.4 : 1, **run 3**). Similarly, in the competitive oxidation of styrene with β,β-dimethylstyrene (**runs 4 and 5**), *cis*-2-octene (**run 6 - 8**) or 2-methyl-2-pentene (**runs 9 and 10**) using **2c**/1-ethylimidazole system, the selectivity for styrene was higher than those observed with **2c** alone (**run 7**) and the (EtioP)MnCl/1-ethylimidazole system (**runs 5, 8** and **10**). These observations again indicate the essential effect of imidazole on the oxygen transfer process mediated by the manganese strapped porphyrin catalyst (**2c**).

Coordination of Imidazole to Manganese Strapped Porphyrin (2c). The spectral changes upon titration of a CH_2Cl_2 solution of **2c** with imidazole

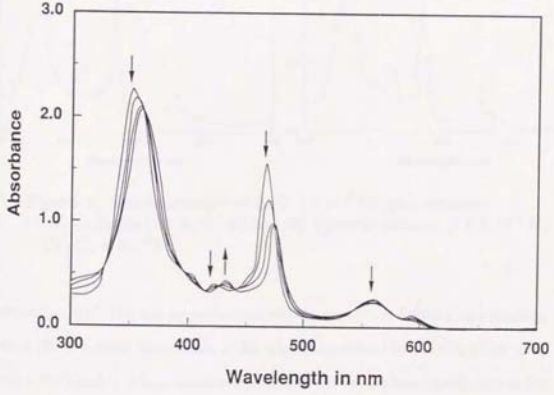

Figure 6. Spectral changes of **2c** (1.8×10^{-5} M) upon titration with imidazole (0 - 3.2×10^{-2} M) in CH_2Cl_2 at 20 °C.

at 20 °C are illustrated in **Figure 6**. Six isosbestic points were observed and the spectral changes were linear with the concentration of imidazole to the first power,[12] indicating that only one imidazole molecule can coordinate to **2c** with an association constant (K) of 2.1 x 10^2 l·mol^{-1}.[13] The molecular model study indicated that the coordination of imidazole to **2c** is likely to occur specifically on the open face of **2c**, since imidazole is too large to be incorporated into the strap cavity.

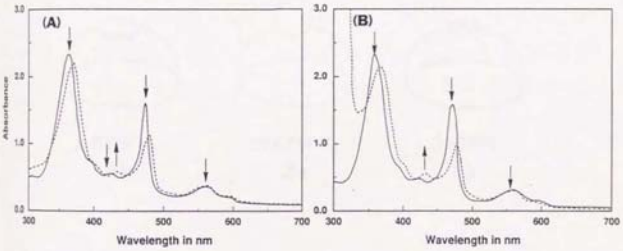

Figure 7. Spectal changes of **2c** (1.8 x 10^{-5} M) upon addition of (**A**) imidazole (1.6 X 10^{-1} M) and (**B**) 2-phenylimidazole (1.6 X 10^{-1} M) in CH_2Cl_2 at 20 °C.

In connection with the low enantioselectivity in **run 10** in **Table I**, the binding constant (K) of 2-phenylimidazole to **2c** were determined in CH_2Cl_2 at 20 °C to be 0.49 x 10^2 l·mol^{-1}. Thus, the coordinating ability of 2-phenylimidazole to **2c** is lower than that of imidazole.

NMR Studies on the Structures of Xylylene-strapped Porphyrins (2a and 3a). In relation to the difference in enantioselectivity between two xylylene-strapped catalysts (**2c** and **3c**) in the presence of imidazole (**runs** 5 and 15), the ^{1}H NMR spectra of the free-base porphyrins (**2a** and **3a**) were measured in $CDCl_3$, where **2a** showed a single 1,4-phenylene signal at δ2.44

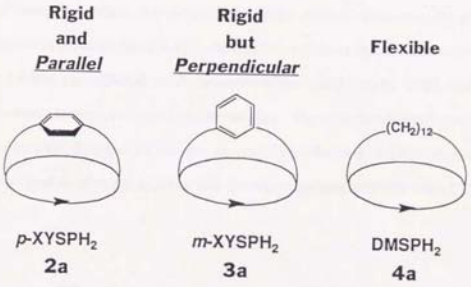

ppm, indicating a parallel conformation of the phenylene moiety with the porphyrin plane on the NMR time scale. On the other hand, as for the 1,3-phenylene moiety of **3a**, the notable upfield shift for the signal of the proton at the 2-position (δ0.30) compared with those for the protons at the 4- and 6-positions (δ5.81) and 5-position (δ6.14) was observed, which indicates a perpendicular conformation of the phenylene moiety with the porphyrin plane.

Mechanism of Asymmetric Epoxidation. The asymmetric oxygen transfer achieved with the chiral manganese strapped porphyrin catalyst - imidazole systems is considered a result of the epoxidation predominantly occurring on the strapped face of the catalyst. In the presence of imidazole, the unstrapped face of the active site is considered to be blocked by the coordination with imidazole, so that the access of olefins and/or iodosobenzene is prohibited. Therefore, the enantioselectivity of the reaction in the presence of imidazole is affected by the structure of the strap in the catalyst (**runs 5**, 15, and **17**) but not affected in the absence of imidazole (**runs 3**, **16**, and 18). When imidazole is coordinated to the catalyst, the enantioselectivity increased in the order: **4c**, **3c**, and **2c**, where the catalyst (**4c**) bearing the longest and relatively flexible strap exhibited the lowest enantioselectivity (**run 17**). The

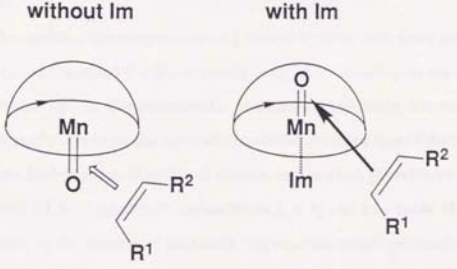

difference in enantioselectivity of the two xylylene-strapped catalysts **2c** and **3c** (**runs 5** and **15**) may be ascribed to the conformational difference of the phenylene moieties, where the phenylene moiety in **2c** oriented in parallel with the porphyrin plane may provide a sterically more hindered cavity on the active site than the vertically oriented phenylene group in **3c**.

In the absence of imidazole, the reaction on the unstrapped open face of the catalyst is allowed, which preferentially affords the epoxides with the opposite configurations. Taking into account the inversion of the stereochemistry of reaction and the decrease in % *ee* of the products (**runs 3**, **16**, and **18**), the epoxidation in the absence of imidazole is considered to occur predominantly on the sterically less hindered unstrapped face of the catalyst with a low steric requirement. When an imidazole with a low coordinating ability such as 2-phenylimidazole is used, the epoxidation on the unstrapped face is less efficiently suppressed, so that the % *ee* of the product decreases (**run 10**).

The results of the competitive oxidation of styrene with more-substituted olefins can also support the above mechanistic understanding on the oxygen transfer reaction. In the presence of a coordinating imidazole, the reaction predominantly occurs on the sterically hindered strapped face of the catalyst, so styrene having a non-substituted olefinic carbon atom is preferred to the 1,2-di- and 1,1,2-tri-substitutd olefins (**runs 1**, **4**, **6**, and **9** in **Table II**). On the other hand, in the absence of imidazole, the reaction occurs predominantly on the sterically less hindered unstrapped face. Therefore, the selectivity for styrene (**runs 2 and 7**) is almost comparable to the case using the non-

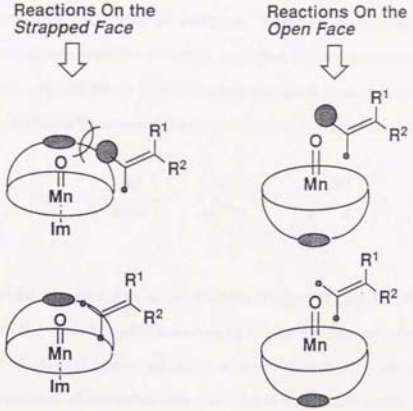

strapped catalyst system ((EtioP)MnCl/1-ethylimidazole) (**runs 3**, and **8**). Thus, the results of competitive oxidation again indicate the difference in steric requirement between the strapped and non-strapped faces of the catalyst.

Asymmetric Oxidation of Sulfides. Based on the successful asymmetric oxygen transfer to olefins described above, asymmetric oxidation of prochiral aryl sulfides by iodosobenzene was examined in the presence of imidazole (**Scheme 5**), where chloroiron complex of *p*-xylylene-strapped

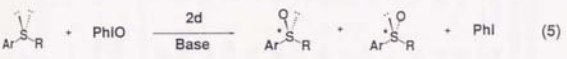

(5)

porphyrin (**2d**) was found to be an effective catalyst (**Table III**).[14] For example, in the oxidation of thioanisole by (+)-**2d** coupled with 600 equiv of imidazole, (*S*)-methyl phenyl sulfoxide was obtained in 71 % yield based on the initial amount of iodosobenzene with the enantiomeric excess of 43 % (**run 2**). Asymmetric sulfoxidation of other aryl sulfides such as *p*-methyl and *p*-bromo-thioanisoles, and methoxymethyl phenyl sulfide also took place in the presence of imidazole (**runs 4**, **6**, and **12 - 14**), where the highest enantioselectivity (up to 71 % *ee*) was obtained in the case of methoxymethyl phenyl sulfide (**runs 12 - 14**). On the other hand, in the absence of imidazole, the enantioselectivity of the reaction virtually disappeared to give racemic sulfoxides, indicating the essential role of imidazole in asymmetric induction (**runs 1**, **5**, and **11**). Five isosbestic points observed in the spectroscopic titration studies demonstrated that **2d** undergoes one-to-one complexation with imidazole ($K = 4.3 \times 10^2$ l·mol^{-1}). Therefore, in the presence of imidazole, the reaction occurs predominantly on the strapped face by the possible blocking of the open face by the coordinating imidazole, while in the absence of

Table III. Asymmetric Oxidation of Sulfides Catalyzed by Chiral Iron Porphyrins.[a]

Run	Catalyst **2d**	Sulfide (ArSR) Ar	R	[Im]$_0$ / [Catalyst]$_0$	T/°C	Time/h	Turnover number[b]	% ee[c]	Confign.[c,d]
1	(+)	C_6H_5	CH_3	0	-43	2.0	67	0	-
2	(+)			600	-43	2.0	142	43	*S*
3	(-)			600	-43	2.0	150	33	*R*
4	(-)	*p*-$CH_3C_6H_4$	CH_3	100	-43	2.0	92	23	(*R*)
5	(-)	*p*-BrC_6H_4	CH_3	0	-23	2.5	178	0	-
6	(-)			100	-23	3.5	30	36	*R*
7	(-)	C_6F_5	CH_3	0	-15	1.5	15	36	(*S*)
8	(-)			100	-15	1.5	55	30	(*S*)
9	(+)	*p*-$CH_3C(O)HNC_6H_4$	CH_3	0	-15	1.5	107	23	(*R*)
10	(+)			600[e]	-15	2.0	60	18	(*R*)
11	(+)	C_6H_5	CH_2OCH_3	0	-43	2.0	30	0	-
12	(+)			100	-43	2.0	40	71	(*R*)
13	(+)			600	-43	2.0	22	70	(*R*)
14	(-)			600	-43	2.0	20	67	(*S*)

[a] In CH_2Cl_2 under nitrogen using 900 μmol of sulfide, 360 μmol of PhIO and 1.8 μmol of **2d**. [b] Calculated from the yield of sulfoxide (GC or gravimetry after isolation) and the amount of **2d**. [c] By ^1H NMR in the presence of (*R*)-1,1'-bi-2-naphthol. [d] The configurations in parentheses were estimated by analogy with the NMR spectral pattern of optically active methyl phenyl sulfoxide. [e] 1-Methylimidazole was used.

imidazole, the reaction is considered to occur on the open face because of the low steric requirement. In sharp contrast, the asymmetric sulfoxidation also occurred even in the absence of imidazole when the substrate with an amide group with a hydrogen-bonding capability (**run 9**) or an electron-poor aromatic group (**run 7**) was used.

Conclusion

In the present paper, the conceptually new chiral metalloporphyrin catalysts (**2c**, **2d**, **3c**, and **4c**) which mediate asymmetric oxygen transfer reaction have been presented. The catalysts are derived from a porphyrin with enantiotopic faces by introducing a strap on one side, and have diastereotopic faces (**II** in **Figure 3**) analogous to the chirally oriented protoheme (protoporphyrin IX) in the active center of cytochrome P-450 (**I**). The reaction proceeds with satisfactory enantioselectivity using the catalyst (**2c**) or (**2d**) when the unstrapped open face was blocked by a coordinating imidazole. Among the recent progress in the field of chiral catalysts, this achievement is of much interest, since the chirality of the catalyst is originating from the C_{2h}-symmetric structure of the porphyrin moiety, which is simply provided by the peripheral substituents upon specific arrangement.

Experimental Section

Materials.

Acetonitrile, triethylamine, and dichloromethane (CH_2Cl_2) were distilled over calcium hydride under dry nitrogen. Toluene and tetrahydrofuran (THF) were distilled over sodium benzophenone ketyl just before use. Dihexyldeuteroporphyrin II dimethyl ester (2,12-bis(2'-(methoxycarbonyl)ethyl)-3,8,13,18-tetramethyl-7,17-dihexylporphine) was synthesized from 4-ethyl-3-(methoxycarbonyl)ethyl-5-methylpyrrole-2-carboxylic acid[15] and 4-ethyl-5-formyl-3-hexylpyrrole-2-carboxylic acid[16] by a similar procedure reported by Collman *et. al.*.[17]

Hydrolysis of Dihexyldeuteroporphyrin II Dimethyl Ester.

Dihexyldeuteroporphyrin II dimethyl ester (1.0 g, 1.41 mmol) was dissolved in a mixture of THF (100 mL) and concentrated hydrochloric acid (100 mL), and stirred at room temperature in the dark for 20 h. The solvents were removed under reduced pressure and the residue was taken up in $CHCl_3$ (100 mL). The organic phase was washed with water until the aqueous phase was neutralized, dried over anhydrous Na_2SO_4, and evaporated to dryness to give dihexyldeuteroporphyrin II (**1**) as a purple powder, which was used in the next reaction without further purification.

***p*-Xylylene-strapped Porphyrin (*p*-XYSPH$_2$, 2a).**[18] To a THF solution (200 mL) of dihexyldeuteroporphyrin II (**1**) (960 mg, 1.41 mmol) in a 1-L round- bottom flask equipped with a dropping funnel were successively added triethylamine (1.0 mL, 7.4 mmol) and isobutyl chloroformate (0.5 mL, 3.4

mmol) by means of hypodermic syringes under dry nitrogen at room temperature to convert **1** into the corresponding mixed anhydride. After the mixture was stirred for 1 h at room temperature, a THF solution (500 mL) of 1,4-xylylenediamine (584 mg, 4.29 mmol) was introduced to the dropping funnel by a syringe and added dropwise to the mixed anhydride solution for a period of 5 h. The mixture was then stirred for 36 h at room temperature under dry nitrogen and evaporated to dryness. The residue dissolved in CH_2Cl_2 (100 mL) was filtered from insoluble fractions by passing through Celite, and the filtrate was concentrated to a small volume, which was chromatographed on silica gel (Wakogel C-300). After a brown band was eluted with CH_2Cl_2, a red band was eluted with $CHCl_3$/ethyl acetate (90/10 v/v), which was collected and evaporated to dryness, and the residue was recrystallized from CH_2Cl_2/hexane to give **2a** as a reddish purple powder (382.3 mg, 35 % yield). FAB-HRMS: Calcd for $C_{50}H_{63}O_2N_6$ (MH^+), m/z 779.5013, obsd m/z 779.5071. UV-vis: λmax (log ε) 401 (5.18), 500 (4.05), 536 (3.97), 566 (3.78), 620 (3.49). ^{1}H NMR: δ10.13 and 10.03 (s x 2, 4H, meso), 4.70 (td, 2H, diastereotopic porph-$CH_2$$CH_2$CO), 4.24 - 3.96 (m, overlapped, 6H, diastereotopic porph-$CH_2$$CH_2$CO (2H) and porph-$CH_2$$C_5H_{11}$ (4H)), 3.76 and 3.55 (s x 2, 12H, porph-CH_3), 3.29 (br, 2H, CONH), 2.97 and 2.36 (m x 2, 4H, diastereotopic porph-$CH_2$$CH_2$CO), 2.58 (d, 4H, $CH_2$$C_6H_4$), 2.44 (s, 4H, C_6H_4), 2.27 (m, 4H, porph-$CH_2$$CH_2$$C_4H_9$), 1.77 - 1.32 (m, overlapped, 12H, porph-$C_2H_4$$CH_2$$C_3H_7$, -$C_3H_6$$CH_2$$C_2H_5$, and -$C_4H_8$$CH_2$$CH_3$), 0.91 (t, 6H, porph-$C_5H_{10}$$CH_3$), -3.55 (br, 2H, core NH). These assignments were supported by 2D NMR.

Preparation and Demetallation of Zinc Complex of *p*-Xylylene-strapped Porphyrin ((*p*-XYSP)Zn, 2b). **2b** was obtained quantitatively by the reaction of **2a** with zinc acetate in $CHCl_3$/MeOH.[19] Demetallation was carried out by shaking a $CHCl_3$ solution of **2b** with 10 % HCl followed by neutralization with aq. $NaHCO_3$.

***m*-Xylylene-strapped Porphyrin (*m*-XYSPH$_2$, 3a).** To a 50-mL round-bottom flask containing a THF solution (25 mL) of **1** (483 mg, 0.71 mmol) were successively added triethylamine (0.51 mL, 3.77 mmol) and isobutyl chloroformate (0.22 mL, 1.7 mmol) under dry nitrogen at room temperature. After stirring for 1 h at room temperature, the resulting mixed anhydride solution was transferred in a nitrogen stream by a syringe to a dropping funnel connected to a 500-mL round-bottom flask containing THF (75 mL). The above mixed anhydride solution was added dropwise to the flask for a period of 10 h, with a simultaneous addition of a THF solution (25 mL) of 1,3-xylylenediamine (140 μL, 1.16 mmol) by a syringe pump through a rubber septum. The reaction mixture was then stirred for 12 h and evaporated to dryness. The residue dissolved in CH_2Cl_2 (100 mL) was filtered through Celite, and the filtrate was chromatographed on silica gel (Wakogel C-300). A red fraction eluted with CH_2Cl_2 was collected and concentrated to a small volume (5 mL), to which hexane (30 mL) was then added, and the mixture was slowly evaporated under reduced pressure to give **3a** as a purple powder (130 mg, 23 % yield). FAB-HRMS: Calcd for $C_{50}H_{63}O_2N_6$ (MH^+), m/z 779.5013, obsd m/z 779.5034. UV-vis: λmax (log ε) 401 (5.14), 501 (3.98), 538 (3.96), 566 (3.75), 620 (3.42). ^1H NMR: δ10.06 and 10.03 (s x 2, 4H, meso), 6.14 (t, 1H,

5-H of C_6H_4), 5.81 (dd, 2H, 4- and 6-H of C_6H_4), 4.67 (td, 2H, diastereotopic porph-CH_2CH_2CO), 4.19 - 4.06 (m, overlapped, 6H, diastereotopic porph-CH_2CH_2CO (2H) and porph-$CH_2C_5H_{11}$ (4H)), 3.75 and 3.53 (s x 2, 12H, porph-CH_3), 2.80 and 2.11 (m x 2, 4H, diastereotopic porph-CH_2CH_2CO), 2.36 - 2.31 (m, overlapped, 6H, porph-$CH_2CH_2C_4H_9$ and diastereotopic $CH_2C_6H_4$), 2.19 (br, 2H, NHCO), 1.76 - 1.34 (m, overlapped, 12H, porph-$C_2H_4CH_2C_3H_7$, -$C_3H_6CH_2C_2H_5$, and -$C_4H_8CH_2CH_3$), 0.92 (t, 6H, porph-$C_5H_{10}CH_3$), 0.30 (s, 1H, 2-H of C_6H_4), -0.64 (d, 2H, diastereotopic $CH_2C_6H_4$), -3.58 (br, 2H, core NH). These assignments were supported by 2D NMR.

Dodecamethylene-strapped Porphyrin (DMSPH_2, 4a). 4a was prepared in 27 % yield from **1** and dodecamethylenediamine in a similar manner to that described for the preparation of **2a**. FAB-HRMS: Calcd for $C_{54}H_{79}O_2N_6$ (MH^+), m/z 843.6264, obsd m/z 843.6264. UV-vis: λmax (log ε) 401 (5.18), 500 (4.05), 536 (3.97), 566 (3.78), 620 (3.49). ^1H NMR: δ10.13 and 10.09 (s x 2, 4H, meso), 4.81 (t, 2H, CONH), 4.67 (dd, 2H, diastereotopic porph-CH_2CH_2CO), 4.24 - 4.07 (m, overlapped, 6H, diastereotopic porph-CH_2CH_2CO (2H) and porph-$CH_2C_5H_{11}$ (4H)), 3.69 and 3.55 (s x 2, 12H, porph-CH_3), 3.28 and 3.10 (td x 2, 4H, diastereotopic porph-CH_2CH_2CO), 2.27 (m, 4H, porph-$CH_2CH_2C_4H_9$), 1.82 - 1.37 (m, overlapped, 12H, porph-$C_2H_4CH_2C_3H_7$, -$C_3H_6CH_2C_2H_5$, and -$C_4H_8CH_2CH_3$), 0.95 (t, 6H, porph-$C_5H_{10}CH_3$), 0.57 (m, 8H, $CONHCH_2$ and $CONHCH_2CH_2$), 0.11 (m, 8H, $CONH(CH_2)_2CH_2$ and $CONH(CH_2)_3CH_2$), -0.22 (br, 8H, $CONH(CH_2)_4CH_2$ and $CONH(CH_2)_5CH_2$), -3.55 (br, 2H, core NH).

Optical Resolutions by HPLC.

Resolutions of the optical antipodes of **2b**, **3a**, and **4a** were carried out by using 0.46 x 250 mm (analytical) or 20 x 500 mm (preparative) HPLC column packed with silica gel coated with cellulose tris(3,5-dimethylphenylcarbamate) as a chiral stationary phase. HPLC experiments with the analytical column were performed on a JASCO Type TWINCLE equipped with a JASCO Type 875-UV variable wavelength detector at a flow rate of 1.0 mL-min^{-1} at room temperature and monitored at 390 nm. HPLC experiments with the preparative column were performed on a JASCO Type 887-PU pump equipped with a JASCO Type 875-UV variable wavelength detector, a JASCO Type 802-SC system controller, and a JASCO Type 892-01 column selector at a flow rate of 10.0 mL-min^{-1} at room temperature and monitored at 410 nm. The HPLC column packs were prepared by the method reported by Okamoto *et. al.*[20]

Resolution of the Antipodes of 2b. 2b (2 mg) was dissolved in CCl_4 (20 mL) containing diethylamine (1 drop), and an aliquot (20 μL) of the solution was subjected to HPLC with the analytical column using hexane/ethanol/diethylamine (96/3/1 v/v) as eluent. Two peaks were observed at 15.2 and 18.6 min. For miligram-scale resolution, 3-mL portions of a CCl_4 solution (50 mL) of **2b** (50 mg) containing diethylamine (two drops) were loaded on the preparative column with hexane/ethanol/diethylamine (84/15/1 v/v) as eluent.

Resolution of the Antipodes of 3a. 3a (2 mg) was dissolved in CCl_4 (20 mL) and an aliquot (20 μL) of the solution was subjected to HPLC with the analytical column using hexane/ethanol (92/8 v/v) as eluent. Two peaks were

observed at 8.4 and 9.6 min. For miligram-scale resolution, 3-mL portions of a CCl_4 solution (50 mL) of **3a** (50 mg) were loaded on the preparative column with hexane/ethanol (88/12 v/v) as eluent.

Resolution of the Antipodes of 4a. Under similar conditions as for **3a**, two peaks were observed at 19.7 and 24.8 min, using hexane/2-propanol/$CHCl_3$ (70/20/10 v/v) as eluent. In this case, the analytical column was also used for a miligram-scale resolution.

Preparation of Chiral Chloromanganese Complexes.[21] To a 50-mL round bottom flask containing an acetic acid/acetic anhydride solution (5 mL/1 mL) of an optically active free-base porphyrin (**2a**, **3a**, or **4a**) (20 mg) was added $MnCl_2$-$4H_2O$ (10 mg), and the mixture was refluxed for 10 h. Then, the reaction mixture was poured into a mixture of saturated aq. $NaHCO_3$ and $CHCl_3$. The organic layer was separated and washed twice with saturated aq. NaCl, dried over anhydrous Na_2SO_4, and evaporated to dryness. Recrystallization of the residue from CH_2Cl_2/hexane gave an optically active manganese complex (**2c**, **3c**, or **4c**) as a brown powder in a quantitative yield. **2c**, UV-vis: λmax (log ε) 360 (5.09), 424 (4.39), 472 (4.92), 559 (4.20), 593 (3.89). **3c** UV-vis: λmax (log ε) 361 (5.05), 420 (4.11), 472 (4.68), 560 (4.10), 593 (3.69).

Preparation of Chiral Chloroiron Complexes.[22] Anhydrous $FeCl_3$ (18 mg) and Fe wire (12 mg) were refluxed in THF (50 mL) for 15h under dry nitrogen. After cooling to room temperature, a THF solution (5 mL) an optically active free base porphyrin (**2a**) (30 mg) was added and the mixture was refluxed for 10 h under nitrogen. Then, the reaction mixture was poured

into a mixture of water and $CHCl_3$. The organic layer was separated and washed twice with 2N HCl, dried over anhydrous Na_2SO_4, and evaporated to dryness. Recrystallization of the residue from CH_2Cl_2/hexane gave an optically active iron complex (**2d**) as reddish brown crystals in 52 % yield. UV-vis: λmax (log ε) 376 (4.75), 503 (4.05), 534 (3.70), 635 (3.41).

Oxidation Reactions.

Asymetric Epoxidation. In a standard experiment, to a 20-mL Schlenk flask containing a stirring bar, a dry CH_2Cl_2 solution (1 mL) of a manganese porphyrin (1.8 μmol), imidazole (10 equiv), and biphenyl or naphthalene (4 ~ 5 mg, GC standard) were successively added. After the solution was degassed and cooled to -10 - -20 °C, an olefin (500 equiv) and iodosobenzene (100 equiv) were added, and the mixture was stirred for 3 h. An aliquot of the reaction mixture was subjected to GC analysis to determine the yield of epoxide. The residue was evaporated and subjected to flash column chromatography on silica gel with hexane/ether (80/20 v/v) as eluent, affording the analytically pure epoxide, which was analyzed by ^1H NMR in $CDCl_3$ containing a chiral shift reagent, tris[3-[(heptafluoropropyl)hydroxymethylene]-(+)-camphorato]europium(III) ($Eu(hfc)_3$), to determine the enantiomeric excess. The absolute configuration was determined by polarimetry with sodium D-line.[23]

Competitive Epoxidation. To a 20-mL Schlenk flask containing a stirring bar, a dry CH_2Cl_2 solution (0.5 mL) of a manganese porphyrin (1.0 μmol), 1-ethylimidazole (10 μmol), and naphthalene (4 ~ 5 mg, GC standard)

were successively added. To this solution were added two olefins (250 μmol each), and then iodosobenzene (100 μmol), and the mixture was stirred at -10 °C under nitrogen for 1 h. The yields of epoxides and the conversions of olefins were determined by GC analysis of an aliquot of the reaction mixture.

Asymmetric Oxidation of Sulfides. To a 20-mL Schlenk flask containing biphenyl (13 mg, GC standard) and the imidazole (1080 μmol) under nitrogen were successively added sulfide (900 μmol) and a CH_2Cl_2 solution of **2d** (1.8 μmol / 1mL) and the solution was degassed by freeze-to thaw cycles. Then iodosobenzene (PhIO) (360 μmol) was added to the flask thermostated at -43 °C. An aliquot of the reaction mixture was subjected to GC analysis to determine the yield of sulfoxide. The residue was evaporated and subjected to flash column chromatography on silica gel with dichloromethane as eluent, affording the analytically pure sulfoxide, which was analyzed by ^1H NMR in $CDCl_3$ containing a chiral shift reagent, (*R*)-1,1'-bi-2-naphtol (1 - 2 equiv of the sulfoxide), to determine the enantiomeric excess.[24] The absolute configuration was determined by polarimetry with sodium D-line.

Determination of Association Constants. Association constants for imidazole coordination to **2c**, equation **[1]**, were measured by spectroscopic titration technique.[12] The data were fitted to the equation **[2]**, using $(A_0 - A_\infty) / (A - A_\infty)$ to calculate the concentration ratio, where A_0 and A_∞ are the absorbances for non-coordinated and coordinated species, respectively, at 472 nm, and the A is the absorbance at any intermediate added imidazole concentration. Values of log *K* were determined from the intercept of the line

$$Mn(P)Cl + x\,Im \underset{}{\overset{K}{\rightleftharpoons}} Mn(P)(Im)_xCl \qquad [1]$$

$$\ln K = \ln ([Mn(P)(Im)_x] / [Mn(P)Cl]) - x \ln [Im] \qquad [2]$$

$$\frac{[Mn(P)(Im)_x]}{[Mn(P)Cl]} = \frac{A_0 - A}{A - A_\infty}$$

for a plot of log $[(A_\infty - A_0) / (A - A_\infty)]$ versus log [imidazole]; the slopes (r values) were 1.02 (0.996) and 1.04 (0.999) for imidazole and 2-phenylimidazole, respectively, indicating the one to one coordination of imidazoles to **2c**. Using a similar technique, the association constant of imidazole to the iron complex **2d** was determined.

Measurements.

^1H NMR spectra were measured in $CDCl_3$ on a JEOL Type GSX-270 spectrometer operating at 270 MHz, where the chemical shifts were determined with respect to internal $CHCl_3$ (δ7.28). Absorption spectra were measured in $CHCl_3$ on a JASCO Type U-best 50 spectrometer by using a quartz cell of 1-cm path length. Circular dichroism spectra were recorded on a JASCO Type J-500 spectropolarimeter in a quartz cell of 1-cm path length using the following parameters: sensitivity, 2 mdeg; time constant, 2 sec; scan speed 10 nm $\cdot$ min^{-1}. Gas chromatographic analyses were performed on an Ohkura Gas Chromatograph Model-103 equipped with a RASCOT stainless capillary column (OV-101, 0.25 mm x 25 m), or a Shimadzu Gas Chromatograph Model GC-14A equipped with a Shimadzu fused silica

capillary column (CBP20-M25-025, 0.2 mm x 25 m). FAB-HRMS measurements were performed on a JEOL JMS-HX110 spectrometer. Optical rotation measurements were performed on a JASCO Model DIP-360 digital polarimeter.

References and Notes

1. (a) Ortiz de Montellano, P. R.; Kunze, K. L.; Belian, H. S. *J. Biol. Chem.* **1983**, *258*, 45. (b) Kunze, K. L.; Mangold, B. L. K.; Wheeler, C.; Belian. H. S.; Ortiz de Montellano, P. R. *J. Biol. Chem.* **1983**, *258*, 4202.

2. (a) Miwa, G. T.; Lu, A. Y. H. The Topology of the Mammalian Cytochrome P-450 Active Site. In *Cytochrome P-450, Structure Mechanism, and Biochemistry*; Ortiz de Montellano, P. R., Ed.; Plenum Press: New York and London, **1986**; pp 77-88. (b) Harris, C.; Philpot, R. M.; Hernandez, O.; Bend, J. R. *J. Pharmacol. Exp. Ther.* **1989**, *248*, 492. (c) Foureman, G. L.; Harris, C.; Guengerich, F. P.; Bend, J. R. *J. Pharmacol. Exp. Ther.* **1986**, *236*, 144. (d) Ortiz de Montellano, P. R.; Fruetel, J. A.; Collins, J. R.; Camper, D. L.; Loew, G. H. *J. Am. Chem. Soc.* **1991**, *113*, 3195.

3. (a) Waxman, D. J.; Light, D. R.; Walsh, C. *Biochemistry* **1982**, *21*, 2499. (b) Takata, T.; Yamazaki, M.; Fujimori, K.; Kim, Y. H.; Iyanagi, T.; Oae, S. *Bull. Chem. Soc. Jpn.* **1983**, *56*, 2300.

4. (a) Groves, J. T.; Myers, R. S. *J. Am. Chem. Soc.* **1983**, *105*, 5791. (b) Groves, J. T.; Viski, P. *J. Am. Chem. Soc.* **1989**, *111*, 8537. (c) Groves, J. T.; Viski, P. *J. Org. Chem.* **1990**, *55*, 3628.

5. (a) Mansuy, D.; Battioni, P.; Renaud, J. P.; Guerin, P. *J. Chem. Soc., Chem. Commun.*, ***1985***, 155. (b) Renaud, J. P.; Battioni, P.; Mansuy, D. *Nouv. J. Chem.* **1987**, *11*, 280.

6. (a) Naruta, Y.; Tani, F.; Maruyama, K. *Chem. Lett.* ***1989***, 1269. (b) Naruta, Y.; Tani, F.; Maruyama, K. *J. Chem. Soc., Chem. Commun.*, ***1990***, 1378. (c) Naruta, Y.; Tani, F.; Ishihara, N.; Maruyama, K. *J. Am. Chem. Soc.* **1991**, *113*, 1378. (d) Naruta, Y.; Tani, F.; Maruyama, K. *Tetrahedron Asymmetry:* **1991**, *2*, 533. (e) Naruta, Y.; Ishihara, N.; Tani, F.; Maruyama, K. *Chem. Lett.* **1991**, 1933. (f) Naruta, Y.; Tani, F.; Maruyama, K. *Tetrahedron. Lett.* **1992**, *33*, 1269.

7. (a) O'Malley, S; Kodadek, T. J. *J. Am. Chem. Soc.* **1989**, *111*, 9116. (b) Collman, J. P.; Zhang, X.; Hembre, R. T.; Brauman, J. I. *J. Am. Chem. Soc.* **1990**, *112*, 5356. (c) Collamn, J. P.; Zhang, X.; Lee, V. J.; Brauman, J. I. *J. Chem. Soc., Chem. Commun.*, ***1992***, 1647. (d) Halterman, R. L.; Jan, S.-T. *J. Org. Chem.* **1991**, *56*, 5253.

8. The direct resolution of the antipodes of the chloroiron compex (**2d**) in a preparative scale failed due to the low solubility of **2d** in the eluent.

9. The yield of styrene oxide, as determined based on the amount of the converted styrene (10.2 %, by GC), was 84 %.

10. When the chiral iron complex ((+)-**2d**) was used as catalyst coupled with imidazole, (*R*)-styrene oxide was formed in 30 % *ee* (18 % yield) under the similar conditions.

11. Use of sodium hypochlorite as oxidant with **2d** / pyridine under the phase transfer conditions (Guilmet, E.; Meunier, B. *Nouv. J. Chem.* **1982**, *6*, 51.) yielded (*R*)-styrene oxide with comparable enantioselectivity (46 % *ee*, 88 % yield).

12. Ariel, S.; Dolphin, D.; Domazeits, G.; James, B. R.; Leung, T. W.; Rettig, S. J.; Trotter, J.; Williams, G. M. *Can. J. Chem.* **1984**, *62*, 755.

13. A similar observation has been reported by Collman *et. al.* for the coordination of 1-methylimidazole to a bromomanganese(III) complex of picnic

basket porphyrin, where only one imidazole binds to form a five- coordinate manganese complex: Collman, J. P.; Brauman, J. I.; Fitzgerald, J. P.; Hampton, P. D.; Naruta, Y.; Michida, T. *Bull. Chem. Soc. Jpn.* **1988**, *61*, 47.

14. The chiral manganese complex ((+)-**2c**) coupled with imidazole also catalyzed the oxidation of thioanisole under similar conditions (96 % yield), but no enantioselection was observed to give racemic methyl phenyl sulfoxide.

15. Chang, C. K. *J. Am. Chem. Soc.* **1977**, *99*, 2819.

16. Battersby, A. R.; Hunt, E.; McDonald, E.; Paine III, J. P.; Saunders, J. *J. Chem. Soc. Perkin Trans. 1*, **1976**, 1008.

17. Collman, J. P.; Denisevich, P.; Konai, Y.; Marrocco, M.; Koval, C.; Anson, F, C. *J. Am. Chem Soc.* **1980**, *102*, 6027.

18. Ogoshi, H.; Sugimoto, H.; Miyake, M.; Yoshida, Z. *Tetrahedron* **1984**, *40*, 579.

19. Buchler, J. W. Static Coordination Chemistry of Metallopophyrins. In *Porphyrins and Metalloporphyrins*; Smith, K. M., Ed.; Elsevier: Amsterdam, Oxford, and New York, **1975**; pp 157 - 231.

20. (a) Okamoto, Y.; Hatada, K. *Chem. Lett.* **1986**, 1237. (b) Okamoto, Y.; Kawashima, M; Hatada, K. *J. Chromatogr.* **1986**, *363*, 173.

21. Jones, R. D.; Summerville, D. A.; Basolo, F. *J. Am. Chem, Soc.* **1978**, *100*, 4416.

22. David, S.; James, B. R.; Dolphin, D. *J. Inorg. Biochem.* **1988**, *28*, 125.

23. See ref. 4(c) and references cited therein.

24. S. Shinkai.; Yamaguchi, T.; Manabe, O.; Toda, F. *J. Chem. Soc., Chem. Commun.*, **1988**, 1399.

CHAPTER 5

A Novel Anion - Binding Chiral Receptor Based on a Metalloporphyrin with Molecular Asymmetry. Highly Enantioselective Recognition of Amino Acid Derivatives.

Abstract

A chiral zinc *N*-methylated strapped porphyrin (**3c**) with molecular asymmetry, featuring a metal atom to bind a carboxylate anion and a rigid *p*-xylylene strap anchored via two amide linkages, was synthesized from mesoporphyrin II with enantiotopic faces, and the optical isomers were resolved by HPLC. By using **3c** as a chiral receptor, the highly enantioselective binding was achieved for the carboxylate anions of *N*-benzyloxycarbonyl-, -*tert*-butoxycarbonyl-, -(3,5-dinitrobenzoyl)-, and -acetyl-amino acids. Infrared studies demonstrated the crucial role of the hydrogen bonding interaction between the receptor and substrates in the chiral recognition.

Introduction

Design of enantioselective receptors has been a major objective in molecular recognition. To achieve high chiroselectivity, a number of recognition features should be incorporated and oriented within the binding site to complement the chemical characteristics of the substrate. Recent developments in this area promise to provide new approaches to enantiomer separation as well as new chiral environments and reagents for asymmetric synthesis and catalyst. In connection with this, asymmetric recognition of amino acids and their derivatives has attracted much attention, and some chiral receptors have been reported.[1] However to date, there have been only a few chiral receptors which are capable of enantioselectively binding carboxylate anions of amino acids, and to our knowledge, the results are not satisfactory for carboxylate salts of amino acids (enantioselectivity < 20 % *ee*).[2]

The author now wishes to describe the molecular design of a novel anion - binding chiral receptor (**3c**) based on a metalloporphyrin with molecular asymmetry, and its prominent ability to enantioselectively recognize carboxylate anions of *N*-protected amino acids.[3] The synthetic strategy here takes advantage of the rigid conformation and enantiotopic structure of mesoporphyrin II, to which the functionalities for (1) electrostatic (central metal), (2) hydrogen bonding (amide linkages), and (3) van der Waals (aromatic strap) interactions are logically incorporated and arranged. By using this strategically designed

receptor, the author has attempted three dimensional (chiral) molecular recognition of *N*-protected amino acid carboxylates .

Results and Discussion

Synthesis of Chiral Metalloporphyrin Receptor 3c. The synthesis of **3c** was achieved in three steps from mesoporphyrin II (**1a**) having enantiotopic faces. Condensation of the mixed acid anhydride of **1a** with 1,4-xylylenediamine gave *p*-xylylene-strapped porphyrin (**3a**),[4] which was reacted with methyl iodide to afford the *N*-methylated strapped porphyrin (**3b**).[5] Comparison of the ^{13}C NMR chemical shift ($CDCl_3$, 25 °C) of the *N*-methyl signal of **2c** (δ 35.5), derived from **3b**, with those of *N*-methylcoproporphyrin I tetramethyl ester (δ 35.6) and *N*-methyletioporphyrin I (**4c**) (δ 34.0) demonstrated that the *N*-methylation occurs exclusively at one of the nitrogen atoms of the pyrrole units linked to the

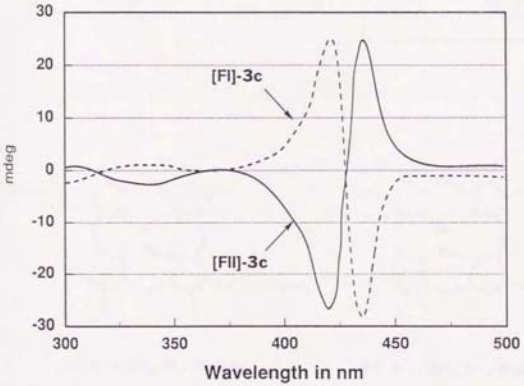

Figure 1. Circular dichroism spectra of the antipodes of **3c** in $CHCl_3$ at room temperature.

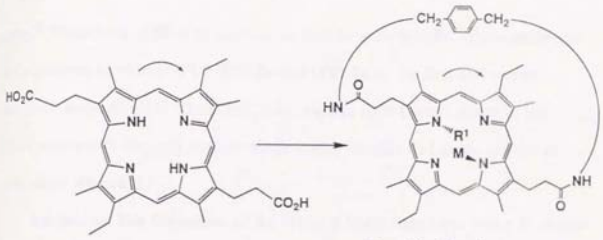

1a

Mesoporphyrin II

3a $R^1 = M = H$

3b $R^1 = CH_3$, $M = H$

3c $R^1 = CH_3$, $M = ZnOAc$

3d $R^1 = CH_3$, $M = ZnX$

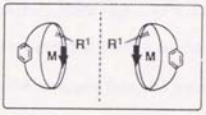

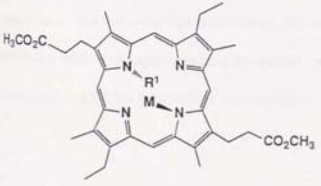

2c $R^1 = CH_3$, $M = ZnOAc$

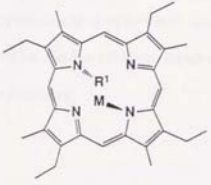

4c $R^1 = CH_3$, $M = ZnOAc$

4d $R^1 = CH_3$, $M = ZnX$

strap.[6] Treatment of **3b** with methanolic $Zn(OAc)_2$ yielded **3c**, whose antipodes were resolved by chiral HPLC (**[FI]-3c** and **[FII]-3c** as the first and second fractions, respectively).[7] These antipodes showed split Cotton effects in the Soret region (426 nm) and perfect mirror-image circular dichroism spectra of each other (**Figure 1**).

Studies on the Structure of 3c. The ^1H NMR signal due to the *N*-methyl group of **3c** (δ -4.04) appeared at the downfield region relative to that of **2c**[8] (δ -4.68), because of the distortion of the porphyrin skeleton induced by strapping.[9] On the contrary, despite this weakened shielding effect of the porphyrin ring, the signal due to the axial acetate group was observed at the upfield region (δ -1.32) compared with that of **2c** (δ -1.04). Thus, the *N*-methyl group is located on the unstrapped face of **3c**, while the acetate group is on the strapped face and more strongly shielded by the proximal *p*-xylylene unit. **Figure 2** shows the molecular structure of an antipode of **3c**, optimized with molecular mechanics (MM2) calculation.[10] Within the chiral binding site of **3c** are arranged (i) a metal atom to bind a carboxylate anion, (ii) two topologically inequivalent amide functions with hydrogen bonding capability, and (iii) a rigid *p*-xylylene strap as an aromatic wall for additional interaction with substrates.

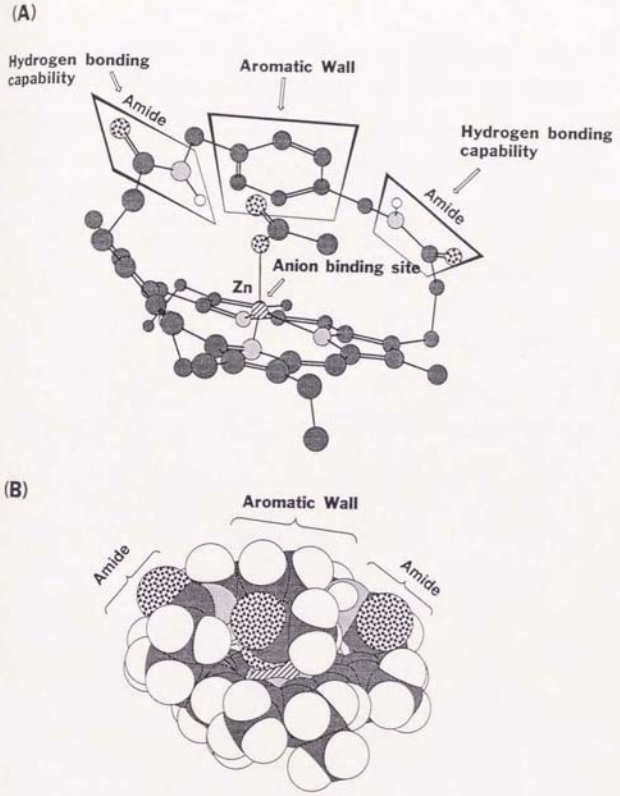

Figure 2. Ball and stick (**A**) and space-filling (**B**) models of an optimized structure of an antipode of **3c**.

Chiral Recognition of Amino Acid Derivatives. Asymmetric binding of carboxylate anions with **3c** was investigated by single - extraction experiment. For example, when a $CHCl_3$ solution of **[Fl]-3c** was shaken with an aqueous solution of *N*-benzyloxycarbonyl-DL-valine (*N*-Cbz-DL-Val) sodium salt (2 equiv), axial ligand exchange took place smoothly and quantitatively to give a mixture of two diastereoisomeric zinc *N*-Cbz-valinate complexes, L-**[Fl]-3d** and D-**[Fl]-3d** (X = $O_2CC^*H(^iPr)NHCbz$) with the mole ratio, as determined by ^1H NMR, of 92 : 8.[11] Upon treatment of the above mixture with trifluoroacetic acid, the

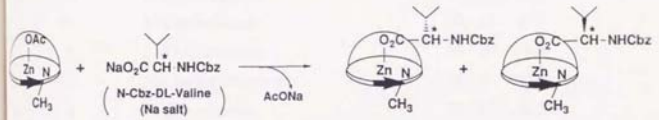

[Fl]-**1b**

L-[Fl]-**1c** 92 %

D-[Fl]-**1c** 8 %

Scheme 1

complexes were completely demetallated to release *N*-Cbz-valine with the L : D ratio, as determined by HPLC, of 90 : 10. Thus, the **[Fl]**-receptor preferentially binds the L-isomer of *N*-Cbz-Val.

Table I summarizes the results of the single - extraction of a variety of racemic substrates with racemic **3c**, where the high enantioselectivities with the ratios of the major to the minor diastereoisomer pairs of 96 : 4 to 23 : 77 were observed for the substrates having NHCO moieties (**runs 1, 3 - 6,** and **8 - 13**). Except for the case of *N*-Cbz-serinate having a hydroxyl function with hydrogen

Table I. Single - Extraction Experiments of Sodium Salts of Racemic *N*-Protected Amino Acids with Racemic **3c**.[13]

run	substrate[a]	[L-**[FI]-** + D-**[FII]-3d**] / [L-**[FII]-** + D-**[FI]-3d**]
1	*N*-Cbz-alaninate	91 / 9 (10.1)
2	*N*-Cbz-*N*-methylalaninate	50 / 50 (1.0)
3	*N*-Cbz-valinate	96 / 4 (21.2)
4	*N*-Boc-valinate	95 / 5 (19.9)
5	*N*-Acetylvalinate	85 / 15 (5.6)
6	*N*-Cbz-leucinate	85 / 15 (5.8)
7	*N*-Cbz-prolinate	50 / 50 (1.0)
8	*N*-Cbz-methioninate	91 / 9 (10.2)
9	*N*-Cbz-serinate	23 / 77 (0.3)
10	*N*-Cbz-phenylglycinate	91 / 9 (9.6)
11	*N*-(3,5-Dinitrobenzoyl)-phenylglycinate	96 / 4 (23.4)
12	*N*-Cbz-phenylalaninate	84 / 16 (5.1)
13	*N*-Cbz-tryptophanate	89 / 11 (8.5)

[a] Cbz: benzyloxycarbonyl, Boc: *tert*-butoxycarbonyl.

bonding capability (**run 9**), **[FI]**- and **[FII]**-receptors preferentially bind L- and D-substrates, respectively.[11] Among the substrates examined, the highest enantioselectivity was observed for *N*-(3,5-dinitrobenzoyl)-phenylglycinate, where the ratio [L-**[FI]**- + D-**[FII]-3d**] / [L-**[FII]**- + D-**[FI]-3d**] of 23.4 was achieved (**run 11**). As for the effect of the *N*-protective group of the substrate, the enantioselectivity for *N-tert*-butoxycarbonyl (Boc) - valinate (19.9, **run 4**) was comparably high to that for the *N*-Cbz analogue (21.2, **run 3**), while the *N*-acetyl analogue was less enantioselectively recognized (5.8, **run 5**). In sharp contrast, no enantioselection was observed for *N*-Cbz-*N*-methylalaninate and *N*-Cbz-prolinate having no NHCO functionality (**runs 2** and **7**).

Mechanism of Chiral Recognition. The high degree of chiral recognition achieved here is considered a result of multiple interaction between the chiral receptor and the substrates. Evidences were given for the hydrogen bond formation *via* the NHCO moieties of the receptor and the substrates. The zinc acetate complex (**3c**) showed a single amide C=O infrared absorption at 1645 cm^{-1} in $CHCl_3$ (**Table II, run 1**), while the *N*-Cbz-glycinate complex (**3d**, X = O_2CCH_2NHCbz) showed an additional amide C=O absorption at a lower wavenumber (1622 cm^{-1}) (**run 2**). As for the carbamate moiety of the binding substrate, the *N*-Cbz-glycinate in **3d** showed the C=O absorption at 1703 cm^{-1} (**run 3**), which was again lower in wavenumber than that of the unstrapped reference complex (**4d**, X = O_2CCH_2NHCbz: 1715 cm^{-1}, **run 4**)). Thus, either of the two NHCO moieties in the receptor molecule participates in the hydrogen

bonding interaction with the substrate. In connection with the lack of enantioselectivity in **runs 2** and **7** in **Table I**, the *N*-methylated analogue of the Cbz-glycinate complex (**3d**, X = $O_2CCH_2N(CH_3)Cbz$), on the contrary, showed no substantial difference in wavenumbers of both amide (1645 cm^{-1}) and carbamate (1692 cm^{-1}) absorptions from those of the reference samples, **3c** (NH*CO*: 1645 cm^{-1}, **run 1** in **Table II**) and **4d** (X = $O_2CCH_2N(CH_3)Cbz$) ($N(CH_3)CO$: 1695 cm^{-1}, **run 5** in **Table II**).

Table II. Wavenumbers of carbonyl infrared absorptions (cm^{-1}) of the zinc complexes **3c, 3d** and **4d** in $CHCl_3$.

run	porphyrin	carboxylate	strap amide	Cbz carbamate
1	**3c** (acetate)	1605	1645	———
2	**3d** (*N*-Cbz-glycinate) (X = O_2CCH_2NHCbz)	1605	1645 1622	1703
3	**3d** (*N*-Cbz-sarcosinate) (X = $O_2CCH_2N(CH_3)Cbz$)	1603	1645	1692
4	**4d** (*N*-Cbz-glycinate) (X = O_2CCH_2NHCbz)	1603	———	1715
5	**4d** (*N*-Cbz-sarcosinate) (X = $O_2CCH_2N(CH_3)Cbz$)	1603	———	1695

Taking all the above results into account, the anionic substrates are bound to the receptor via (1) the bond - forming (electrostatic) interaction between the carboxylate functionality of the substrate and the zinc atom of the receptor, and (2) the hydrogen bonding interaction of the NHCO functionality of the substrate with either of the two amide moieties of the receptor, as schematically illustrated in **Figure 3**. An additional repulsive or attractive interaction of the amino acid residue with the *p*-xylylene unit (aromatic wall) of the receptor would accomplish the three - dimensional recognition of the chiral substrate.

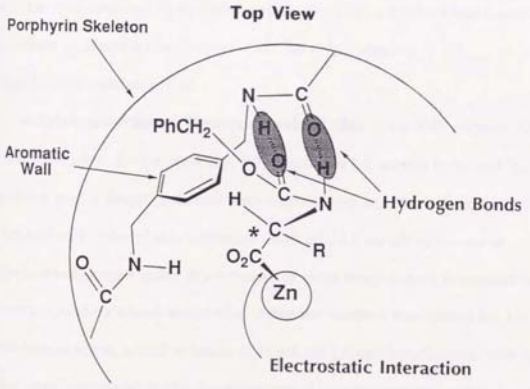

Figure 3. Schematic representation of the proposed structure of **3d** bound with *N*-Cbz-amino acid.

Experimental Section

Materials.

Tetrahydrofuran (THF) was distilled over sodium benzophenone ketyl just before use. Mesoporphyrin II dimethyl ester (2,12-bis(2'-(methoxycarbonyl)ethyl)-3,8,13,18-tetramethyl-7,17-diethylporphine) was synthesized from 4-methyl-3-(methoxycarbonyl)ethyl-5-methylpyrrole-2-carboxylic acid[12] and 4-methyl-5-formyl-3-ethylpyrrole-2-carboxylic acid by a similar procedure reported by Collman *et. al.*.[13] Mesoporphyrin II dicarboxylic acid (**1a**) was obtained by hydrolysis of the dimethyl ester by using a similar procedure as described in Chapter 4 for the preparation of dihexyldeutereoporphyrin II.

***p*-Xylylene-strapped Mesoporphyrin II (3a).** To a THF solution (320 mL) of mesoporphyrin II (**1a**) (594 mg, 1.0 mmol) in a 1-L round- bottomed flask equipped with a dropping funnel were successively added triethylamine (0.7 mL, 5.3 mmol) and isobutyl chloroformate (0.31 mL, 2.4 mmol) by means of hypodermic syringes under dry nitrogen at room temperature to convert 1a into the corresponding mixed anhydride. After the mixture was stirred for 1 h at room temperature, a THF solution (170 mL) of 1,4-xylylenediamine (409 mg, 3.0 mmol) was introduced to the dropping funnel by a syringe and added dropwise to the mixed anhydride solution over a period of 5 h. The mixture was stirred for additional 36 h at room temperature under dry nitrogen and evaporated to

dryness. The residue dissolved in CH_2Cl_2 (200 mL) was filtered from insoluble fractions by passing through Celite, and the filtrate was concentrated to a small volume, which was chromatographed on silica gel (Wakogel C-300). After a brown band was eluted with CH_2Cl_2, a red band was eluted with $CHCl_3$/acetone (90/10 v/v), which was collected and evaporated to dryness, and the residue was recrystallized from CH_2Cl_2 / hexane to give **3a** as a reddish purple powder (300 mg, 45 % yield). FAB-MS, m/z 667 (MH^+).

***p*-Xylylene-strapped N-methylmesoporphyrin II (3b).** In a 500-mL round - bottomed flask equipped with a reflux condenser were placed **3a** (300 mg, 0.45 mmol), $CHCl_3$ (160 mL), methyl iodide (30 mL, 0.48 mol), and acetic acid (10 mL), and the mixture was stirred at 55 °C. After 40 h, the reaction mixture was poured into saturated aq. $NaHCO_3$. The organic layer separated was washed successively with aq. ammonia (28 %) and saturated aq. NaCl, dried over anhydrous Na_2SO_4, and evaporated to dryness. The residue dissolved in a minimum volume of CH_2Cl_2 was loaded on a silica gel column (Wakogel, C-200) prepared from $CHCl_3$ slurry. Unreacted 3a was first eluted with $CHCl_3$/acetone (90/10 v/v) as a red band. The red protonated porphyrin fraction remained at the top of the column was eluted with CH_2Cl_2/ethanol/diethylamine (90/9/1 v/v), collected, and evaporated. Recrystallization of the residue from CH_2Cl_2/hexane gave **3b** as a purple powder (153 mg, 50 % yield). FAB-HRMS for $C_{43}H_{49}N_6O_2$ (MH^+): calcd m/z 681.3917; obsd 681.3963.

The zinc acetate complex of *p*-Xylylene-strapped

N-methylmesoporphyrin II (3c). To a $CHCl_3$ solution (10 mL) of **3b** (68 mg, 0.1 mmol) was added a saturated methanolic $Zn(OAc)_2$ (2 mL) and the mixture was refluxed for 2 h. The reaction mixture was cooled and washed twice with saturated aqueous CH_3CO_2Na. The organic layer separated was dried over anhydrous Na_2SO_4 and filtered. The filtrate was evaporated to dryness under reduced pressure, and the residue was recrystallized from CH_2Cl_2/cyclohexane to give **3c** as purple crystals in quantitative yield. Anal. Calcd for $C_{45}H_{50}N_6O_4Zn \cdot CH_2Cl_2 \cdot 1/2(C_6H_{12}) \cdot H_2O$: C, 61.99; H, 6.37; N, 8.85. Found: C, 62.30; H, 6.26; N, 8.97. FAB-HRMS for $C_{45}H_{47}N_6O_2Zn$ (M^+ - OAc): calcd m/z 743.3052; obsd 743.3052. UV-vis λmax ($CHCl_3$), nm (log ε): 625 (3.40), 583 (3.90), 541 (3.84), 426 (5.04). ^1H NMR ($CDCl_3$, 55 °C): δ 10.24, 10.13, 9.98, 9.92 (s x 4, 4H, meso), 5.46 and 4.66 (d x 2, 4H, C_6H_4), 4.50 - 4.34 (m, overlapped, 4H, diastereotopic porph-CH_2CH_2CO (3H), $CHaHbC_6H_4CH_2$ (1H), and N-H (1H)), 4.17 (q, 2H, porph-CH_2CH_3), 4.05 - 3.95 (m, overlapped, 3H, diastereotopic porph-CH_2CH_2CO (1H) and porph-CH_2CH_3 (2H)), 3.73, 3.68, 3.52, 3.16 (s x 4, 12H, pyr-CH_3), 3.52 - 3.43 (overlapped, 2H, $CHaHbC_6H_4CH_2$ (1H), N-H (1H)), 3.04 (ddd, diastereotopic porph-CH_2CH_2CO (1H)), 2.77 (ddd, 1H, diastereotopic porph-CH_2CH_2CO), 2.71(d, 1H, $CH_2C_6H_4CHcHd$), 2.45 (dd, 1H, diastereotopic porph-CH_2CH_2CO), 2.08 (d, 1H, $CH_2C_6H_4CHcHd$), 2.00 and 1.80 (t x 2, 6H, porph-CH_2CH_3), 0.70 (dd, 1H, diastereotopic porph-CH_2CH_2CO), -1.32 (s, 3H, CH_3CO_2), -4.04 (s, 3H, N-CH_3). These assignments were supported from the 2D-COSY-NMR. IR ($CHCl_3$, 25 °C) 3291 (br, NH), 1645 (amide C=O), 1605

(carboxylate C=O) cm^{-1}.

Optical Resolutions by HPLC.

Resolutions of the optical antipodes of **3c** was carried out by using 0.46 x 250 mm (analytical) or 20 x 500 mm (preparative) HPLC column packed with silica gel coated with cellulose tris(3,5-dimethylphenylcarbamate) as a chiral stationary phase. HPLC experiments with the analytical column were performed on a JASCO Type TWINCLE equipped with a JASCO Type 875-UV variable wavelength detector at a flow rate of 1.0 mL·min^{-1} at room temperature and monitored at 390 nm. HPLC experiments with the preparative column were performed on a JASCO Type 887-PU pump equipped with a JASCO Type 875-UV variable wavelength detector, a JASCO Type 802-SC system controller, and a JASCO Type 892-01 column selector at a flow rate of 10.0 mL·min^{-1} at room temperature and monitored at 410 nm. Column; CHIRALCEL OD (Daicel), eluent; hexane / 2-propanol (90 / 10 v/v)

Chiral Recognition Experiments. A $CHCl_3$ (2 mL) solution of **3c** (10 μmol) was stirred for 10 h with an aqueous solution (2 mL) of the substrate (100 μmol) at room temperature. The organic layer separated was washed with water, dried over Na_2SO_4, and filtered, and the residue after stripping off the volatile fraction was subjected to ^1H NMR analysis in $CDCl_3$ (0.5 mL). **3c** was quantitatively converted into **3d** in every case. The diastereoisomer ratios of **3d** were determined from the intensity ratios of the two well - distinguishable *N*-methyl signals, since the signals due to the axial ligands were poorly

separated except for the alaninate and valinate complexes.

Measurements.

^1H NMR spectra were measured in $CDCl_3$ on a JEOL Type GSX-270 spectrometer operating at 270 MHz, where the chemical shifts were determined with respect to internal $CHCl_3$ (δ 7.28). Absorption and spectra were measured in $CHCl_3$ on a JASCO Type U-best 50 spectrometer by using a quartz cell of 1-cm path length. Infra red spectra were measured on a JASCO Type IR-5300 spectrometer using a NaCl cell of 1-mm path length. Circular dichroism spectra were recorded on a Jasco Type J-720 spectropolarimeter with the following parameters: sensitivity, 10 mdeg; step resolution, 2 nm / data; response, 4 sec; scan speed, 50 nm-min^{-1}; accumulation, 16 times, using a quartz cell of 1-cm path length; optical density of sample ($CHCl_3$), 2.0 at 424 nm.

References and Notes

1. For amino acids and their derivatives: (a) Peacock, S. C.; Domeier, L. A.; Gaeta, F. C. A.; Helgeston, R. C.; Timko, J. M.; Cram, D. J. *J. Am. Chem. Soc.* **1978**, *100*, 8190. (b) Davidson, R. B.; Bradshaw, J. S.; Jones, B. A.; Dalley, N. K.; Christensen, J. J.; Izatt, R. M. *J. Org. Chem.* **1984**, *49*, 353. (c) Rebek, J., Jr.; Askew, B.; Ballester, P.; Doa, M. *J. Am. Chem. Soc.* **1987**, *109*, 4119. (d) Sanderson, P. E. J.; Kilburn, J. D.; Still, W. C. *J. Am. Chem. Soc.* **1989**, *111*, 8314. (e) Liu, R.; Sanderson, P. E. J.; Still, W. C. *J. Org. Chem.* **1990**, *55*, 5184. (f) Jeong, K.-S.; Muehldorf, A. V.; Rebek, J., Jr. *J. Am. Chem. Soc.* **1990**, *112*, 6144. (g) Hong, J,.-I.; Namgoong, S. K.; Bernardi, A.; Still, W. C. *J. Am. Chem. Soc.* **1991**, *113*, 5111. (h) Galan, A.; Andreu, D.; Echavarren, A. M.; Prados, P.; de Mendoza, J. *J. Am. Chem. Soc.* **1992**, *114*, 1511.

2. Echavarren, A.; Galan, A.; Lehn, J.-L.; de Mendoza, J. *J. Am. Chem. Soc.* **1989**, *111*, 4994.

3. For use of chiral porphyrins for molecular recognition: (a) Le Maux, P.; Bahri, H,: Simonneaux, G. *J. Chem. Soc., Chem. Commun.*, **1992**, 1350. (b) Aoyama, Y.; Uzawa, T.; Saita, K.; Tanaka, Y.; Toi, H.; Ogoshi, H.

Tetrahedron Lett. **1988**, *29*, 5271.

4. For chiral strapped porphyrins: see chapter 4.

5. For chiral *N*-alkylated porphyrins: see chapters 1 and 2.

6. The transformation of **3c** into **2c** was accomplished by acidolysis of the amide linkages, followed by esterification of the resulting CO_2H moieties of **1b** with MeOH / H_2SO_4, and metalation of the dimethyl ester **2b** with $Zn(OAc)_2$.

7. See other chapters in this thesis.

8. Derived from **3c** according to ref 6.

9. The intensity ratio of the Q-band III (535 nm) to Q-band IV (501 nm) of **3a** (0.88) was higher than that of the unstrapped analogue (**2a**) (0.73). A similar tendency has been reported for some distorted strapped porphyrins: Morgan, B,; Dolphin, D.; Jones, R. H.; Jones, T.; Einstein, F. W. B. *J. Org. Chem.* **1987**, *52*, 4628.

10. The CAChe Worksystem (SONY Tektronics) was used.

11. The diastereoisomers of **3d** were identified on the basis of the ^{1}H NMR spectra of the authentic samples prepared from **(Fl)-3c** and the optically pure substrates. The diastereoisomer ratios were determined from the intensity ratios of the two well - distinguishable *N*-methyl signals.

12. Chang, C. K. *J. Am. Chem. Soc.* **1977**, *99*, 2819.

13. Collman, J. P.; Denisevich, P.; Konai, Y.; Marrocco, M.; Koval, C.; Anson, F, C. *J. Am. Chem Soc.* **1980**, *102*, 6027.

CHAPTER 6

Diastreoselective and Enantioselective Hydrogen Transfer from Alcohols to Carbonyl Compounds Catalyzed by Aluminum Porphyrins. Stereochemical Aspects.

Abstract

Highly diastereoselective reductions of methylcyclohexanones with alcohols such as 2-propanol, (-)-borneol, or (±)-isoborneol were brought about by using chloroaluminium porphyrins, (5,10,15,20-tetraphenylporphinato) aluminum chloride or (etioporphinato) aluminum chloride, as catalysts. When an optically active alcohol such as (-)-isoborneol was used, enantioselective reductions of prochiral phenones such as isopropyl- or cyclohexyl- phenyl ketone took place. ^{1}H NMR and UV-Vis studies demonstrated the coordination of ketone and alcohol to the central aluminum atom of the catalyst, and the acyclic transition model by the simultaneous participation of two aluminum porphyrin molecules was proposed for the hydrogen transfer from alcohol to ketone.

Introduction

The reactions of metalloporphyrins have received particular attentions in relation to biochemical systems.[1] Since reactions take place as for the substrate and/or the reagent coordinated to the metal on a rigid macrocycle of porphyrin, notable stereospecificities are expected and some investigations in stereochemical aspects have been made in exploiting metalloporphyrins as cytochrome P-450 model systems.[2]

The authors have investigated the reactions of aluminum porphyrins and found ambiphilic features, nucleophilicity of axial ligand and Lewis acidity. Bases such as 1-methylimidazole coordinate to the central metal from the back side of the original axial group due to the Lewis acidity of aluminum atom, and affect the reactivities of the axial ligand.[3] Recently, Inoue *et al.* found that aluminum porphyrin can coordinatively activate carbonyl compounds such as cyclic esters for nucleophilic attack.[4]

In the present chapter is described the novel coordinative activation of carbonyl compounds by aluminum porphyrin developed in the Meerwein-Ponndorf-Verley (MPV) type reduction of aldehydes or ketones with secondary alcohols using the aluminum porphyrins, (TPP)AlX (**1a**) and (EtioP)AlX (**1b**) (EtioP : Etioporphinato-I) as catalysts. The author also provides here the results of the detail investigation of diastereoselective and

1a (TPP)AlX

$R^1 = R^2 = H$, $R^3 = C_6H_5$

1b (EtioP)AlX

$R^1 = CH_3$, $R^2 = C_2H_5$, $R^3 = H$

enantioselective reductions of various ketones and discusses the stereochemical course of the hydrogen transfer process.

Experimental Section

Materials. All ketones were distilled over calcium hydride or anhydrous calcium sulfate under dry nitrogen. 2-Propanol was distilled over magnesium treated with iodine under nitrogen atmosphere. (±)-Isoborneol was recrystallized from ethanol. (+)-Camphor was reduced by $LiAlH_4$ in ether to give (-)-isoborneol contaminated with 11 % (+)-borneol, and the crude mixture thus obtained was subjected to esterification with *o*-nitrobenzoyl chloride / pyridine, followed by steam distillation, to give (-)-isoborneol free from (+)-borneol as a distillate, which was further purified by careful sublimation to afford optically pure (-)-isoborneol (m.p. 209 - 210 °C, $[a]^{25}_D$ -34.0° (c 5, ethanol)).[5] Commercial 2-methylcyclohexanol (*cis/trans* = 27/73) was distilled over anhydrous magnesium sulfate under nitrogen. 2-Methylcyclohexanol with a *cis/trans* isomer ratio of 54/46 was prepared by the reduction of 2-methylcyclohexanone with 2-propanol in the presence of $Al(OCH(CH_3)_2)_3$.[6] 5,10,15,20-Tetraphenylporphine ($TPPH_2$) was synthesized from pyrrole and benzaldehyde in propionic acid and recrystallized from chloroform / methanol.[7] Etioporphyrin-I ($EtioPH_2$) was synthesized from t-butyl 4-ethyl-3,5-dimethylpyrrole-2-carboxylate and recrystallized from chloroform / methanol.[8] Trimethylaluminum (Me_3Al) and diethylaluminum chloride (Et_2AlCl) were fractionally distilled under reduced pressure in a nitrogen

atmosphere. $Al(OCH(CH_3)_2)_3$ distilled under reduced pressure was dissolved in $CHCl_3$ and stored under nitrogen. (-)-Menthyl chloroformate, prepared by the reaction of (-)-menthol with 2 equiv. of phosgene in the presence of quinoline,[9] was dissolved in benzene (1.0 M) and stored under nitrogen. All the solvents used were purified by the standard procedures under nitrogen.

Preparation of Aluminum Porphyrin (1). (5,10,15,20-Tetraphenylporphinato)aluminum chloride ((TPP)AlCl, **1a** (X = Cl)) and (etioporphinato)aluminum chloride ((EtioP)AlCl, **1b** (X = Cl)) were prepared respectively by the reaction of the corresponding free-base porphyrins with 1.2 equiv. of Et_2AlCl in CH_2Cl_2 at room temperature under nitrogen, followed by evaporation of the volatile fractions under reduced pressure.[10] (TPP)AlMe (**1a**, X = CH_3) was prepared by the equimolar reaction between $TPPH_2$ and Me_3Al in CH_2Cl_2 at room temperature under nitrogen.[11] (TPP)$AlOCH(CH_3)_2$ was prepared by the reaction of (TPP)AlMe (**1a**, X = CH_3) with 40 equiv. of 2-propanol in CH_2Cl_2 at room temperature, followed by evaporation to dryness at 55 °C under reduced pressure.[12]

Reduction of Substituted Cyclohexanones with Alcohols catalyzed by Aluminum Porphyrins (1a, 1b). General procedures for the reductions of substituted cyclohexanones with alcohols catalyzed by aluminum porphyrins (**1a**, **1b**) are represented by the following example : To a 50-mL round bottom flask equipped with a three-way stopcock containing 0.5 mmol of (TPP)AlCl (**1a**,

X = Cl) under dry nitrogen, 2-methylcyclohexanone (2.5 mmol) was added by using a hypodermic syringe, and the mixture was stirred for a few minutes at room temperature. Then, a solution of (±)-isoborneol in $CHCl_3$ (2.5 mmol in 4 mL) was added, and the mixture was stirred at 30 °C. Aliquots of the reaction mixture were periodically taken out by means of a hypodermic syringe in a nitrogen stream, and subjected to gas chromatographic (GC) analyses (PEG 20M, column temp; 100 °C initially, then increased at 3 °C/min) to determine the yield and the isomer ratio of 2-methylcyclohexanol produced. For isolation of 2-methylcyclohexanol from the reaction mixture, 2.5 mL of the above reaction mixture after 8 h (100 % yield) was poured into hexane (10 mL), the mixture was filtered from the insoluble catalyst residue, and the filtrate was evaporated by water aspirator to leave an oily residue, which was chromatographed on a silica gel with hexane / $CHCl_3$ (2/1) as eluent to give 164 mg (92 % isolated yield) of an isomeric mixture of 2-methylcyclohexanol (*cis*/*trans* = 5/95) as identified by ^1H NMR and GC/MS analyses. In the case of the reduction with 2-propanol, 2.5 mL of $CHCl_3$ was used as solvent.

Reduction of Prochiral Ketones with (-)-Isoborneol catalyzed by (TPP)AlCl (1a, X = Cl). A representative example of the reduction of prochiral ketones with (-)-isoborneol catalyzed by (TPP)AlCl (**1a**, X = Cl) is as follows : To a stirred mixture of (TPP)AlCl (0.5 mmol) and isopropyl phenyl ketone (2.0 mmol) in $CHCl_3$ (1.5 mL), a $CHCl_3$ solution of (-)-isoborneol (2.0 mmol/1.5 mL)

was added under dry nitrogen, and the mixture was stirred at 55 °C. After 2 h, 0.1 mL of the reaction mixture was taken out and an aliquot was subjected to GC analysis (PEG-20M, 150 °C), by which the yield of 2-methyl-1-phenyl-1-propanol was determined to be 96 %. The residue was treated at room temperature with (-)-mentyl chloroformate (1.0 M benzene solution, 5 equiv. with respect to the alcohol) in the presence of pyridine to afford a diastereoisomeric mixture of (-)-mentyl 2-methyl-1-phenyl-1-propyl carbonate with a GC peak area ratio of 1 : 7.3, which corresponds to 76 % *ee* of the parent alcohol. The reaction mixture remained was poured into hexane (10 mL), from which the insoluble catalyst residue was removed by filtration. The greenish oil, left after the evaporation of the filtrate, was chromatographed on a silica gel with hexane / acetone (10/1) as eluent to afford a crude alcohol, which was subjected to preparative TLC (silica gel, hexane / ethyl acetate (9/1)) to afford 280 mg (93 % isolated yield) of 1-phenyl-2-methyl-1-propanol, as identified by GC-MS and ^{1}H NMR analyses. $[\alpha]^{25}_D$ of the isolated alcohol, after trap-to-trap distillation, was +35.3° (c 5.0, ether), from which the optical purity was estimated to be 72 % (*R*).[13] In excellent agreement with this, the diastereoisomer ratio of the mentyl carbonate derived from the isolated alcohol, as determined by GC analysis, was 1/6.7, which corresponds to 74 % *ee* of the parent alcohol.

Measurements. Gas chromatographic analyses were performed on a Ohkura Model 103 gas chromatograph equipped with a Rascot stainless capillary column (PEG 20M, 30 m), a flame ionization detector, and a Shimadzu Chromatopak C-R3A data processor. GC-MS spectra were taken on a Shimadzu model QP-1000 gas chromatograph / mass spectrometer. ^{1}H NMR analyses were performed in $CDCl_3$ on a JEOL model JNM-GX 400 spectrometer operating at 399.7 MHz, where the chemical shifts were determined with respect to $CHCl_3$ (d 7.28). UV-Vis spectra were recorded on a JASCO model Ubest-50 spectrophotometer, using a quartz cell of 1-cm path length. Optical rotation measurements were performed on a JASCO model DIP-360 digital polarimeter.

Results and Discussion

Reduction of Aldehydes and Ketones. The system of (TPP)AlCl (**1a**, X = Cl) combined with secondary alcohols such as 2-propanol and (±)-isoborneol is found to be effective for the reduction of aldehydes and ketones under mild conditions. For example, cyclohexanone, hexanal and benzaldehyde were reduced by 2-propanol to cyclohexanol,1-hexanol, and benzylalcohol, respectively, with 80, 84, 40 yields, in $CHCl_3$ at 30 °C for 3 h. (*1S*)-(-)-Borneol, a secondary alcohol, was also effective for reduction of cyclohexanone in the presence of (TPP)AlCl, affording cyclohexanol in 88 % yield. Similarly, use of a primary alcohol such as benzyl alcohol coupled with (TPP)AlCl brought about the reduction of cyclohexanone, although very slowly (6 %, 30 °C, 3h). On the other hand, use of *t*-butylalcohol with no carbinol nydrogen, combined with (TPP)AlCl, resulted in no reduction of cyclohexanone under the same conditions. Thus, (TPP)AlCl successfully catalyzed the reduction of aldehydes or ketones with alcohols under the catalytic transfer of the carbinol hydrogen to the carbonyl groups was involved. In marked contrast, when **1a** (X = $OCH(CH_3)_2$) coupled with 2-propanol showed very low catalytic activity in the reduction of benzaldehyde.

Diastereoselective Reduction of Substituted Cyclohexanones with Alcohols catalyzed by Aluminum Porphyrins (1a, 1b). With respect to the

stereochemical course of this hydrogen process, it is noteworthy that reductions of mono-substituted cyclohexanones (**Table 1**). For example, the reduction of 2-methylcyclohexanone with (±)-isoborneol catalyzed by (TPP)AlCl (mole ratio : 5/5/1) proceeded smoothly at 30 °C to afford 2-methylcyclohexanol and camphor quantitatively (runs 1 - 3), where the *cis/trans* isomer ratio of 2-methylcyclohexanol produced is time-dependent. As clearly illustrated in **Figure 1**, the *cis/trans* isomer ratio of the product was 93/7 in the reaction for 0.3 h (93 % yield), which gradually changed with time, even after the quantitative consumption of the 2-methylcyclohexanone, to attain the constant *cis/trans* ratio 5/95 in 5 h. A very similar stereochemical profile was observed

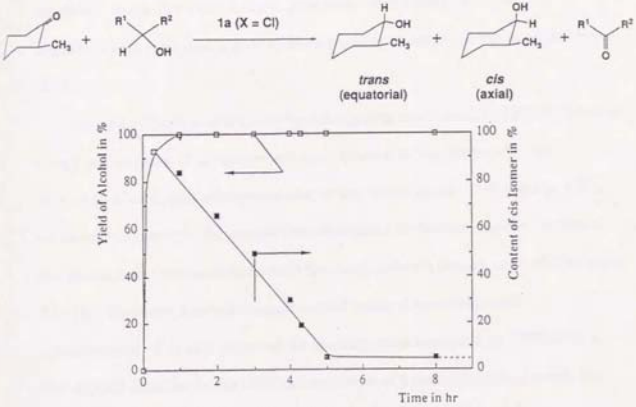

Figure 1. Reduction of 2-methylcyclohexanone with (±)-isoborneol catalyzed by (TPP)AlCl (1, X = Cl) in $CHCl_3$ at 30 °C. Time course of the reaction. $[2\text{-Methylcyclohexanone}]_0$ = $[(\pm)\text{-isoborneol}]_0$ = 1.0 M, $[(TPP)AlCl]_0$ = 0.2 M.

for the reaction catalyzed by (EtioP)AlCl (**1b**, X = Cl), where the *cis/trans* isomer ratio of 2-methylcyclohexanol formed in 80 % yield in 0.3 h changed from 93/7 to 5/95 after 6 h, although the ketone had been completely consumed within 1 h (runs 7 - 9). Thus, in the reductions with (±)-isoborneol using the chloroaluminum porphyrins (TPP)AlCl and (EtioP)AlCl as catalysts, 2-methylcyclohexanone is once reduced stereoselectively to the corresponding *cis* alcohol, which gradually epimerizes to the *trans* alcohol with also a high stereoselectivity. In sharp contrast, the attempted reduction of 2-methylcyclohexanone with (±)-isoborneol using aluminum tris(2-propoxide) ($Al(OCH(CH_3)_2)_3$), a representative catalyst for the hydrogen transfer reaction,[14] or **1a** (X = $OCH(CH_3)_2$), proceeded very slowly under similar conditions and exhibited a poor stereoselectivity throughout the reaction (runs 10, 11)

For the reduction of 2-methylcyclohexanone catalyzed by (TPP)AlCl, use of (-)-borneol in place of (±)-isoborneol also resulted in the stereoselective formation of *cis*-2-methylcyclohexanol at the initial stage (17 % yield in 0.3 h, *cis*-isomer content; 91 %), where the subsequent *cis*-to-*trans* epimerization of the product also occurred to furnish the final *cis/trans* isomer ratio of 5/95 (runs 12 - 14). However, the reaction proceeded much slower than with (±)-isoborneol. Use of 2-propanol for the reduction catalyzed by (TPP)AlCl or (EtioP)AlCl resulted in the efficient reduction of 2-methylcyclohexanone, but

Table 1. Reduction of Methylcyclohexanones with Secondary Alcohols.[a]

					cyclohexanol	
run	cyclohexanone	alcohol	catalyst	time, h	yield, %[d]	*cis/trans*[d]
1	2-methyl	(±)-isoborneol	(TPP)AlCl	0.3	93	93/ 7
2				3.0	100	51/49
3				5.0	100	5/95
4[b]				0.17	47	>99/<1
5[b]				0.5	100	96/ 4
6[b]				3.0	100	94/ 6
7			(EtioP)AlCl	0.3	80	93/ 7
8				3.0	100	48/52
9				6.0	100	5/95
10			$Al(OCH(CH_3)_2)_3$	0.3	15	72/28
11				3.0	49	65/35
12		(-)-borneol	(TPP)AlCl	2.0	17	91/ 9
13				4.0	87	11/89
14				7.0	100	5/95
15[c]		2-propanol	(TPP)AlCl	0.3	52	58/42
16[c]				3.0	85	7/93
17[c]			(EtioP)AlCl	0.3	45	60/40
18[c]				3.0	78	7/93
19[c]			$Al(OCH(CH_3)_2)_3$	0.3	13	55/45
20[c]				3.0	55	55/45
21	3-methyl	(±)-Isoborneol	(TPP)AlCl	1.0	64	16/84
22				6.0	100	85/15
23	4-methyl	(±)-Isoborneol	(TPP)AlCl	1.0	63	83/17
24				6.0	100	7/93

a) $[Ketone]_o/[alcohol]_o/[catalyst]_o$ = 2.5 mmol/2.5 mmol/0.5 mmol, in $CHCl_3$ (4.0 mL) at 30 °C under N_2. b) $[Ketone]_o/[alcohol]_o/[catalyst]_o$ of 2.5 mmol/20.0 mmol/0.5 mmol. c) in 2.5mL of $CHCl_3$. d) Determined by GC.

the *cis*-isomer content was low even at the initial stage compared with the above two cases (runs 15 - 18).

The system of (±)-isoborneol coupled with (TPP)AlCl or (EtioP)AlCl was also applicable to the stereoselective reduction of other substituted cyclohexanones. Examples shown in **Table 1** are the reductions of 3- and 4-methylcyclohexanones with the (±)-isoborneol - (TPP)AlCl system at 0 °C (runs 21 - 24). In both cases, the substrates were once reduced stereoselectively to the corresponding axial alcohols (*trans*-3-methylcyclohexanol, *cis*-4-methylcyclohexanol)[15], which gradually epimerized to the alcohols of opposite configuration in the subsequent stage. Thus, in the reduction of methylcyclohexanones with (±)-isoborneol catalyzed by aluminum porphyrin, the configuration of the alcohols formed at the initial stage demonstrates that the hydrogen transfer to the carbonyl group of the parent ketones preferentially occurs from the equatorial direction with respect to the cyclohexane ring.

In relation to the concomitant configurational change of the produced alcohols in the above processes, of interest to note is the fact that use of a large excess of (±)-isoborneol with respect to the substrate resulted in suppression of the product epimerization. An example is shown by the reduction of 2-methylcyclohexanone with the ratio $[2\text{-methylcyclohexanone}]_0/[(\pm)\text{-isoborneol}]_0/[(TPP)AlCl]_0$ of 5/40/1 at 30 °C, which proceeded to afford

2-methylcyclohexanol in 47 and 100 % yield in 0.17 and 0.5 h, respectively, with the *cis*-isomer contents of >99 and 96 % (runs 4, 5). Furthermore, the high content of the *cis* isomer thus observed remained unchanged even upon standing the reaction mixture for additional 2.5 h (runs 6).

Reduction of Prochiral Ketones with (-)-Isoborneol catalyzed by (TPP)AlCl (1a, X = Cl). Asymmetric reductions of prochiral ketones were attempted by using the system of (TPP)AlCl as catalyst coupled with an optically active alcohol such as (-)-isoborneol in $CHCl_3$ with the ratio $[ketone]_0/[alcohol]_0/[(TPP)AlCl]_0$ of 4/4/1 (**Table II**). Under the conditions examined, various prochiral phenones were catalytically reduced to the corresponding alcohols in excellent yields, and the highest enantioselectivity was observed for the reduction of isopropyl phenyl ketone (2-methyl-1-phenylpropan-1-one) (runs 13 - 17). For example, in the reduction conducted at 30 °C for 10 h, 1-phenyl-2-methyl-1-propanol was formed in 70 % yield in 76 % *ee* (*R*) (run 13). The reduction proceeded quantitatively upon prolonged reaction, keeping the optical purity of the product unchanged (> 99 % yield in 30 h, 72 % *ee*, run 15). Elevating the reaction temperature resulted in a noticeable acceleration of the reduction without decreasing the enantioselectivity ; the reaction performed at 55 °C proceeded to give 1-phenyl-2-methyl-1-propanol in 96 % yield in only 2 h with *ee* of 72 % (*R*) (run 17). The asymmetric reductions of other prochiral phenones (runs 1 - 12, 18 -

Table 2. Reduction of Prochiral Ketones with (-)-Isoborneol catalyzed by (TPP)AlCl.[a]

				carbinol	
run	ketone	temp, °C	time, h	yield, %[b]	*e.e*, %[c]
1	PhCOMe	0	2.0	57	28
2			4.0	95	28
3			8.0	98	0
4	PhCOEt	0	4.0	19	30
5			8.0	83	23
6			10.0	98	5
7	PhCOPr	0	1.5	40	30
8			4.0	93	20
9			7.0	> 99	11
10	PhCO^{t}Bu	20	4.0	53	35
11			6.0	94	30
12			12.0	> 99	10
13	PhCO^{i}Pr	30	4.0	42	70
14			10.0	70	76
15			30.0	> 99	72
16		55	0.5	73	72
17			2.0	96	72
18	PhCO *cyclo*-Hex	55	1.0	61	48
19			7.0	83	48
20	PhCO^{t}Bu	55	1.0	39	33
21			10.0	74	33
22	^{t}BuCOMe	30	6.0	28	32
23			12.0	50	32

a) $[Ketone]_0/[(-)\text{-Isoborneol}]_0/[(TPP)AlCl]_0$ = 2.0/2.0/0.5 (in mmol) in $CHCl_3$ (3.0 mL) under N_2. b) By GC. c) By GC as the corresponding (-)-menthyl carbonates.

21) and an aliphatic ketone such as *tert*-butyl methyl ketone (pinacolone) (runs 22, 23) with (-)-isoborneol catalyzed by (TPP)AlCl also proceeded to give the corresponding alcohols in excellent yields with the e.e. ranging from 20 - 48 %. It should be noted that all the alcohols predominantly formed with the (-)-isoborneol - (TPP)AlCl system have (*R*)-configuration.

In the reductions of phenones with primary alkyl groups attached to the carbonyl group (runs 1 - 12), the optical purity of the produced alcohols gradually decreased with time under the conditions examined. The representative example is shown by the reduction of phenyl propyl ketone with the (-)-isoborneol - (TPP)AlCl system at 30 °C, where the *ee* of the product formed in 1.5 h (40 % yield) decreased from 30 % to 20 (4 h, 93 % yield) and 11 % (7 h, > 99% yield) (runs 7 - 9), indicating the presence of racemization.

Epimerization of Methylcyclohexanols in the Presence of (TPP)AlCl (1a, X = Cl). In the reduction of ketone with alcohol catalyzed by aluminum porphyrin, the initial stereochemistry of the carbinol carbon atom of the products eventually changes (epimerization or racemization), as described in the above sections. Similar stereochemical profiles have been observed for some hydrogen transfer reactions reported to date, and are ascribed to the reversible nature of the reaction.[16] The reversible nature of the hydrogen transfer reaction catalyzed by aluminum porphyrin could be well demonstrated by the combination of appropriate ketones and alcohols. For example, in the

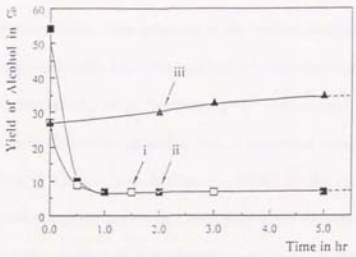

Figure 2. Epimerization of 2-methylcyclohexanol in the presence of 2-methylcyclohexanone catalyzed by (TPP)AlCl (1, X = Cl) or $Al(OCH(CH_3)_2)_3$ in $CHCl_3$ at 30 °C. $[Alcohol]_0/[ketone]_0/[catalyst]_0 = 5/1/1$ ($[alcohol]_0 = 1.0$ M). (i) $[Cis]_0/[trans]_0 = 54/46$, cat. 1 (X = Cl). (ii) $[Cis]_0/[trans]_0 = 27/73$, cat. 1 (X = Cl). (iii) $[Cis]_0/[trans]_0 = 27/73$, cat. $Al(OCH(CH_3)_2)_3$.

presence of (TPP)AlCl (0.2 equiv.) as catalyst at 30 °C, the reduction of 2-methylcyclohexanone with 2-propanol (1 equiv./1 equiv.) to give 2-methylcyclohexanol and acetone proceeded to attain the plateau at 85 % conv., while the plateau was established at 15 % conv. under the same conditions for the reduction of acetone with 2-methylcyclohexanol to give 2-propanol and 2-methylcyclohexanone. In connection with the reversible nature of the reaction, the addition of methylcyclohexanone (5 equiv.) to the isomeric mixture of 2-methylcyclohexanol (*cis/trans* = 54/46) (5 equiv.) in the presence of (TPP)AlCl (1 equiv.) at 30 °C in $CHCl_3$ brought about the epimerization of 2-methylcyclohexanol to furnish the *cis/trans* isomer ratio of

10/90 in 0.5 h and the constant ratio at 7/93 after 2 h (**Figure 2, i**). Nearly the same *trans*-isomer content was attained in the epimerization of 2-methylcyclohexanol with the initial *cis/trans* isomer ratio of 27/73 (**Figure 2, ii**). The epimerization of 2-methylcyclohexanol[17] in the presence of (TPP)AlCl was observed to be slow without added ketone (*cis/trans* isomer ratio, 54/46 initially, 25/75 in 0.5 h, and the constant ratio 7/93 after 5 h). Thus, in the hydrogen transfer reaction with aluminum porphyrin catalyst, the epimerization of the alcohol once produced is mediated by the existing carbonyl compounds, whereupon the product undergoes re-oxidation to lose the original stereochemistry. The epimerization of 2-methylcyclohexanol (*cis/trans* isomer ratio : 27/73) also took place in the presence of 2-methylcyclohexanone and $Al(OCH(CH_3)_2)_3$ but with very poor stereoselectivity to attain the plateau at the *cis/trans* isomer ratio of 35/65 (**Figure 2, iii**).

Coordinative Interaction between Aluminum Porphyrin and Ketones or Alcohols. We have previously reported that the Lewis acidity of (TPP)AlCl (**1a**, X = Cl) is so high that it can be coordinated by and activate the carbonyl group of cyclic esters for nucleophilic attack.[4] A similar coordinative interaction was observed by ^1H NMR for the mixture of (TPP)AlCl and a ketone such as acetophenone. In the ^1H NMR spectrum of the mixture with the mole ratio $[acetophenone]_0/[(TPP)AlCl]_0$ of 1/0.63 in $CDCl_3$ at 27 °C, all the signals due to acetophenone were observed to shift by 0.11 to 0.16 ppm upfield from

those in the absence of (TPP)AlCl.[18] For example, the signal due to the methyl group, which appears in the absence of (TPP)AlCl as a sharp singlet at 2.60 ppm, was observed at 2.44 ppm with significant line broadening. Thus, acetophenone is in the proximity of (TPP)AlCl, and affected by the magnetic shielding effect due to the ring current of porphyrin.

The ^{1}H NMR spectrum in $CDCl_3$ at 27 °C of the mixture of 2-propanol and (TPP)AlCl ($[alcohol]_0/[(TPP)AlCl]_0$ = 1/0.125), where the broadened signals assignable to CH_3, CH and OH groups of 2-propanol (δ 0.78, 3.15 and 1.06 ppm) were upfield-shifted from those in the absence of (TPP)AlCl.[18] The possibility of the ligand exchange reaction of (TPP)AlCl with 2-propanol to form $(TPP)AlOCH(CH_3)_2$ and HCl could be excluded by the comparison of the above spectrum with that of $(TPP)AlOCH(CH_3)_2$ (CH_3: δ -1.92, CH: δ -2.10) separately prepared. Thus, the upfield shifts for the signals of 2-propanol are also ascribed to the coordinative interaction with (TPP)AlCl.

The UV-Vis spectral patterns for (TPP)AlCl in acetone and 2-propanol (Figures 3b and 3c) were both different from that in CH_2Cl_2 (**Figure 4a**) but similar to those for the six-coordinate complexes from **1** and Lewis bases such as 1-methylimidazole and tetraethylammonium acetate in CH_2Cl_2.[3,10] This observation and the NMR profiles mentioned above demonstrate the possible coordinations of ketone and alcohol with (TPP)AlCl from the back side to generate the six-coordinate complexes. In sharp contrast, no change was

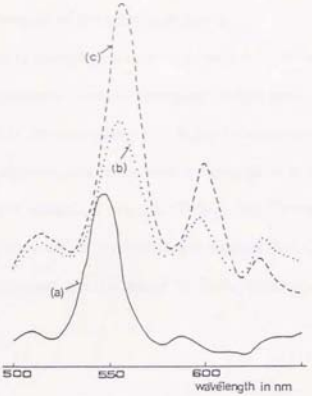

Figure 3. UV–vis spectra of (TPP)AlCl in (a) CH_2Cl_2, (b) acetone, and (c) 2-propanol under N_2 at room temperature.

observed for the NMR spectra of ketone and alcohol upon mixing with (TPP)AlOCH$(CH_3)_2$, which is much inferior to (TPP)AlCl in terms of both catalytic activity and stereoselectivity. Thus, in the reduction catalyzed by the chloroaluminum porphyrins, (TPP)AlCl and (EtioP)AlCl, the hydrogen transfer from carbinol to carbonyl group is affected by the coordinative interactions with the Lewis acidic metal centre of the catalyst. The attempted reaction of cyclohexanone and 2-propanol with (TPP)AlCl in basic solvents such as tetrahydrofuran and pyridine resulted in no reduction of the substrate, probably due to the neutralization of the Lewis acidity of the catalyst by the

preferential coordination of the solvent molecule.

The reduction of methylcyclohexanones with secondary alcohols catalyzed by aluminum porphyrin involves two competitive hydrogen transfer processes, one of which leads to the reduction of methylcyclohexanones to the axial alcohols, and the other results in the slow epimerization of the axial alcohols once produced to the equatorial alcohols (**Table I** and **Figure 1**). High stereoselectivities observed in both processes suggest that these two reactions proceed with a prominent steric effect of the bulky catalyst, chloroaluminum porphyrin.

Conclusion

The diastereoselective and enantioselective hydrogen transfer reactions were observed in the reduction of ketones with alcohols by using the chloroaluminum porphyrins, (TPP)AlCl and (EtioP)AlCl, as catalysts. The coordinative interactions are present both for the ketones and alcohols with the Lewis acidic aluminum atom of the catalyst, leading to the facile hydrogen transfer under mild conditions. The reactions take place with a marked steric effect of the bulky porphyrin ligand around the metal centre. Apart from the biological viewpoints, limited attempts have been reported to utilize metalloporphyrins as catalyst for synthetic reactions. The present development discloses *a potential utility of metalloporphyrin as catalyst to provide a new strategy for the steric control in organic syntheses.*

LIST OF PUBLICATIONS

CHAPTER 1

(1) "Chiral N-Substituted Porphyrins Related to Heme Inactivation Products. First Crystallographic Determination of Absolute Stereochemistry and Correlation with Circular Dichroism."
K. Konishi, Y. Takahata, T. Aida, S. Inoue, and R. Kuroda,
J. Am. Chem. Soc. in press.

CHAPTER 2

(2) "Stereochemical Studies on Reversible Metal-Nitrogen Transfer of Alkyl and Aryl Groups in Chiral Cobalt(III) Porphyrins. Relevance to the Mechanism of a Metabolic Heme Inactivation Process."
K. Konishi, T. Sugino, T. Aida, and S. Inoue,
J. Am. Chem. Soc. 113, 6487-6491 (**1991**).

CHAPTER 3

(3) "Photoinduced Conformational Ruffling of Distorted Porphyrin. Optical Resolution and Photochemical Behavior of Chiral "Single-Armed" Porphyrin Complexes."
K. Konishi, M. Miyazaki, T. Aida, and S. Inoue,
J. Am. Chem. Soc. 112, 5639-5640 (**1990**).

(4) "Molecular Motions of Porphyrin Macrocycles. Racemization Profiles of Chiral Meso-Alkenyl "Armed" Porphyrin Complexes"
K. Konishi, Y. Mori, T. Aida, S. Inoue,
to be submitted, not included in this thesis.

CHAPTER 4

(5) "Asymmetric Epoxidation of Olefins Catalyzed by Manganese Complexes of Chiral "Strapped' Porphyrins with Diastereotopic Faces. A Novel Strategy for Stereochemical Modeling of the Active Site of Cytochrome P-450."

K. Konishi, K. Oda, K. Nishida, T. Aida, and S. Inoue

J. Am. Chem. Soc. 113, 1313-1317 (**1992**).

(6) "Asymmetric Oxidation of Sulfides Catalysed by an Iron Complex of C_2-Chiral Strapped Porphyrin as a Conceptually New P-450 Model Catalyst."

L-c. Chiang, K. Konishi, T.Aida, and S. Inoue,

J. Chem. Soc., Chem. Commun., 254-256 (**1992**).

CHAPTER 5

(7) "A Novel Anion - Binding Chiral Receptor Based on a Metalloporphyrin with Molecular Asymmetry. Highly Enantioselective Recognition of Amino Acid Derivatives."

K. Konishi, K. Yahara, H. Toshishige, T. Aida, and S. Inoue,

J. Am. Chem. Soc. submitted.

(8) "Shape-selective Anion - Binding Receptor Based on a Metalloporphyrin"

K. Konishi, H. Saito, T. Aida, S. Inoue,

to be submitted, not included in this thesis.

CHAPTER 6

(9) "Hydrogen Transfer from Alcohols to Carbonyl Compounds Catalyzed by Aluminum Porphyrins. Stereochemical Aspects."
K. Konishi, T. Aida, and S. Inoue,
J. Org. Chem. 55, 816-820 (**1990**).

(10) "Highly Stereoselective Hydrogen Transfer from Alcohols to Carbonyl Compounds Catalyzed by Aluminum Porphyrins."
K. Konishi, K. Makita, T. Aida, and S. Inoue,
J. Chem. Soc., Chem. Commun., 643 - 644 (**1988**).

Other Publications

(11) "Selective Synthesis with Metalloporphyrin Catalysts"
S. Inoue, T. Aida, and K. Konishi,
J. Mol. Cat. 74, 121 - 129 (**1992**).


Kodak Color Control Patches
© Kodak, 2007 TM: Kodak
Blue
Cyan
Green
Yellow
Red
Magenta
White
3/Color
Black
Kodak Gray Scale
C
Y
M
© Kodak, 2007 TM: Kodak
A 1 2 3 4 5 6 M 8 9 10 11 12 13 14 15 B 17 18 19